The Abdus Salam International Centre for Theoretical Physics

United Nations Educational, Scientific and Cultural Organization

IAEA International Atomic Energy Agency

2332-11

School on Synchrotron and FEL Based Methods and their Multi-Disciplinary Applications

19 - 30 March 2012

Inelastic x-ray scattering: principles and applications

Filippo Bencivenga
Elettra, Trieste - Italy

Inelastic x-ray scattering: principles and applications

Filippo Bencivenga

OUTLINE

Introduction

High resolution inelastic x-ray scattering (IXS)

- Collective atomic dynamics
- Neutrons vs. X-rays
- Basic theory and instrumentation
- Experimental highlights

Inelastic x-ray "Raman" scattering (XRS)

- Experimental/theoretical aspects
- Scattering vs. absorption spectroscopy
- Experimental highlights

Introduction: inelastic X-ray spectrum

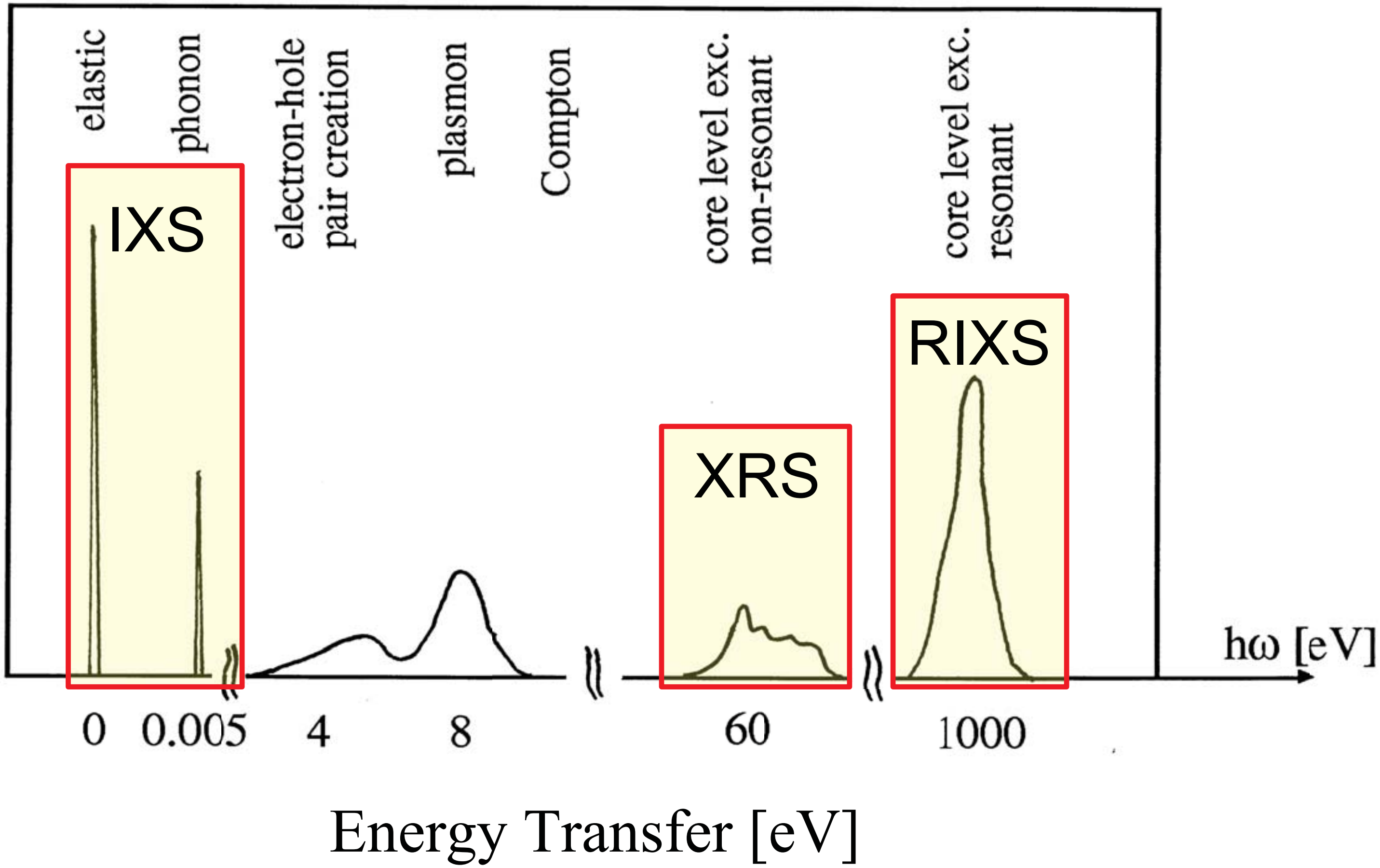

high-resolution Inelastic X-ray Scattering (IXS)

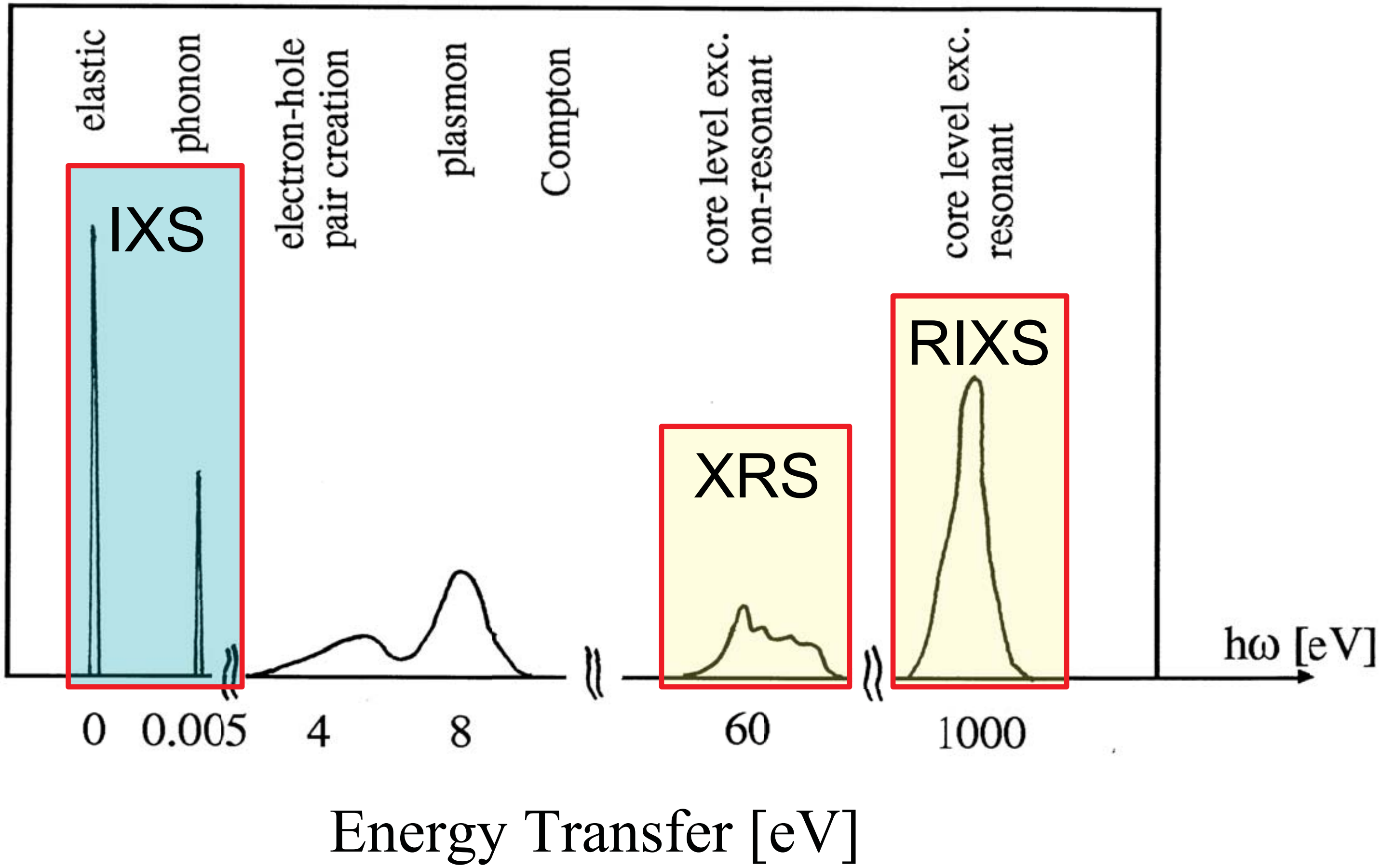

IXS: collective atomic dynamics

The simpler case

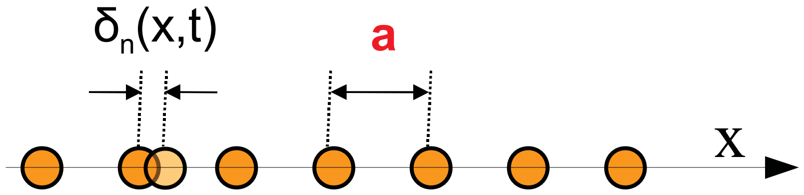

Information:

- Interatomic Structure (**a**)
- Interaction Potential (**β**)

$U = -\beta x^2$

$\delta_n(x,t) = \delta_{n,0} \exp[i(kx-\omega t)]$

Phonons → Eigenstates of vibrational field

$\omega(k)$ → Dispersion relation

$\omega = |(4\beta/M)^{1/2} \sin(ka/2)|$

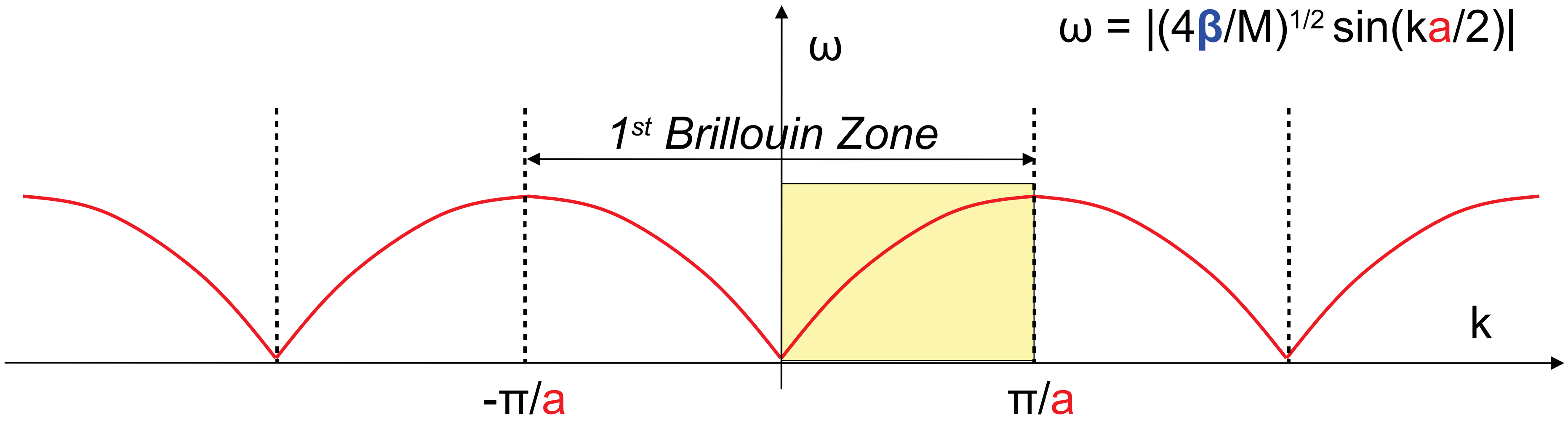

IXS: collective atomic dynamics

One step forward: 3D lattice

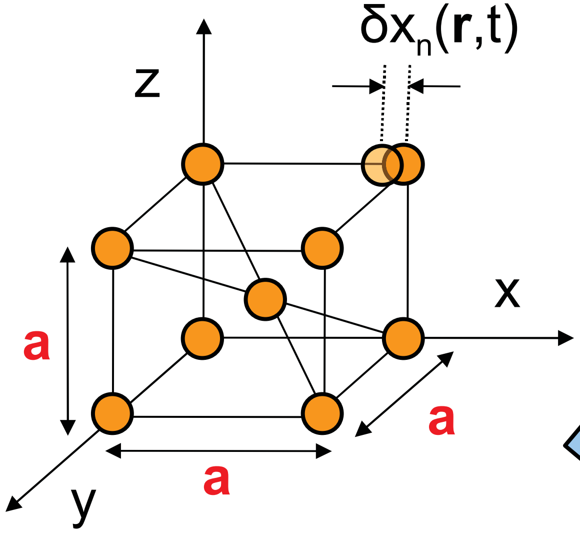

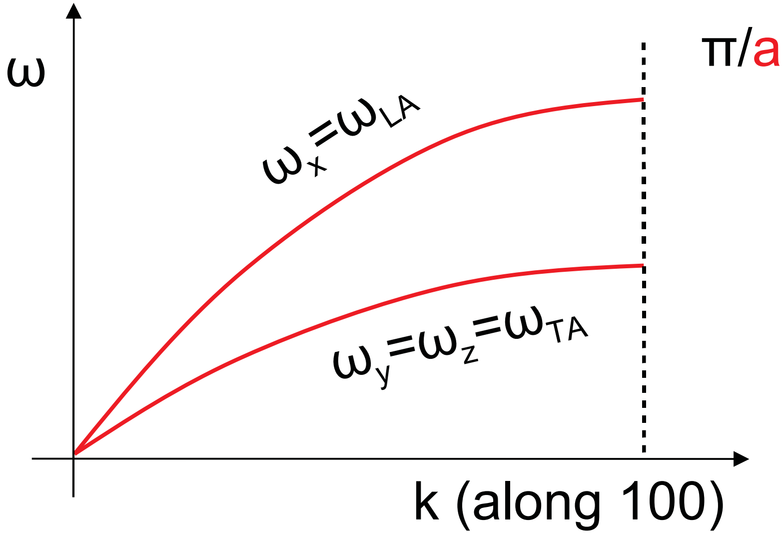

$$\omega = |(\mathbf{c}_{ij}/\rho)^{1/2}\sin(ka^*)|$$

$$U = -\boldsymbol{\beta}|\mathbf{r}|^2 \qquad \mathbf{r} = (x,y,z)$$

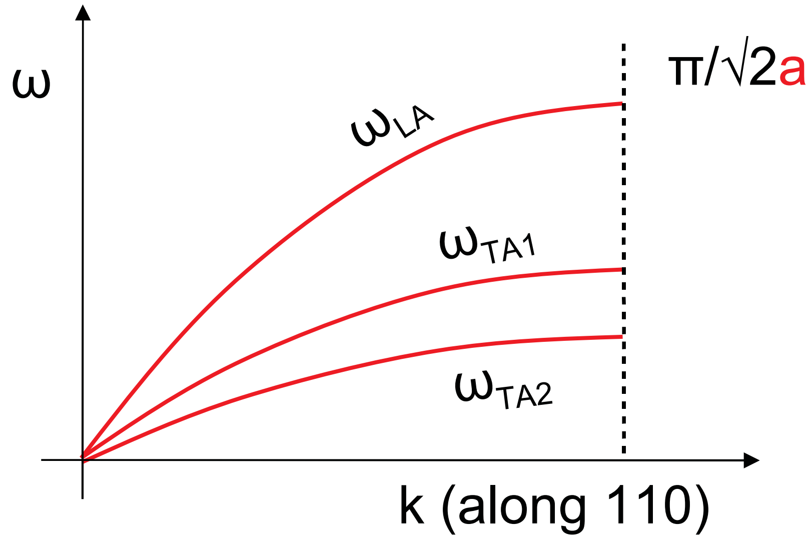

Information:

- Interatomic Structure (**a**)
- Interaction Potential (**β**)
- Anisotropy (elasticity: $\mathbf{c}_{ij}$)

IXS: collective atomic dynamics

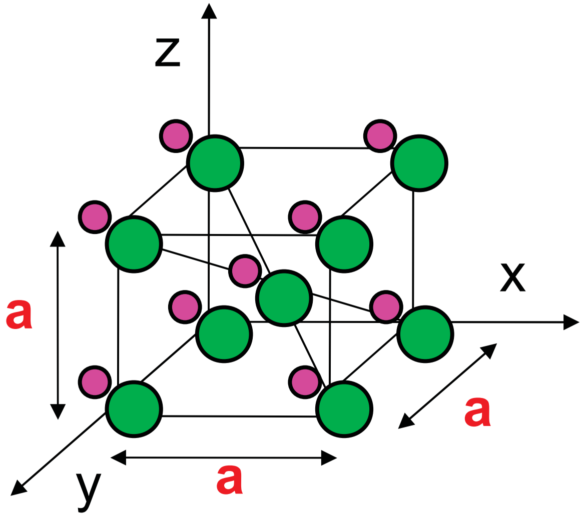

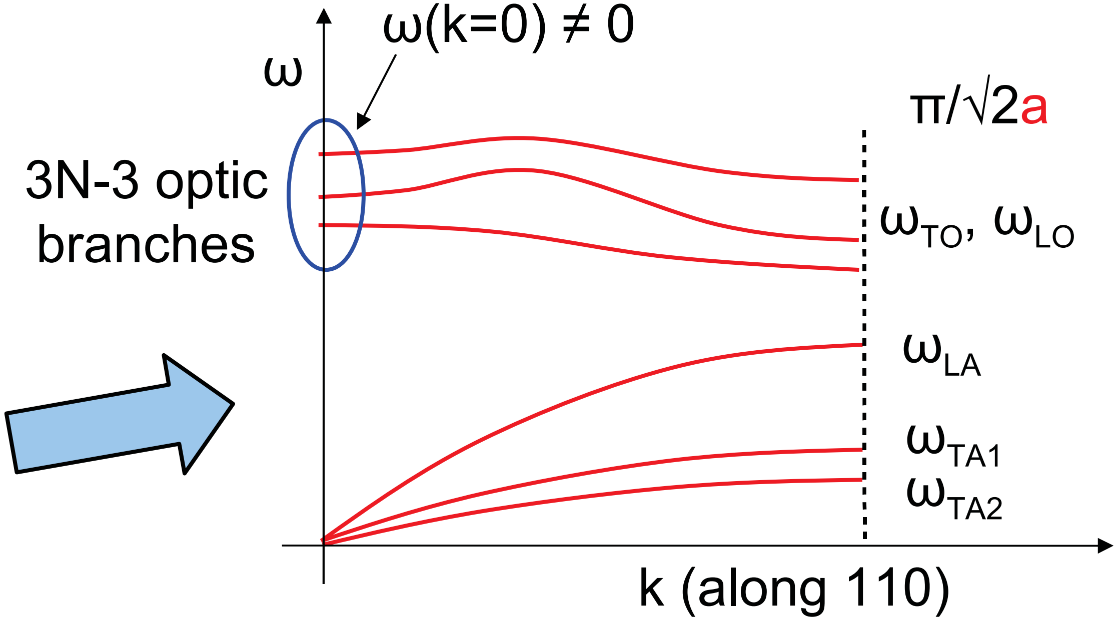

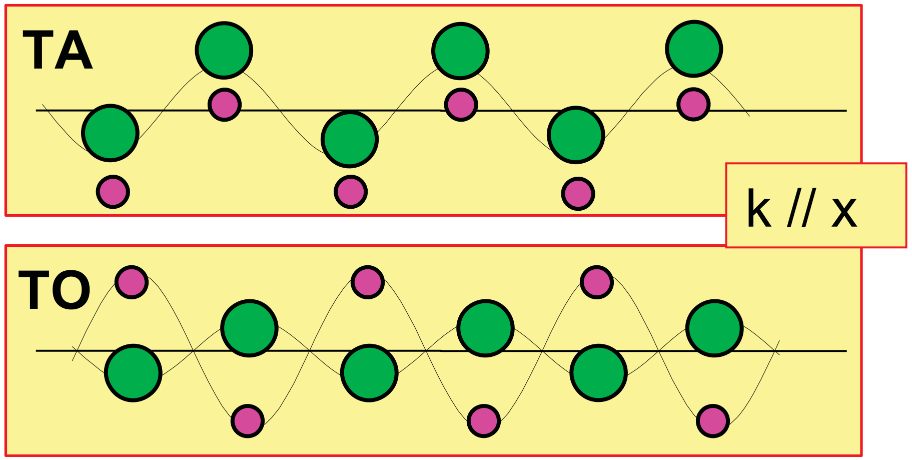

Information:

- Interatomic Structure (**a**)
- Interaction Potential (**β**)
- Anisotropy (elasticity: c_{ij})
- Intramolecular vibrations

IXS: collective atomic dynamics

The most complex case: disordered systems

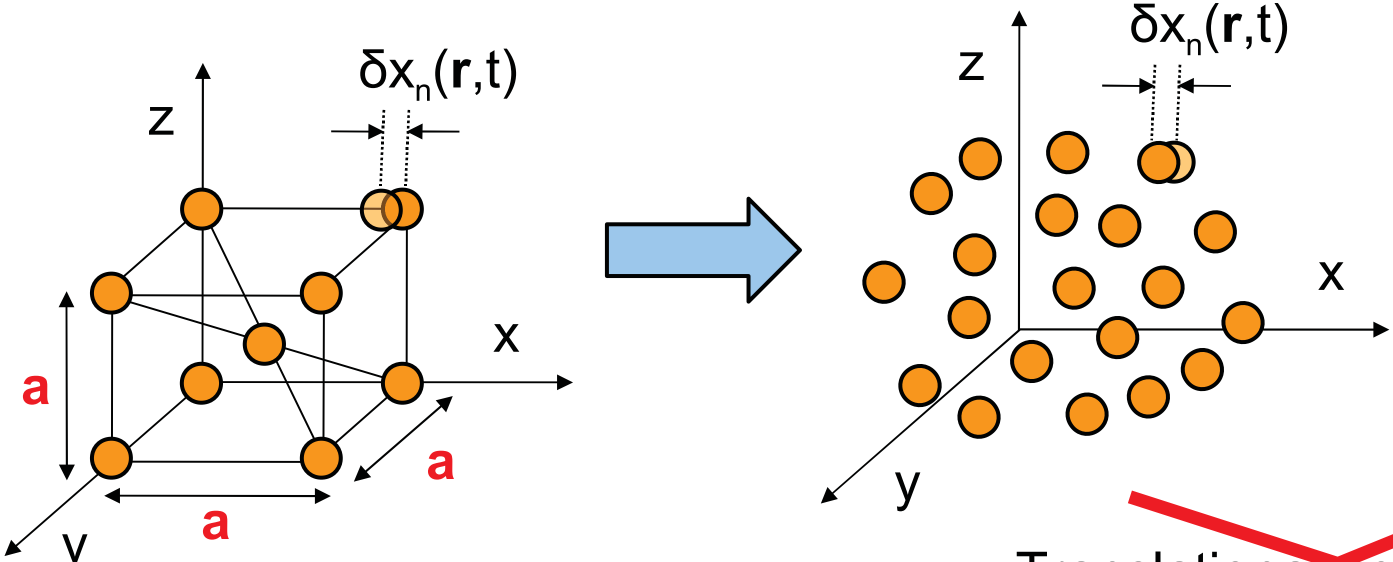

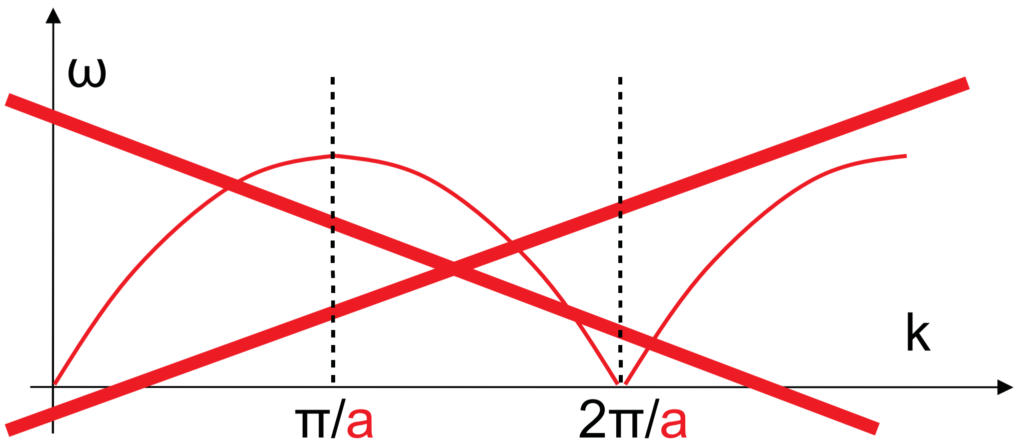

~~Translational periodicity (a)~~

~~Brillouin Zones~~

~~Eingenstates ~ exp[i(kx-ωt)]~~

IXS: collective atomic dynamics

The most complex case: disordered systems

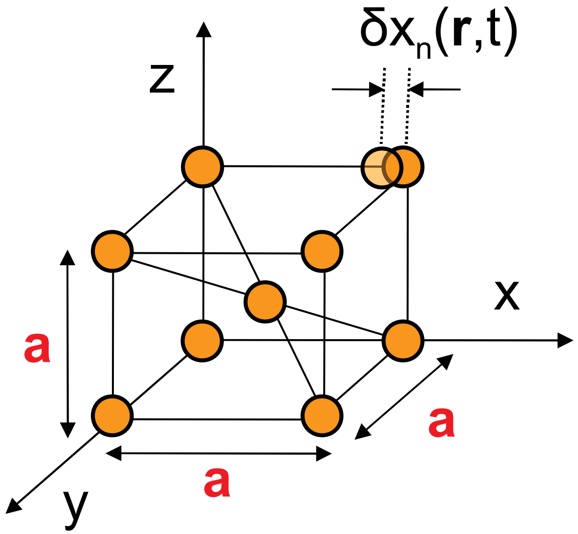

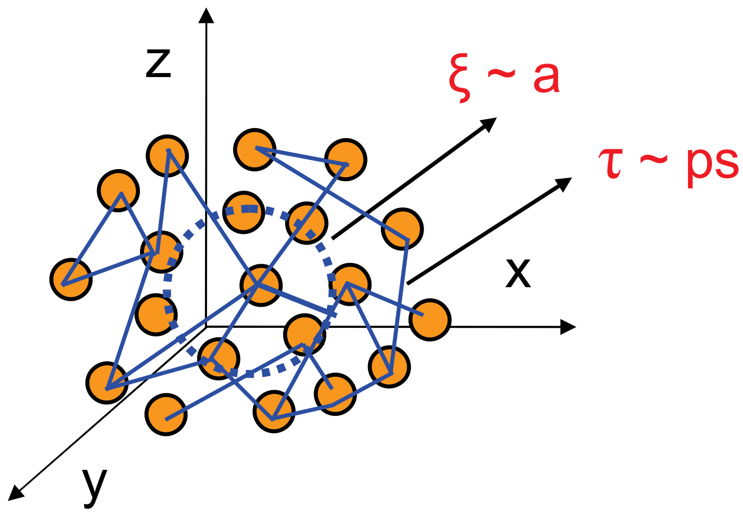

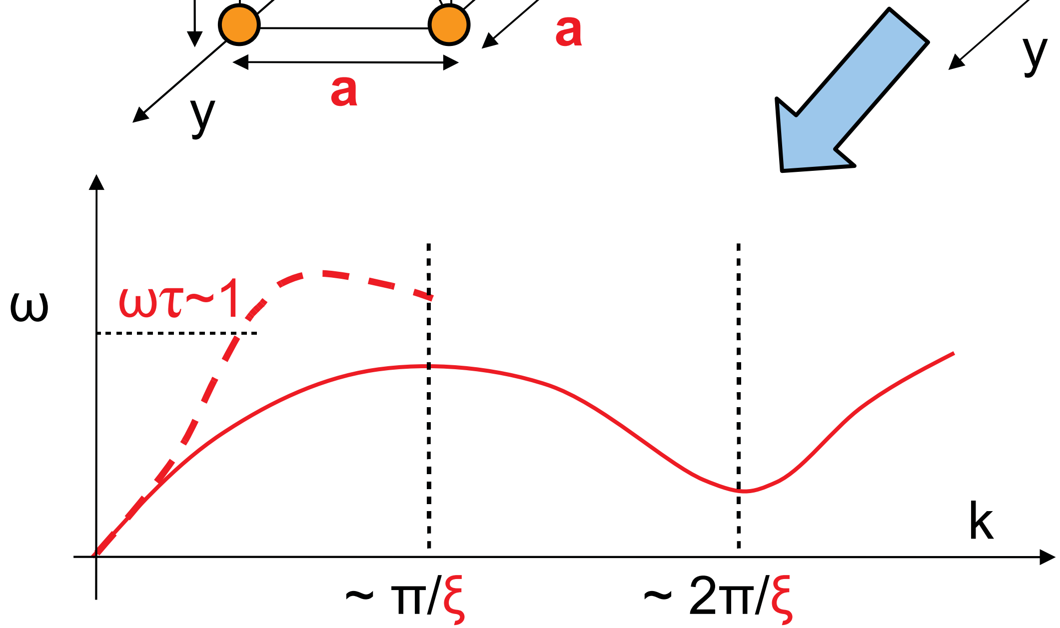

<u>Information:</u>

- Interatomic Structure (**ξ**)
- Interaction potential
- Topological disorder
- Relaxation processes
- "Lineshape" (anharmonicity, etc…)

An example…

Diamond: fcc symmetry + 2 C atoms each lattice site @ ±(¼,¼,¼)

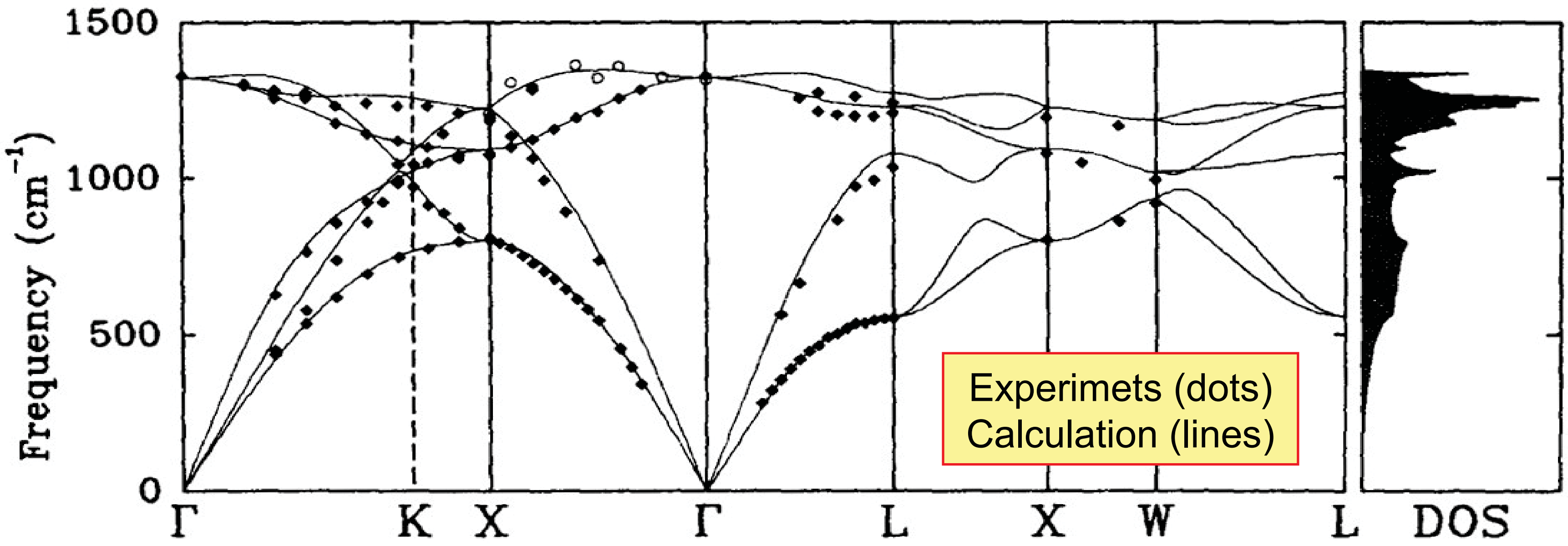

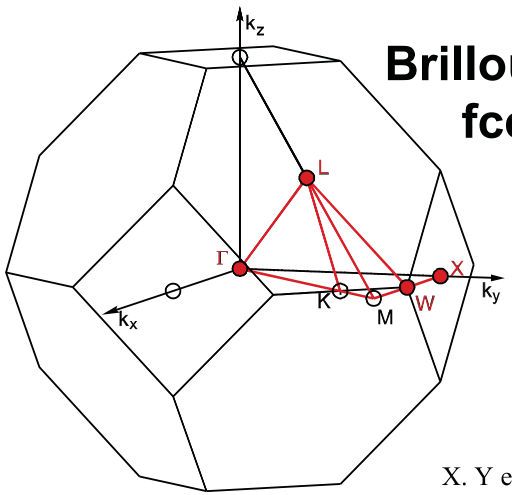

Brillouin zones for fcc symmetry

X. Y et al., PRB 48 (1993)

Information:

- **Structure** and **Elasticity** (sound velocities)
- **Interaction potential** and **Anharmonicity**
- **Dynamical istabilities** (phonon softening)
- **Electron-phonon coupling**
- **Thermodynamics** (c_V, λ, Θ_D, S_D, etc …)

How can we measure Atomic Dynamics?

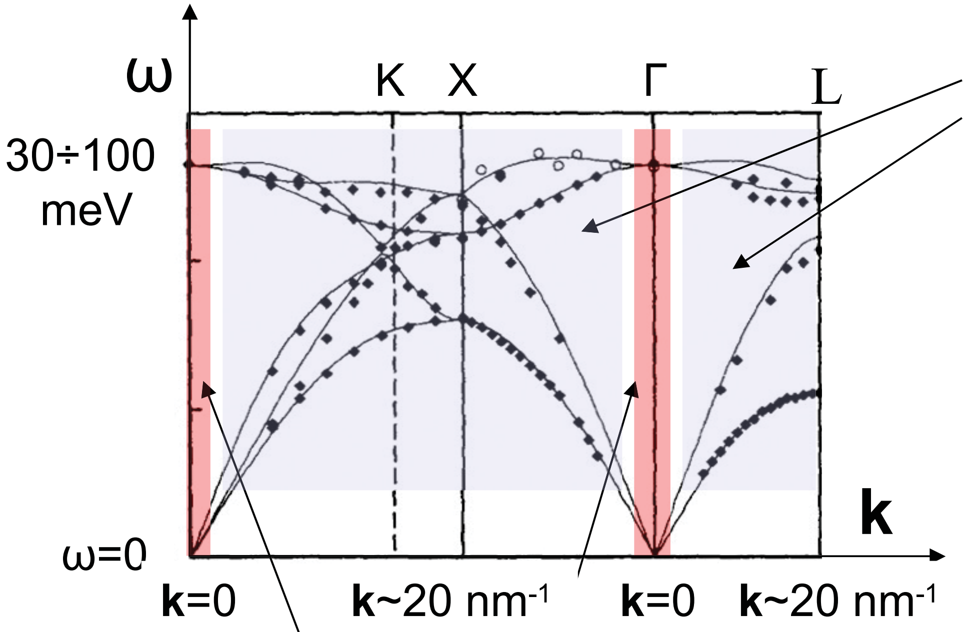

- Probe wavelenght (2π/|**k**|) < 0.1 nm
- Probe energy (E) > 30÷100 meV

- Inelastic Light Scattering (Brillouin & Raman)
- Ultrasonics
- Transient Grating
- Etc …

Inelastic scattering:

$E = E_{out} - E_{in}$

$\mathbf{k} = \mathbf{k}_{out} - \mathbf{k}_{in}$

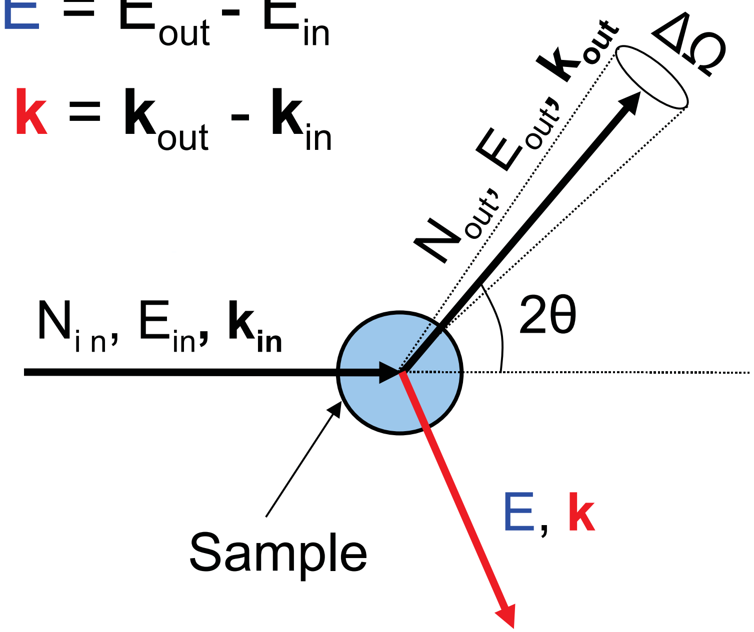

Cross section: $\frac{\partial^2\sigma}{\partial\Omega\partial E} \sim N_{out}/N_{in}$

Neutrons vs. X-rays

$\lambda_{in} = 1 Å$ ⇨ $E_{in} = 82\ meV$

$\lambda_{in} = 1 Å$ ⇨ $E_{in} = 12.4\ keV$

$E > 4\ meV \rightarrow \Delta E/E_{in} = 0.05$

$E > 4\ meV \rightarrow \Delta E/E_{in} = 3 \cdot 10^{-7}$

Moderate energy resolution ⇩ **100 INS instruments** + **Spin sensitive**, **Better contrast**, **"Older" technique**

Very high energy resolution ⇩ **4 IXS instruments**

Inelastic scattering:

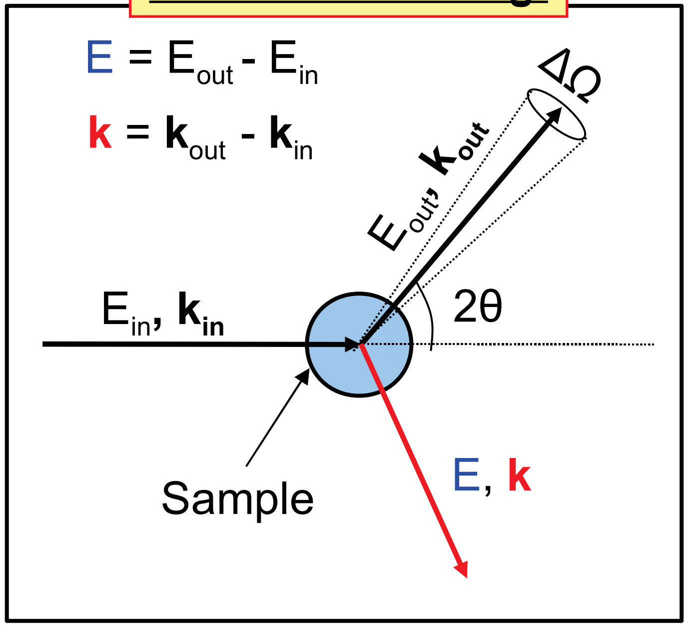

Why X-rays?

Neutrons vs. X-rays

$\lambda_{in} = 1Å$ ⇒ $E_{in} = 82$ meV

$\lambda_{in} = 1Å$ ⇒ $E_{in} = 12.4$ keV

$E = E_{out} - E_{in}$ & $\mathbf{k} = \mathbf{k}_{out} - \mathbf{k}_{in}$

$E_{out} \neq E_{in}$

$$\frac{|\mathbf{k}|^2}{2|\mathbf{k}_{in}|^2} = 1 - E/E_{in} + \cos(2\theta)(1-2E/E_{in})^{1/2}$$

$E_{out} \approx E_{in}$

$$|\mathbf{k}| = 2|\mathbf{k}_{in}|\sin(\theta)$$

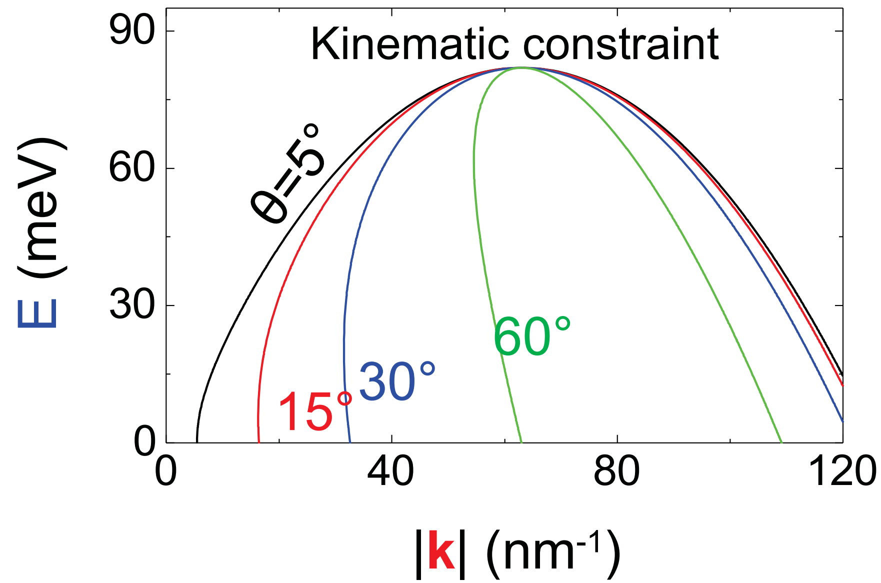

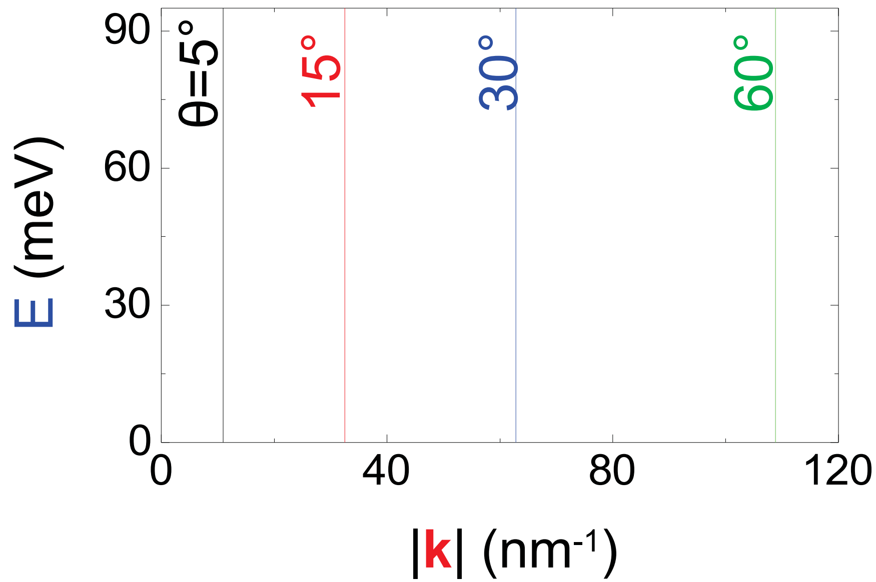

Neutrons vs. X-rays

λ_{in} = 1Å ➔ E_{in} = 82 meV

λ_{in} = 1Å ➔ E_{in} = 12.4 keV

$E = E_{out} - E_{in}$ & $\mathbf{k} = \mathbf{k}_{out} - \mathbf{k}_{in}$

Neutrons: $E_{out} \neq E_{in}$

$$\frac{|\mathbf{k}|^2}{2|\mathbf{k}_{in}|^2} = 1 - E/E_{in} + \cos(2\theta)(1 - 2E/E_{in})^{1/2}$$

X-rays: $E_{out} \approx E_{in}$

$$|\mathbf{k}| = 2|\mathbf{k}_{in}|\sin(\theta)$$

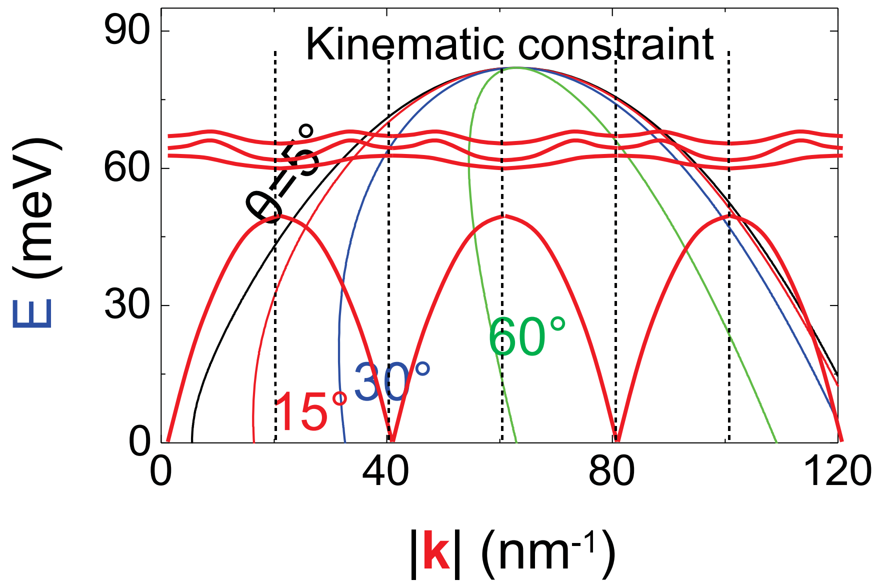

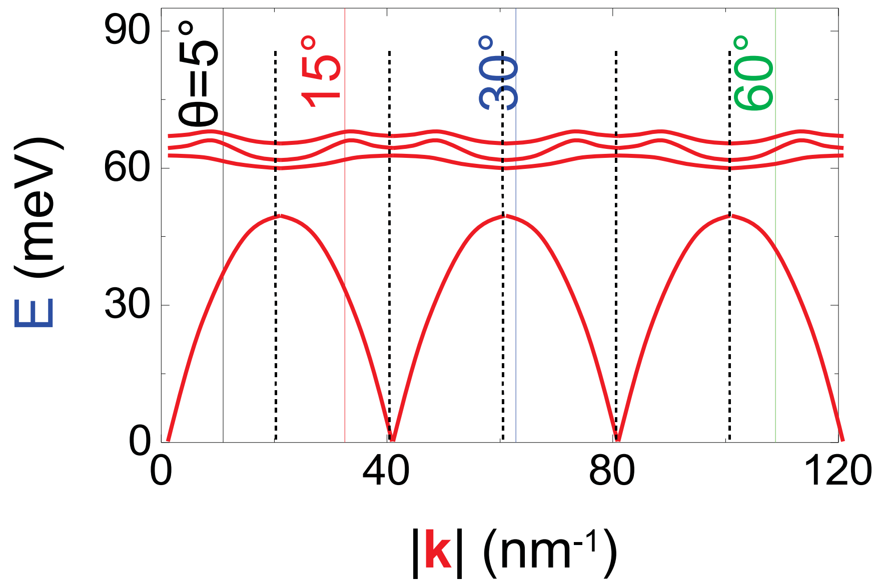

Neutrons vs. X-rays

Inelastic excitations in disordered systems

Neutrons	X-rays
λ_{in} = 1Å E_{in} = 82 meV	λ_{in} = 1Å E_{in} = 12.4 keV

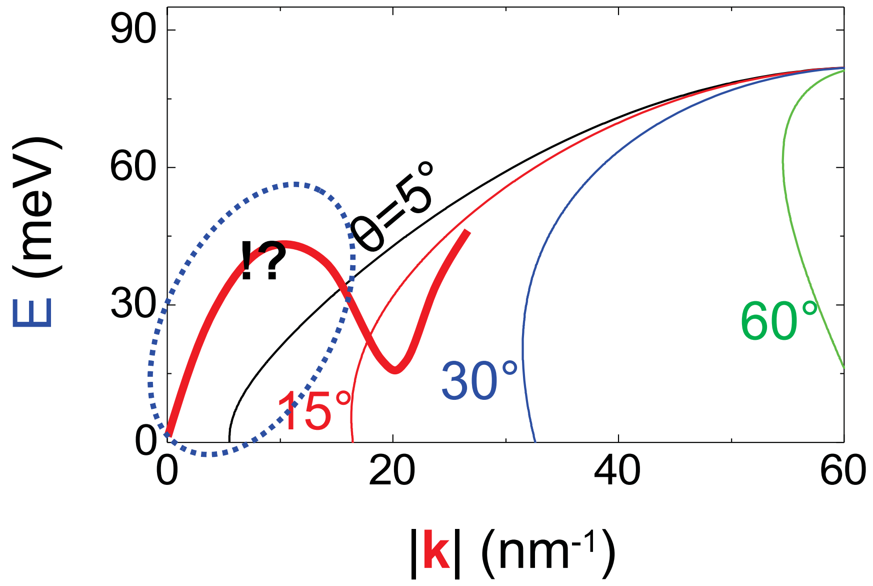

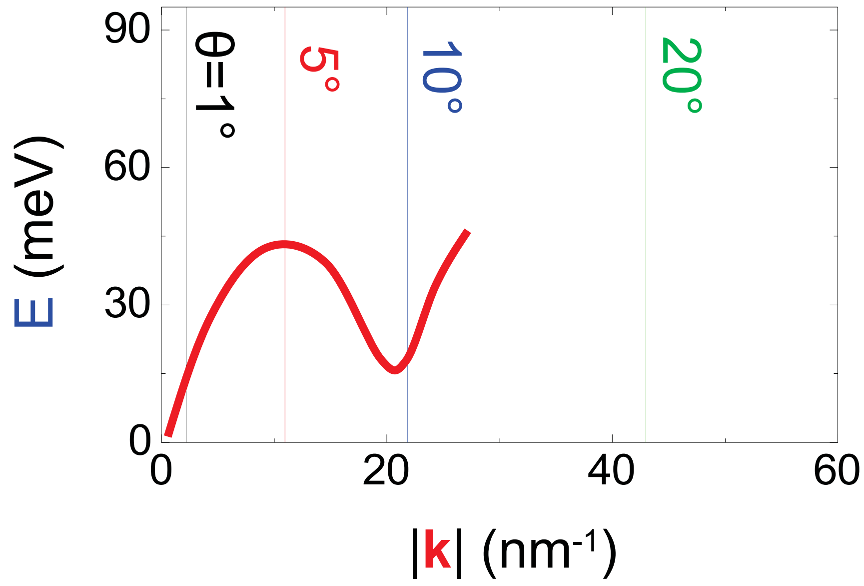

Neutrons vs. X-rays

$\lambda_{in} = 1Å$ ⇨ $E_{in} = 82$ meV

$\lambda_{in} = 1Å$ ⇨ $E_{in} = 12.4$ keV

E > 4 meV → $\Delta E/E_{in} = 0.05$

E > 4 meV → $\Delta E/E_{in} = 3 \cdot 10^{-7}$

Neutrons:

Moderate energy resolution

⇩

100 INS instruments

\+

Spin sensitive

Better contrast

"Older" technique

X-rays:

Very high energy resolution

⇩

3 IXS instruments

Why X-rays?

No kinematical constraints (Disordered systems)

Small beams (small samples: high pressure, exotic materials, etc…)

No incoherent cross section

Basic theoretical aspects

$$H_{int}=(e/m_e c)\sum_j[(e/2c)\mathbf{A}_j\cdot\mathbf{A}_j+\mathbf{A}_j\cdot\mathbf{p}_j+\text{magnetic}]$$

A is the vector potential of electromagnetic field

p is the momentum operator of the electrons

j is the summation over all electrons of the system

1st order perturbation theory

A·A term → one photon (non-resonant) scattering

$$\frac{\partial^2\sigma}{\partial\Omega\partial E} = r_0^{\,2}(\varepsilon_{in}\cdot\varepsilon_{out})^2(k_{in}/k_{out})\sum_I P_I|\langle I|\exp\{i\mathbf{k}\cdot\mathbf{r}_j\}|F\rangle|^2\delta(E-E_{out}+E_{in})$$

Basic theoretical aspects

$$\frac{\partial^2\sigma}{\partial\Omega\partial E} = r_0^2(\boldsymbol{\varepsilon}_{in}\cdot\boldsymbol{\varepsilon}_{out})^2(k_{in}/k_{out})\sum_i P_i|\langle I|\exp\{i\mathbf{k}\cdot\mathbf{r}_j\}|F\rangle|^2\delta(E-E_F+E_I)$$

The key assumption:

<u>Adiabatic approximation</u> → $|I\rangle=|I_n\rangle|I_e\rangle$ and $|F\rangle=|F_n\rangle|F_e\rangle$

$$\frac{\partial^2\sigma}{\partial\Omega\partial E} = r_0^2(\varepsilon_{in}\cdot\varepsilon_{out})^2(k_{in}/k_{out})\; F(|\mathbf{k}|)^2\; S(\mathbf{k},E)$$

Thomson scattering cross section

Molecular form factor ($|I_e\rangle$, $|F_e\rangle$)

<u>**Dynamic structure factor**</u>

The dynamic structure factor

S(**k**,E) is the **SPACE** and **TIME** Fourier transform of G(**r**,t)

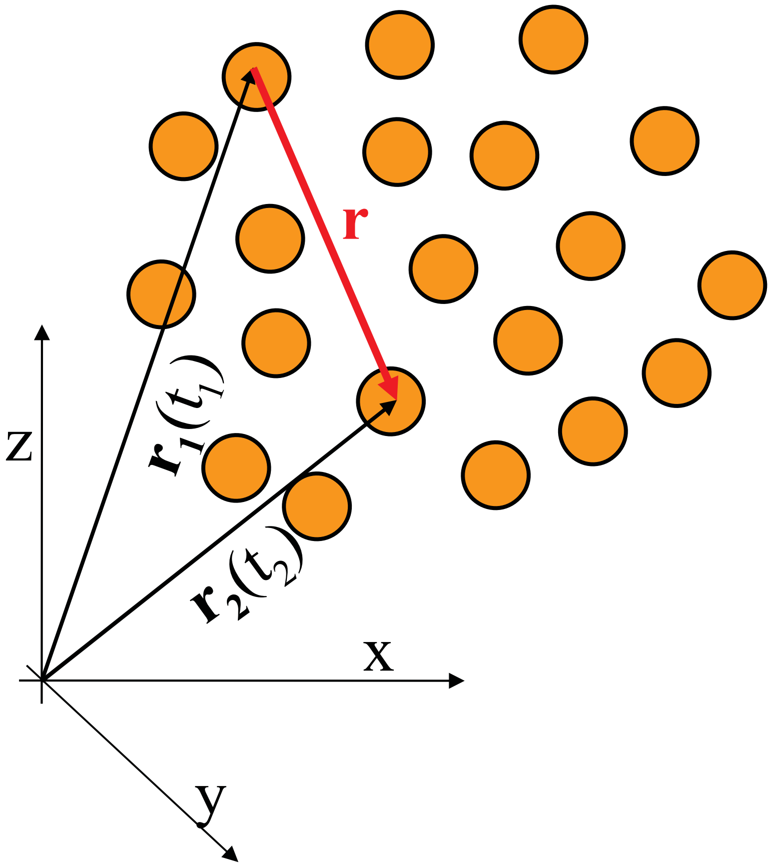

G(**r**,t) is the probability to find two distinct particles at positions $\mathbf{r}_1(t_1)$ and $\mathbf{r}_2(t_2)$, separated by the distance $\mathbf{r}=\mathbf{r}_2-\mathbf{r}_1$ and the time interval $t=t_2-t_1$.

Basic IXS instrumentation

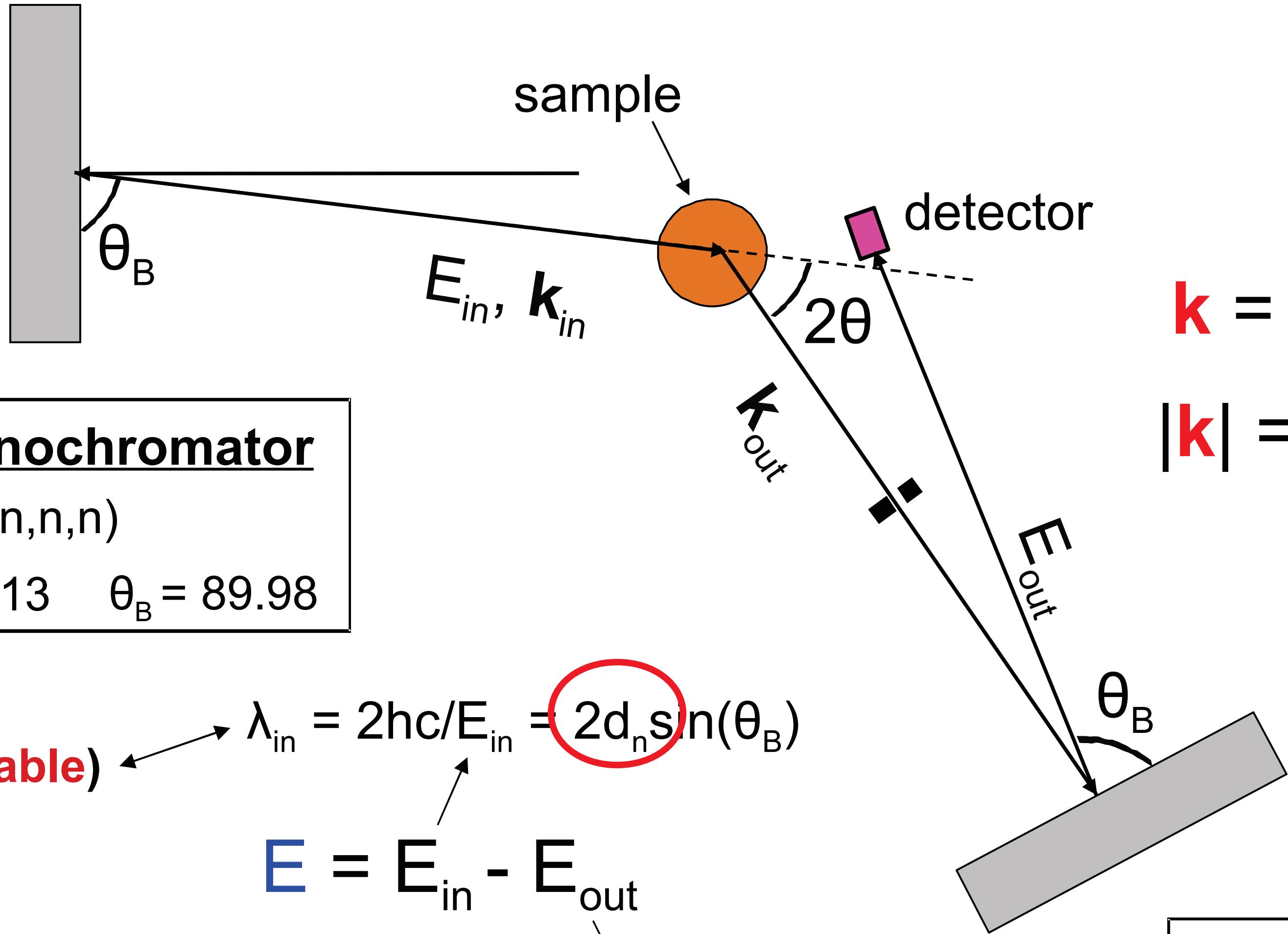

$\mathbf{k} = \mathbf{k}_{out} - \mathbf{k}_{out}$

$|\mathbf{k}| = 4\pi \sin(\theta)$

Monochromator

Si(n,n,n)

n=7-13 $\theta_B = 89.98$

λ_{in} **(tunable)** ↔ $\lambda_{in} = 2hc/E_{in} = 2d_n \sin(\theta_B)$

$E = E_{in} - E_{out}$

λ_{out} **(constant)** ↔ $\lambda_{out} = 2hc/E_{out} = 2d_n \sin(\theta_B)$

$\Delta E/E = \Delta\lambda_{in}/\lambda_{in} \sim \cot(\theta_B)$

Analyser

Si(n,n,n)

n=7-13 $\theta_B = 89.98$

Basic IXS instrumentation

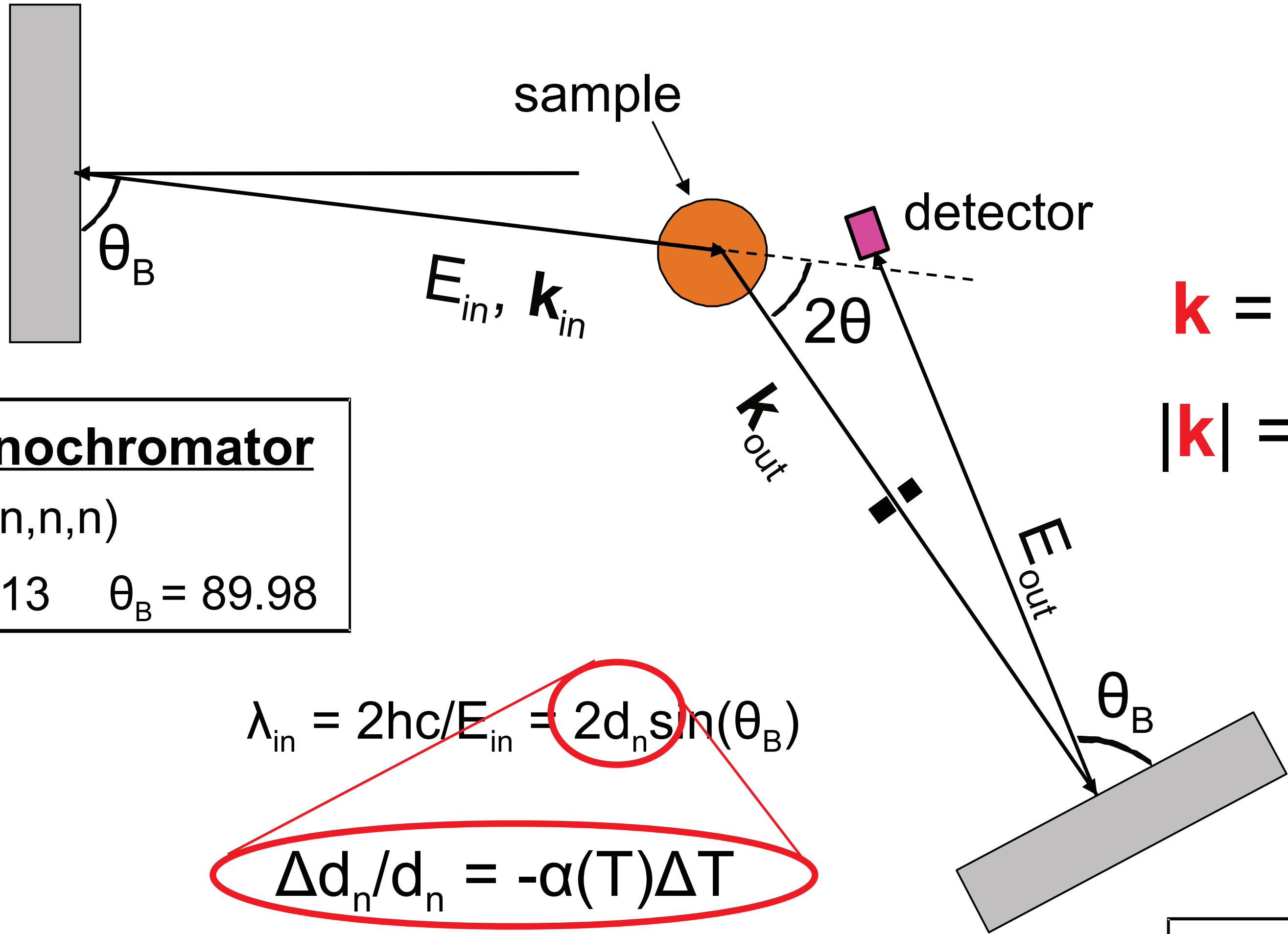

$\mathbf{k} = \mathbf{k}_{out} - \mathbf{k}_{out}$

$|\mathbf{k}| = 4\pi \sin(\theta)$

Monochromator

Si(n,n,n)

n=7-13 $\theta_B = 89.98$

$\lambda_{in} = 2hc/E_{in} = 2d_n \sin(\theta_B)$

$\Delta d_n / d_n = -\alpha(T)\Delta T$

Analyser

Si(n,n,n)

n=7-13 $\theta_B = 89.98$

$\alpha \sim 2.58\cdot10^{-6}$
$\Delta T \sim$ mK

$(E/\Delta E)_{MAX} \sim 0.5\cdot10^{8}$
< 1 meV @ 27 keV

R. Verbeni et al., XXX ??? (1996)

Basic IXS instrumentation

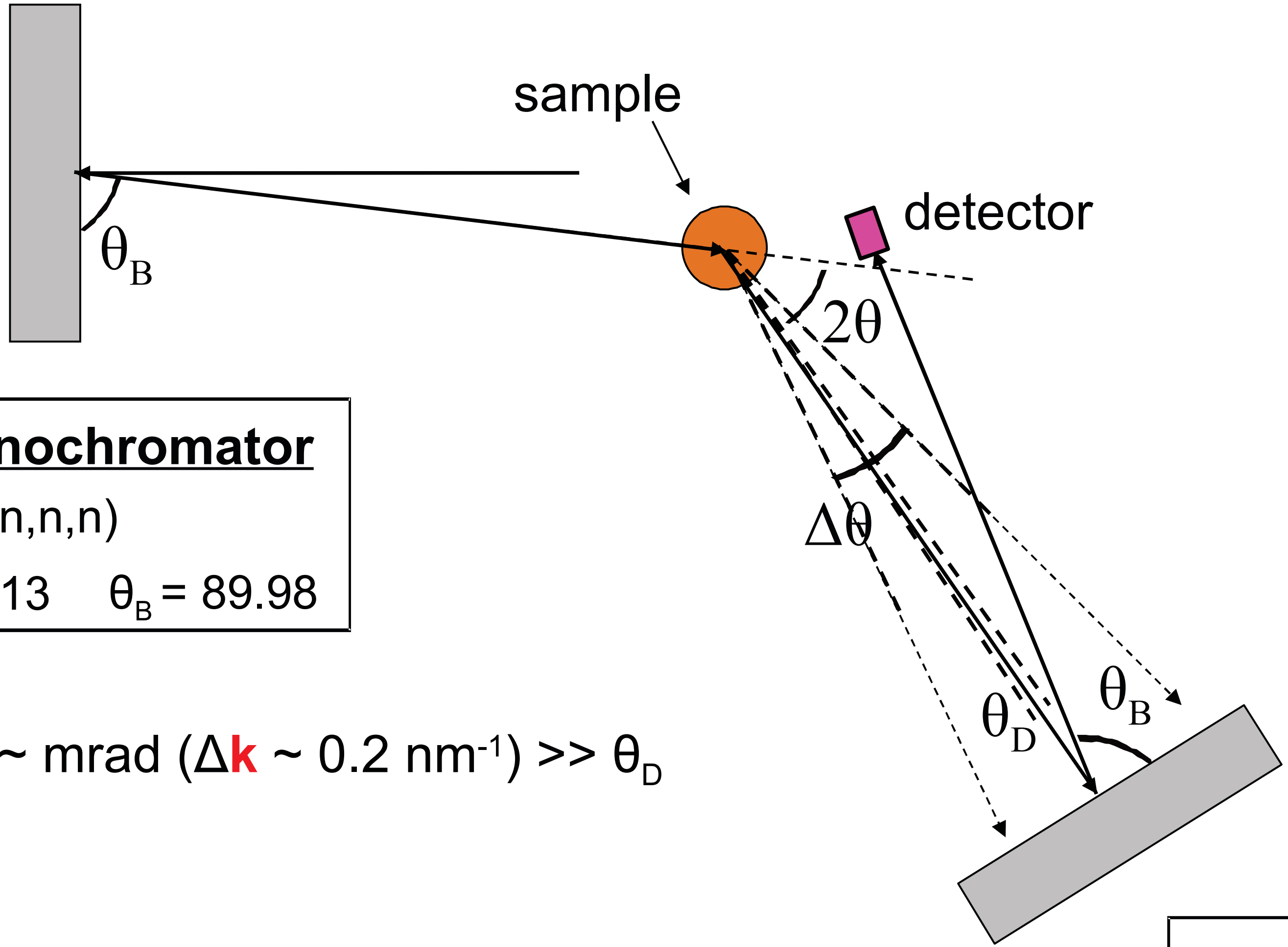

Monochromator

Si(n,n,n)

n=7-13 θ_B = 89.98

$\Delta\theta$ ~ mrad (Δ**k** ~ 0.2 nm^{-1}) >> θ_D

Analyser

Si(n,n,n)

n=7-13 θ_B = 89.98

Basic IXS instrumentation

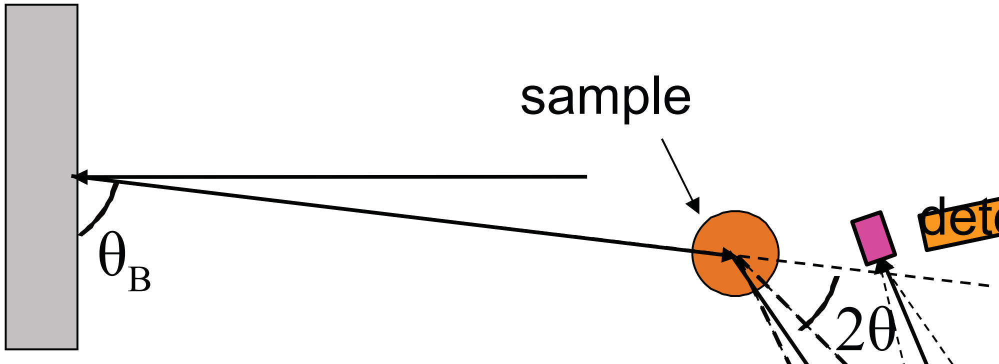

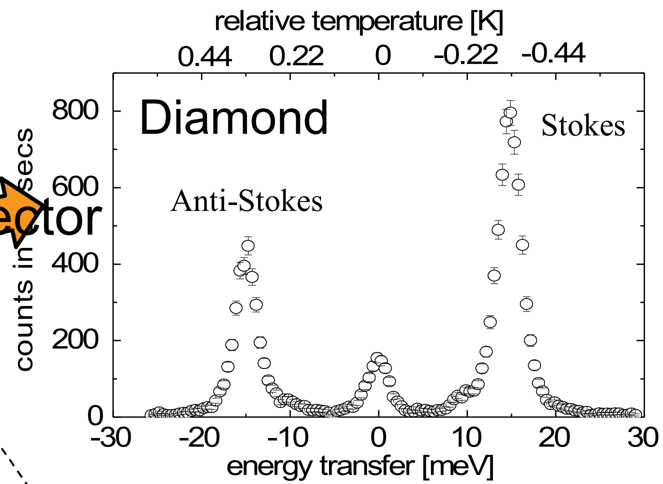

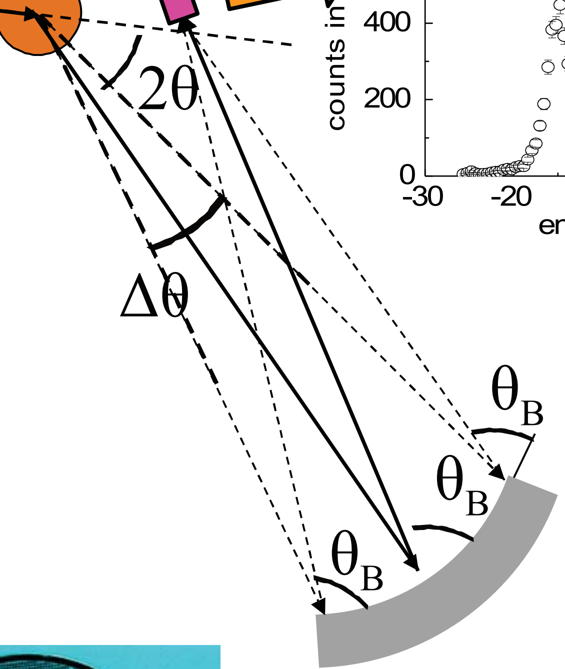

Monochromator

Si(n,n,n)

n=7-13 θ_B = 89.98

$\Delta\theta$ ~ mrad (Δ**k** ~ 0.2 nm^{-1}) >> θ_D

≈ 12000 flat Si "perfect" single crystals (0.6x0.6 mm^2) that approximate a spherical surface

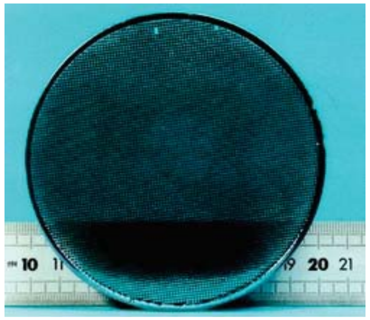

Analyser

Si(n,n,n)

n=7-13 θ_B = 89.98

C. Masciovecchio et al., NIMA 111 (1996)

ID-28 at the ESRF (Grenoble, France)

Spot size: 300 x 120 μm² (H x V) – FWHM (max)
30 x 20 μm² (H x V) – FWHM (min)

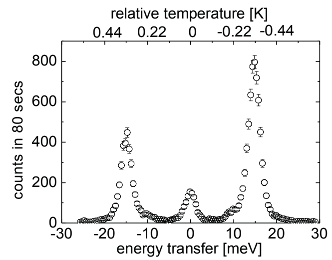

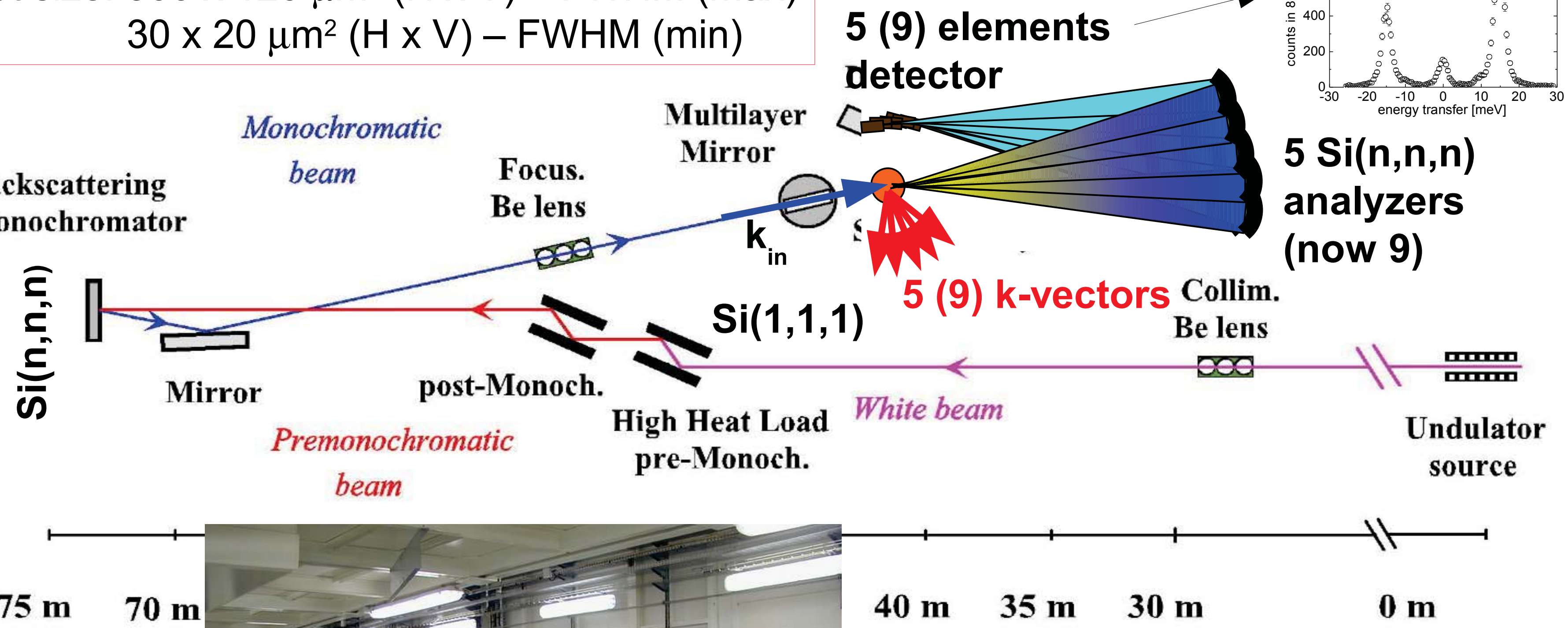

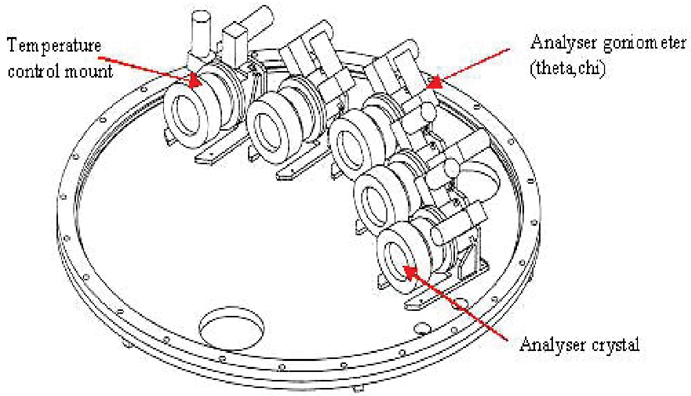

Data Analysis

$$I(k,E)-T*I_{EC}(k,E) = A(k)*f(E,T)*S(k,E) \otimes R(E) + B(k)$$

= known value/function

= measurable function

Empty cell scattering

Sample transmission

Measured IXS signal

Scaling factor

Detailed balance (statistical population of vibrational modes at a given T – accounting for the Stokes to Anti-Stokes intensity ratio)

Model function

Resolution function

Background

No incoherent and multiple scattering corrections

Empty cell scattering often negligible

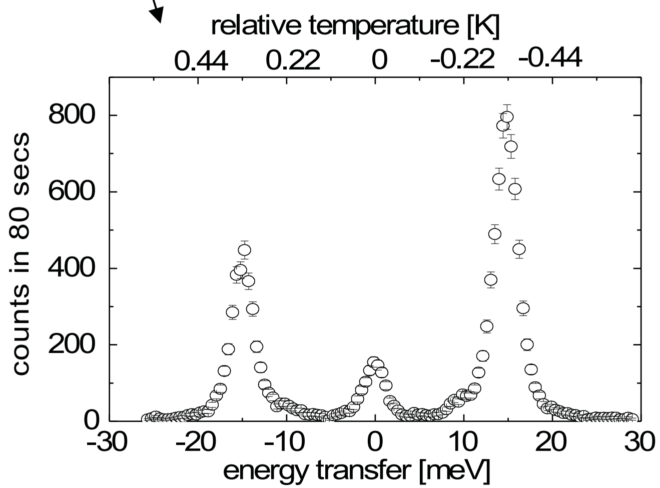

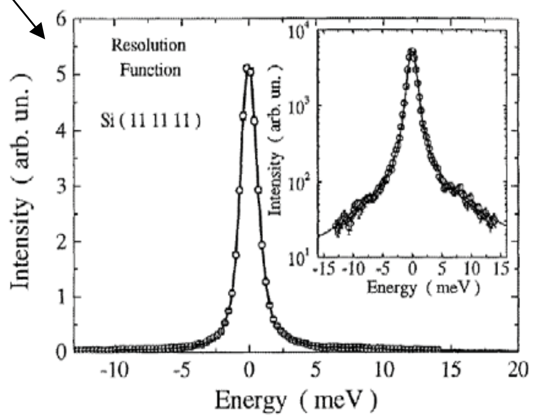

The E-dependence (linashape) of the measured IXS signal can be directly linked to the model S(k,E)

Experimental highlights (1)

Collective dynamics in water (IXS to overcome <u>kinematic constraints</u>)

<u>Inelastic Neutron Scattering (D_2O):</u>

2 experiments, 2 results: <u>why?</u>

<u>A possible interpretation:</u>

- <u>High frequency mode</u> → **D**
- <u>Low frequency mode</u> → **O**

$\Omega_{HF}/\Omega_{LF} \sim (m_O/m_D)^{1/2} \sim 2$

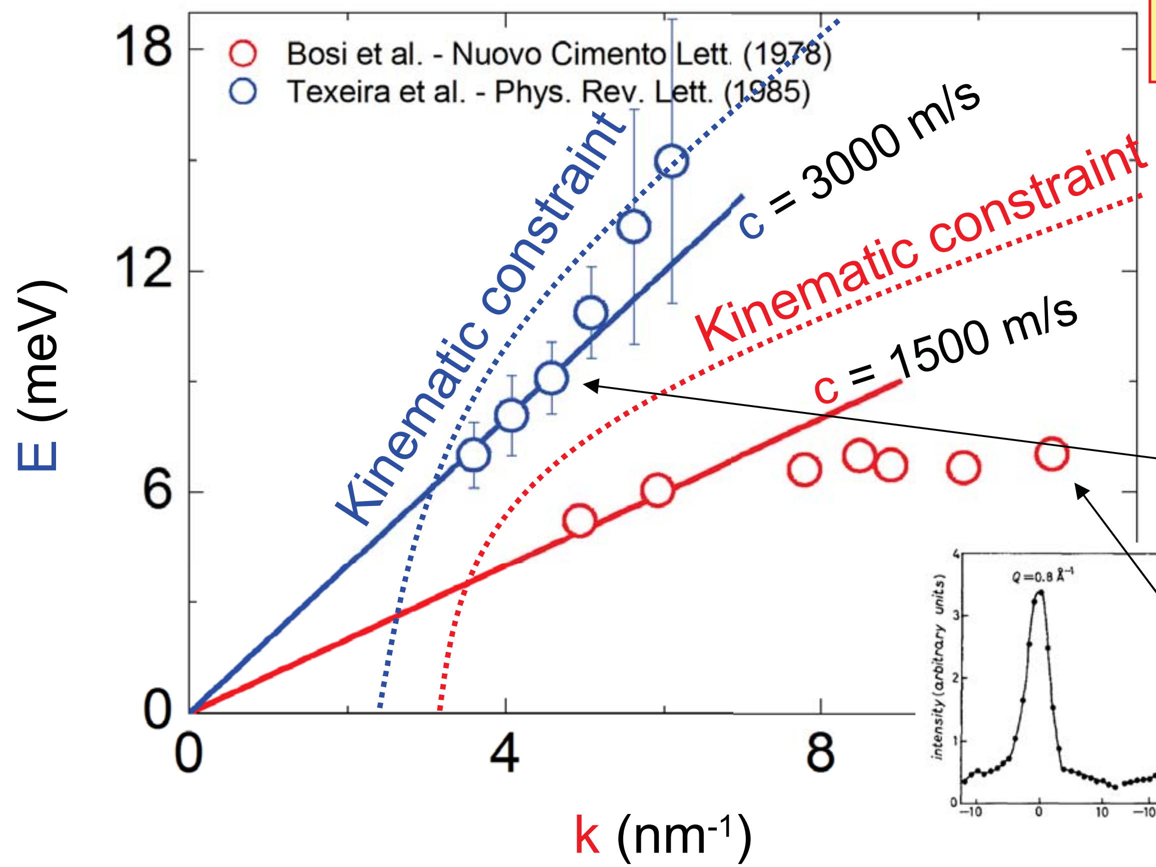

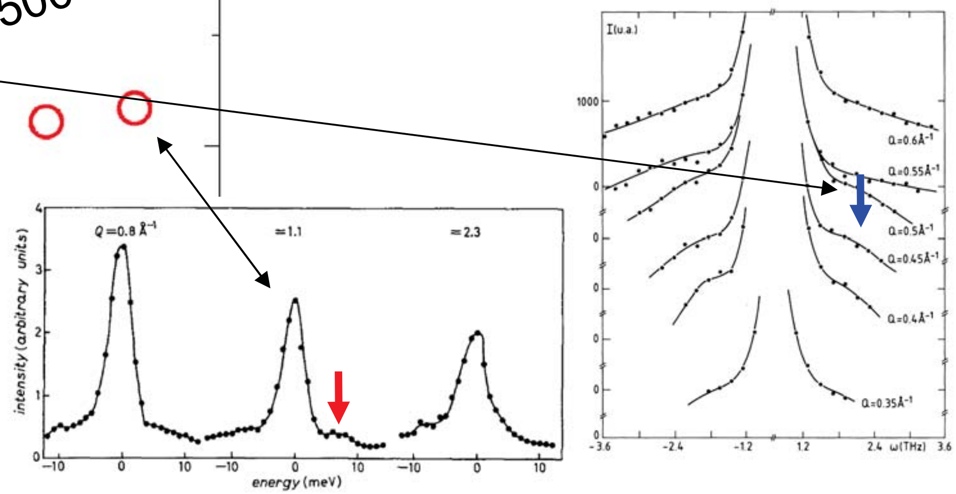

Experimental highlights (1)

Collective dynamics in water

<u>Inelastic Neutron Scattering vs. Inelastic X-ray Scattering (H_2O vs. D_2O)</u>

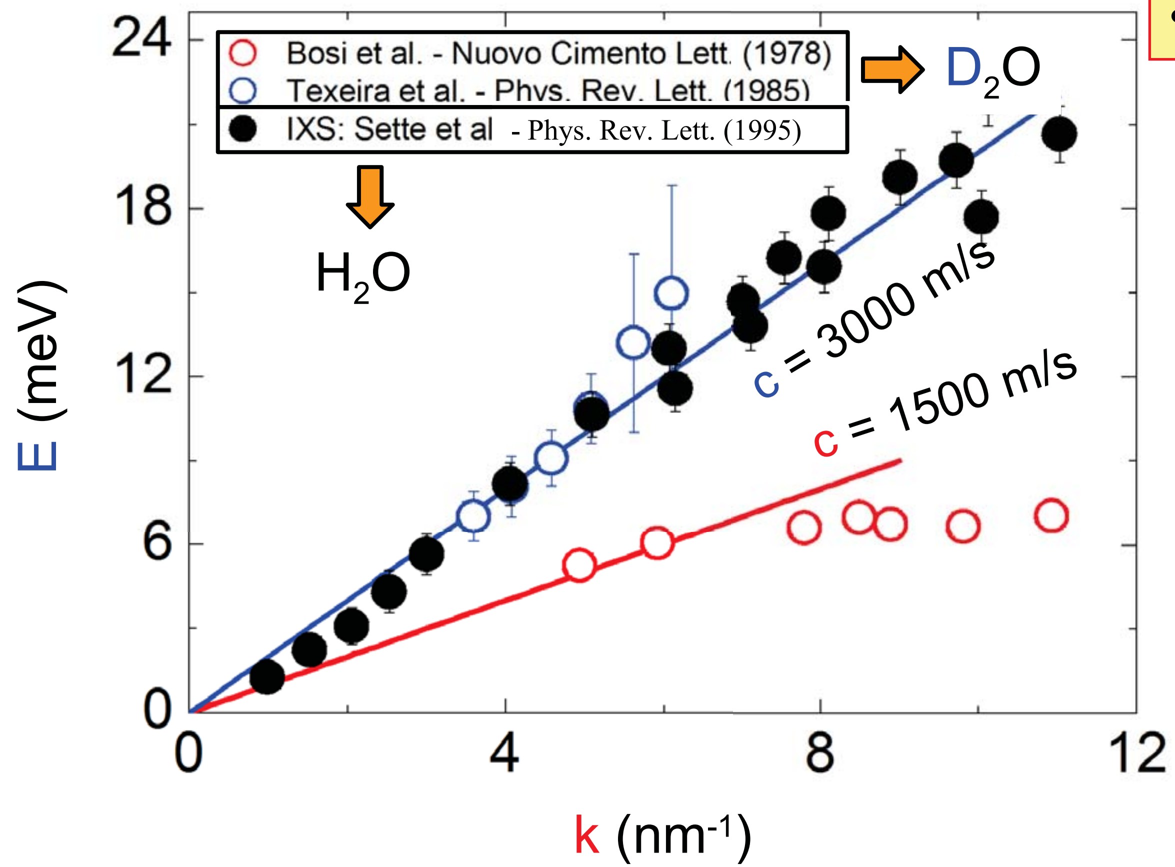

<u>A possible interpretation:</u>

- <u>High frequency mode</u> → **D**
- <u>Low frequency mode</u> → **O**

$\Omega_{HF}/\Omega_{LF} \sim (m_O/m_D)^{1/2} \sim 2$

Data analysis

$$S(k,E) = \frac{A_{qe}}{E^2+\Gamma^2} + \frac{A_{inel}}{(E^2-E_p^{\,2})^2+(E*\Gamma)^2}$$

Lorentian peak (quasi elastic scattering)

Damped harmonic oscillator (inelastic excitations)

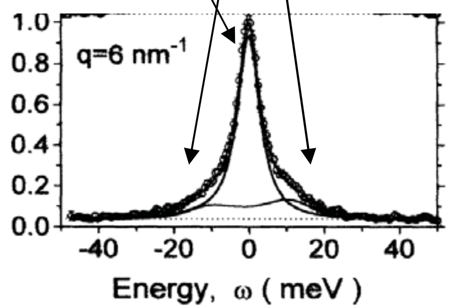

Experimental highlights (1)

Collective dynamics in water

<u>Inelastic Neutron Scattering vs. Inelastic X-ray Scattering (H_2O vs. D_2O)</u>

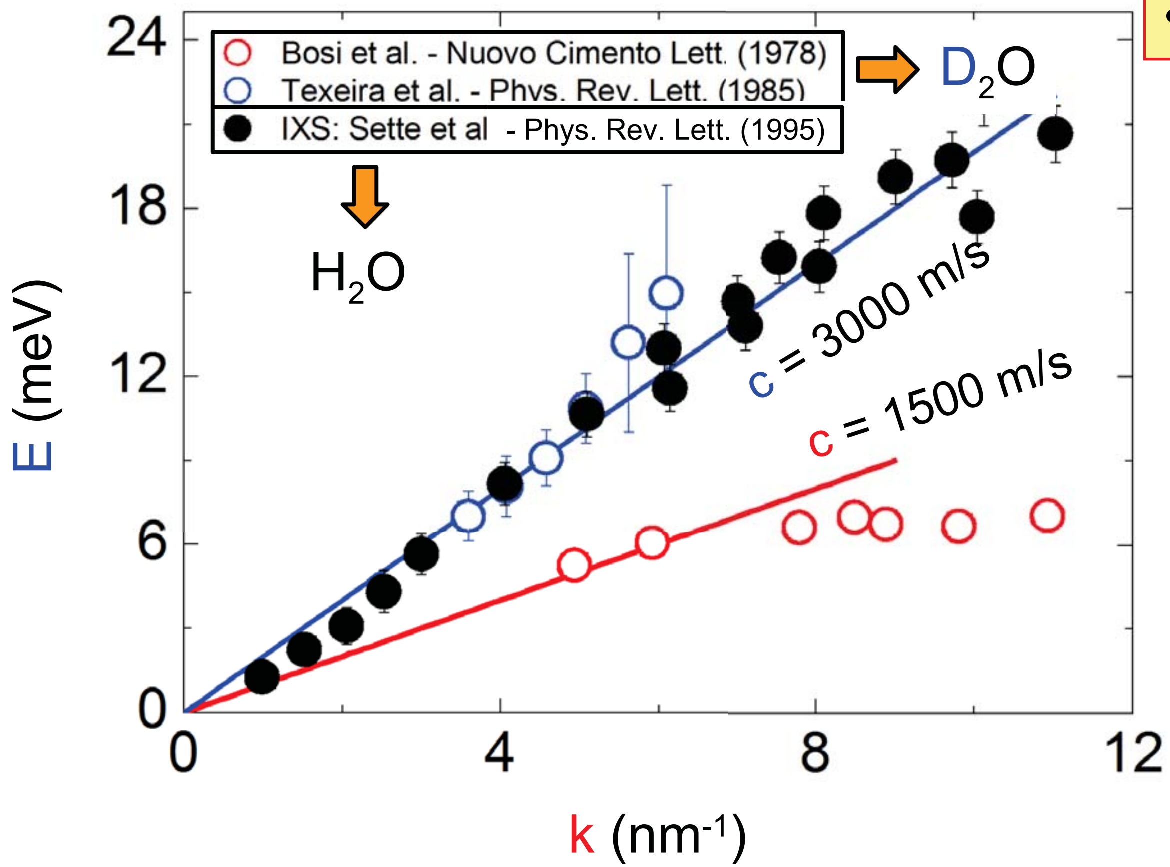

<u>A possible interpretation:</u>

- <u>High frequency mode</u> → **D**
- <u>Low frequency mode</u> → **O**

$\Omega_{HF}/\Omega_{LF} \sim (m_O/m_D)^{1/2} \sim 2$

<u>High frequency mode:</u>

Expected for H_2O…

$\Omega_{IXS}/\Omega_{INS} \sim (m_H/m_D)^{1/2} \sim 1.4$

Experimental highlights (1)

Collective dynamics in water

Inelastic Neutron Scattering vs.
Inelastic X-ray Scattering (H_2O vs. D_2O)

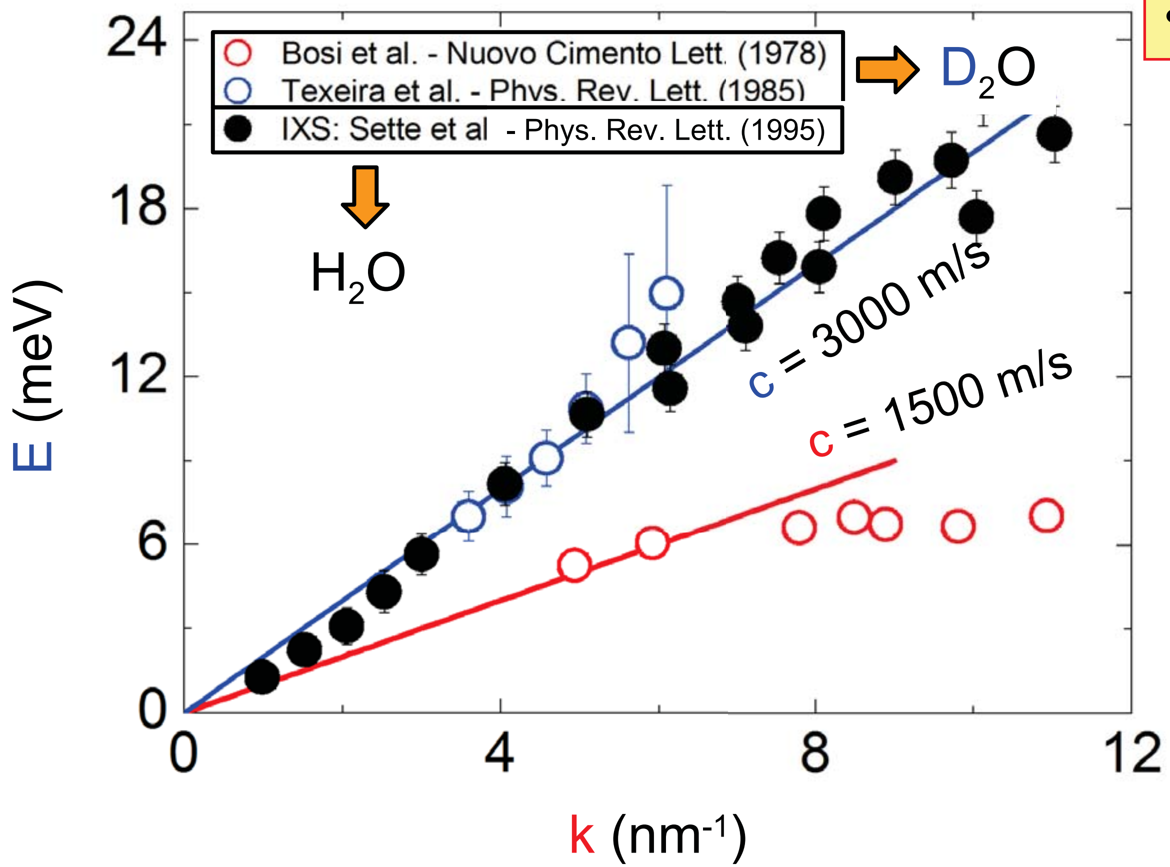

A possible interpretation:

- High frequency mode → **D**
- Low frequency mode → **O**

$\Omega_{HF}/\Omega_{LF} \sim (m_O/m_D)^{1/2} \sim 2$

High frequency mode:

but… $\Omega_{IXS}=\Omega_{INS}$

Experimental highlights (1)

Collective dynamics in water

IXS: no kinematic constraints
→ low-k data can be obtained

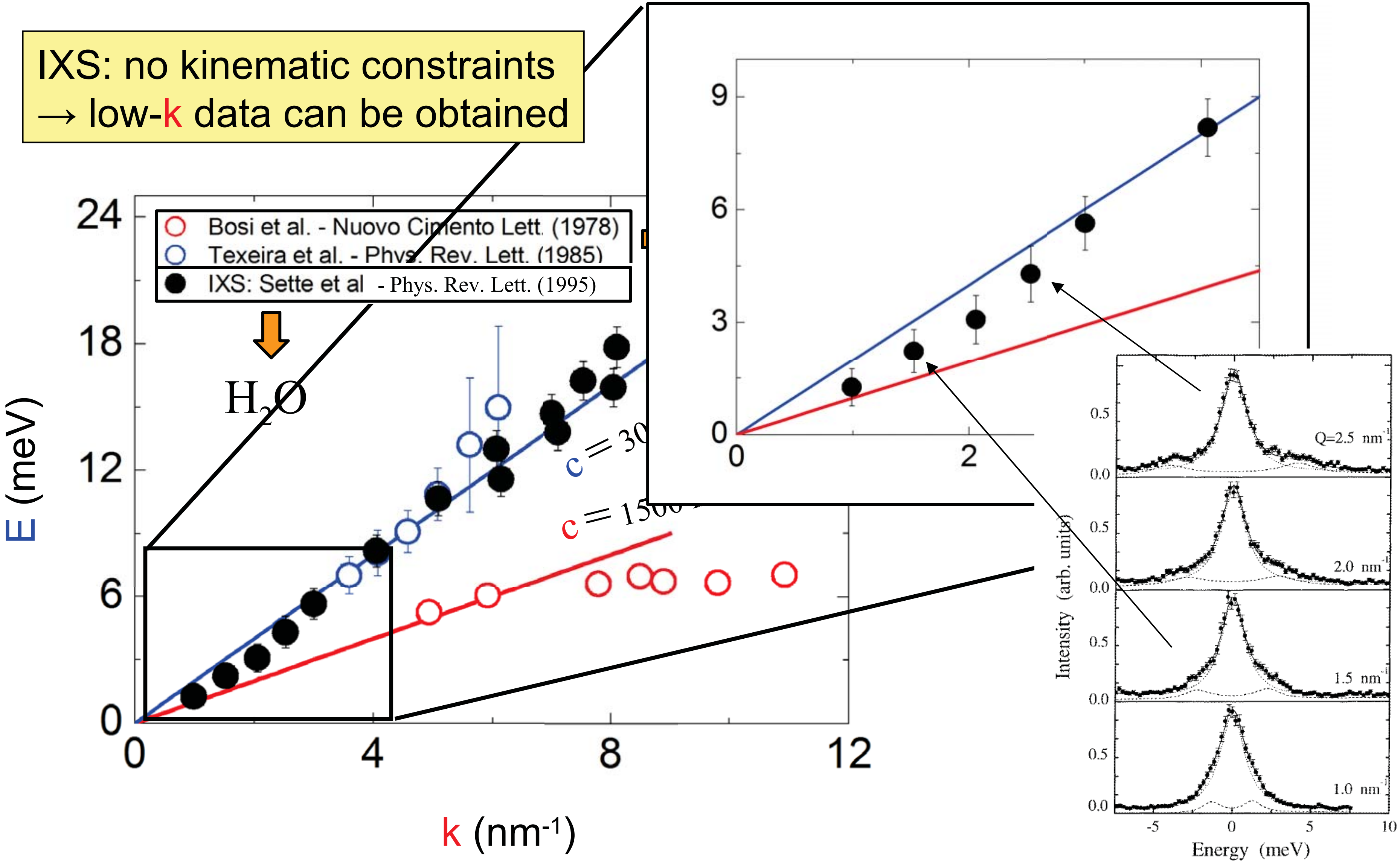

Experimental highlights (1)

Collective dynamics in water (viscoelasticity)

<u>Viscoelasticity:</u>

The sound velocity ($c=E/\hbar k$) is not constant but depends on $E\tau/\hbar$

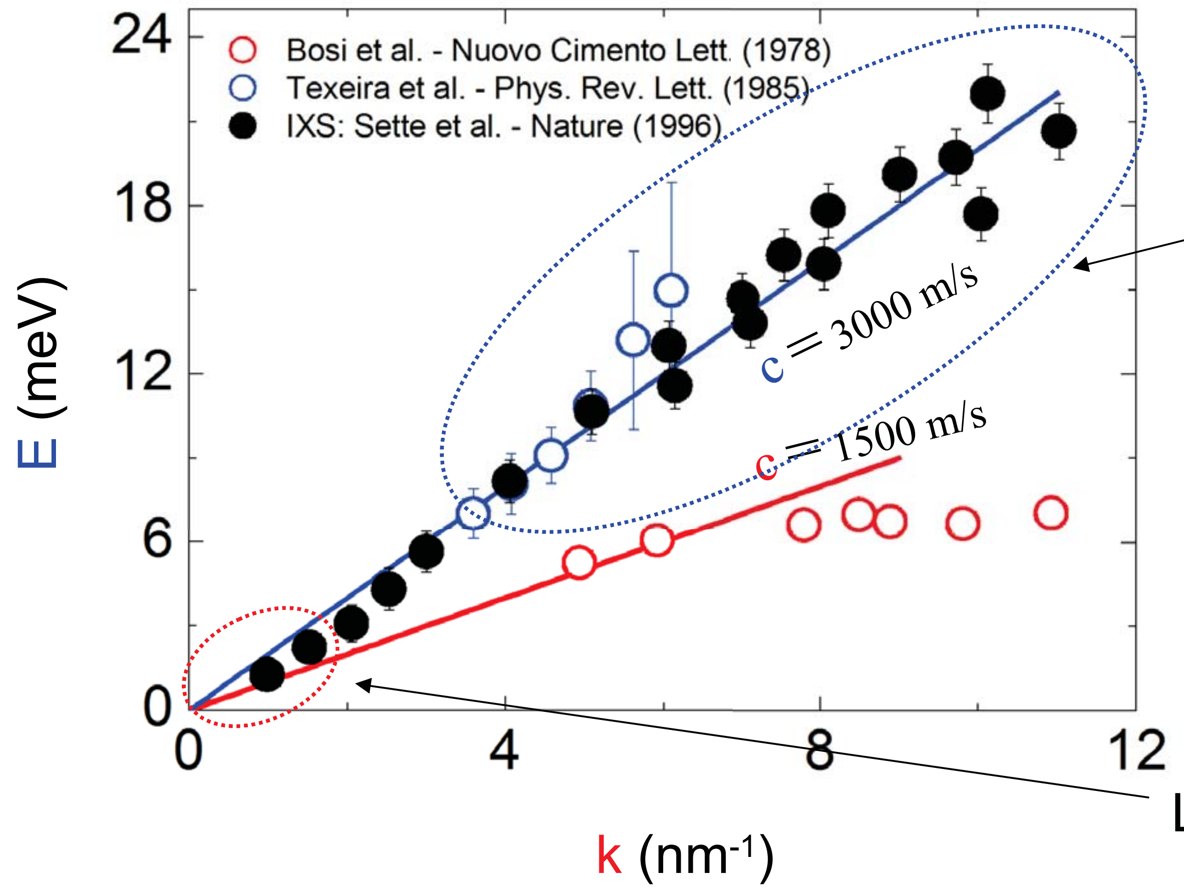

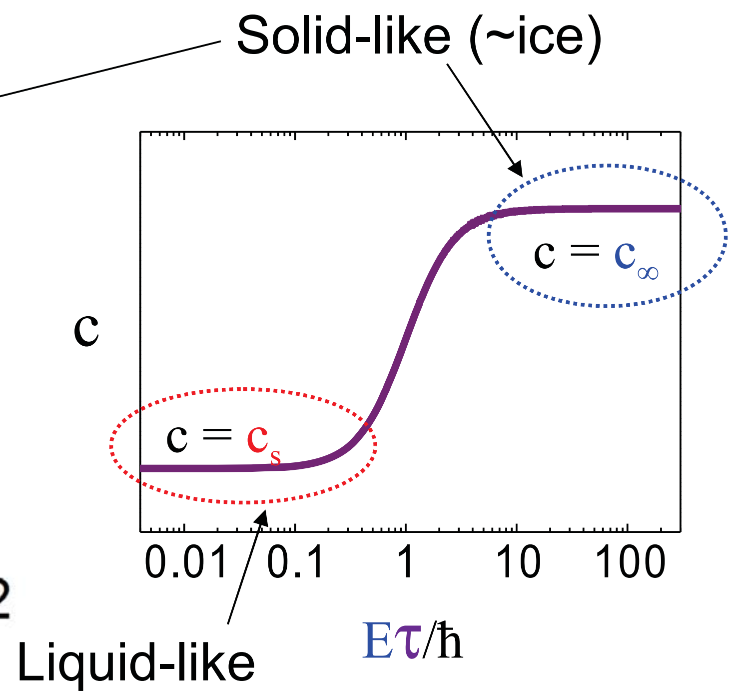

Experimental highlights (1)

Collective dynamics in water (viscoelasticity)

Information we can get from each spectrum:

1) High and low frequency sound velocity (c_{inf} and c_0)[a,b]
2) High/low frequency damping (lifetime) of inelastic excitations[a,b] → Viscosity/anhrmonicity/local disorder
3) Relaxation time[a,b] → hints on the physical processes responsible for the viscoelatic transition
4) Thermal properties (heat diffusion, specific heat)[b]
5) Characteristic energy of inelastic excitations (from the peak energy of the function $J_L(k,E)=E^2S(k,E)$)[a,b]

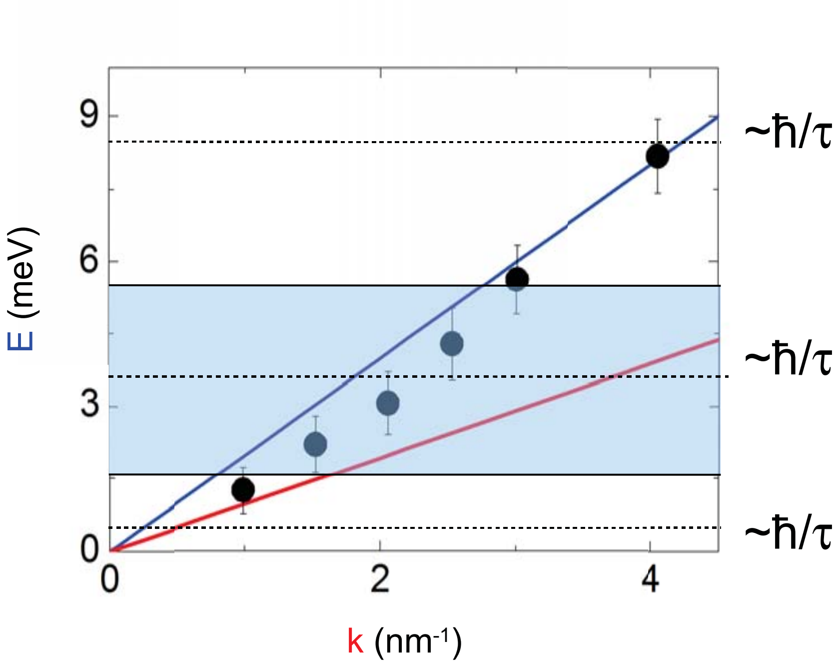

Data analysis

Viscoelastic model function

$$S(k,E) = A_{inel} \frac{E_0^2(k)*m'(k,E)}{[E^2-E_0^2(k)-E*m''(k,E)]^2+[E*m(k,E)]^2}$$

m'(k,E) and m''(k,E) are the real and imaginary part of the FT of memory function, respectively related with viscous and elastic response of the fluid.

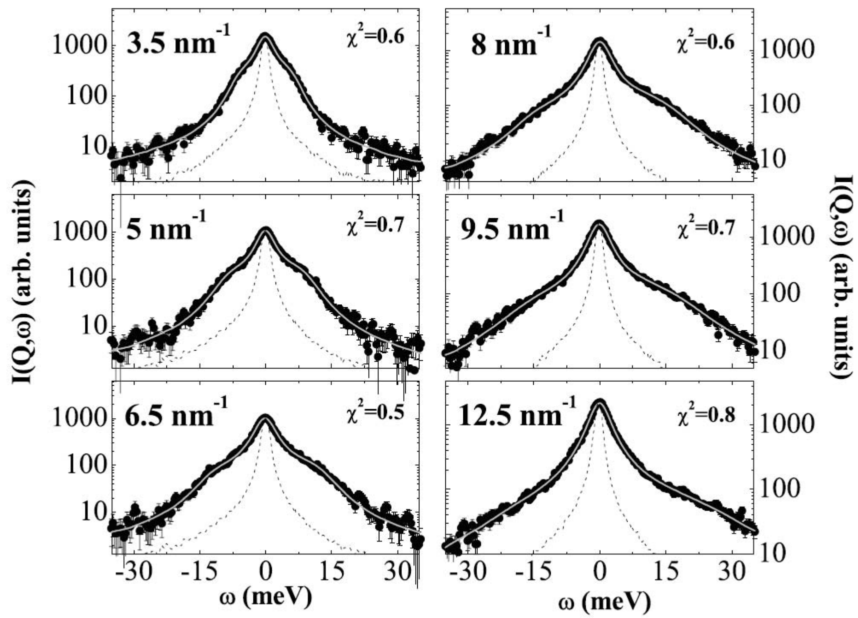

F. Bencivenga et al., PRE 75 (2007)

Experimental highlights (1)

Collective dynamics in water (viscoelasticity)

Information we can get from each spectrum:

1) High and low frequency sound velocity (c_{inf} and c_0)[a,b]
2) High/low frequency damping (lifetime) of inelastic excitations[a,b] → Viscosity/anhrmonicity/local disorder
3) Relaxation time[a,b] → hints on the physical processes responsible for the viscoelatic transition
4) Thermal properties (heat diffusion, specific heat)[b]
5) Characteristic energy of inelastic excitations (from the peak energy of the function $J_L(k,E)=E^2S(k,E)$)[a,b]

c_0 vs (P,T,ρ) = adiabatic sound velocity (classical hydrodynamics)[a,b,c]
c_{inf} ~ sound velocity in glassy/crystalline water (elastic medium)[a,b]

Low frequency damping vs (P,T,ρ) proportional to viscosity (class. hydrod.)[a,b,c]
High frequency damping as in glassy water (elastic medium)[a,b]

Arrhenius temperature dependence (τ=const*exp{E_a/k_BT}) in the liquid phase[a,b,c]; ~ constant in the supercritical phase[b]; "diverging" (vs T) in the supercooled liquid phase (only by IUVS data)[c].

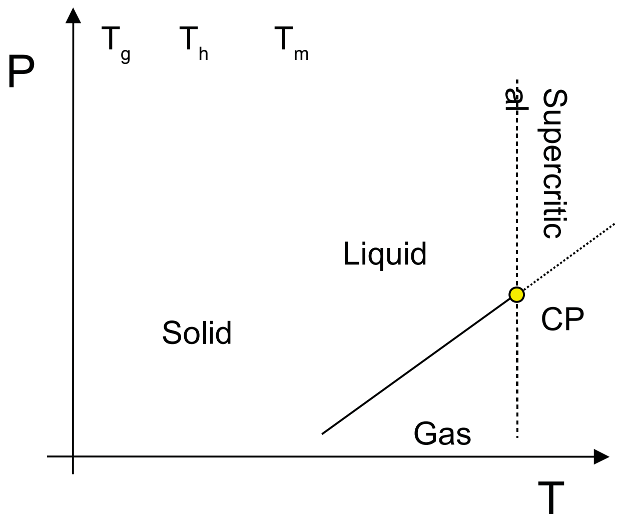

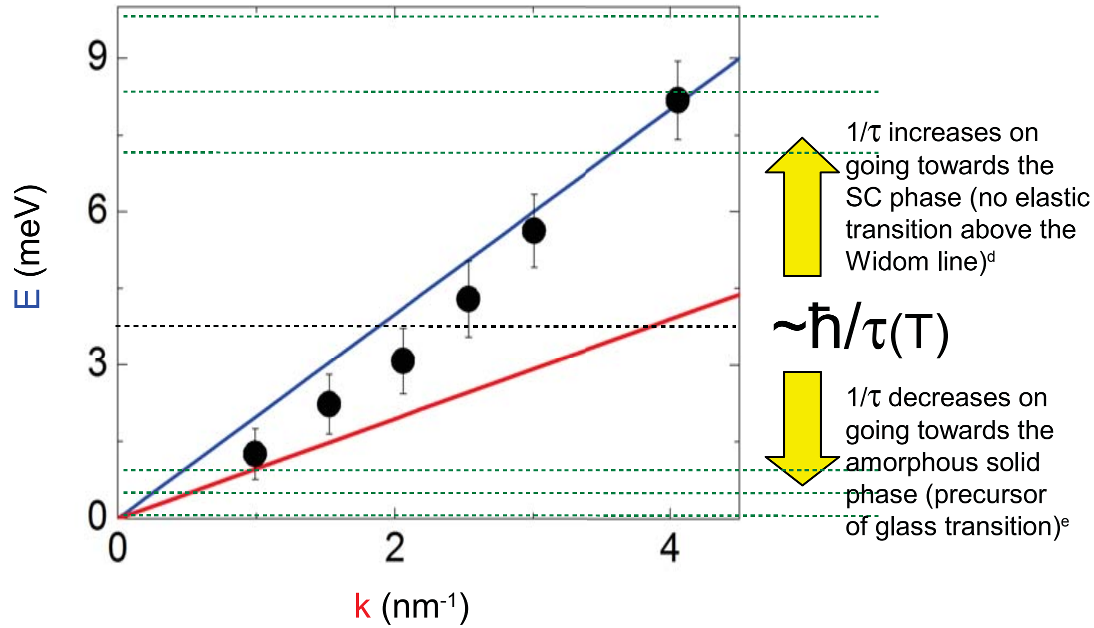

a) G. Monaco et al., PRE 60 (1999) – constant density vs T (liquid)
b) F. Bencivenga et al., PRE 75 (2007) – vs density and T (liquid and SC)
c) C. Masciovecchio et al., PRL 92 (2004) – vs T (IUVS data, supercooled)

d) G.G. Simeoni et al., Nat. Phys. 6 (2010).
e) IXS experiments on various glass formers → F. Sette et al., Nature 280 (1998); T. Scopigno et al., Science 302 (2003)

Experimental highlights (1)

Collective dynamics in water (transverse mode)

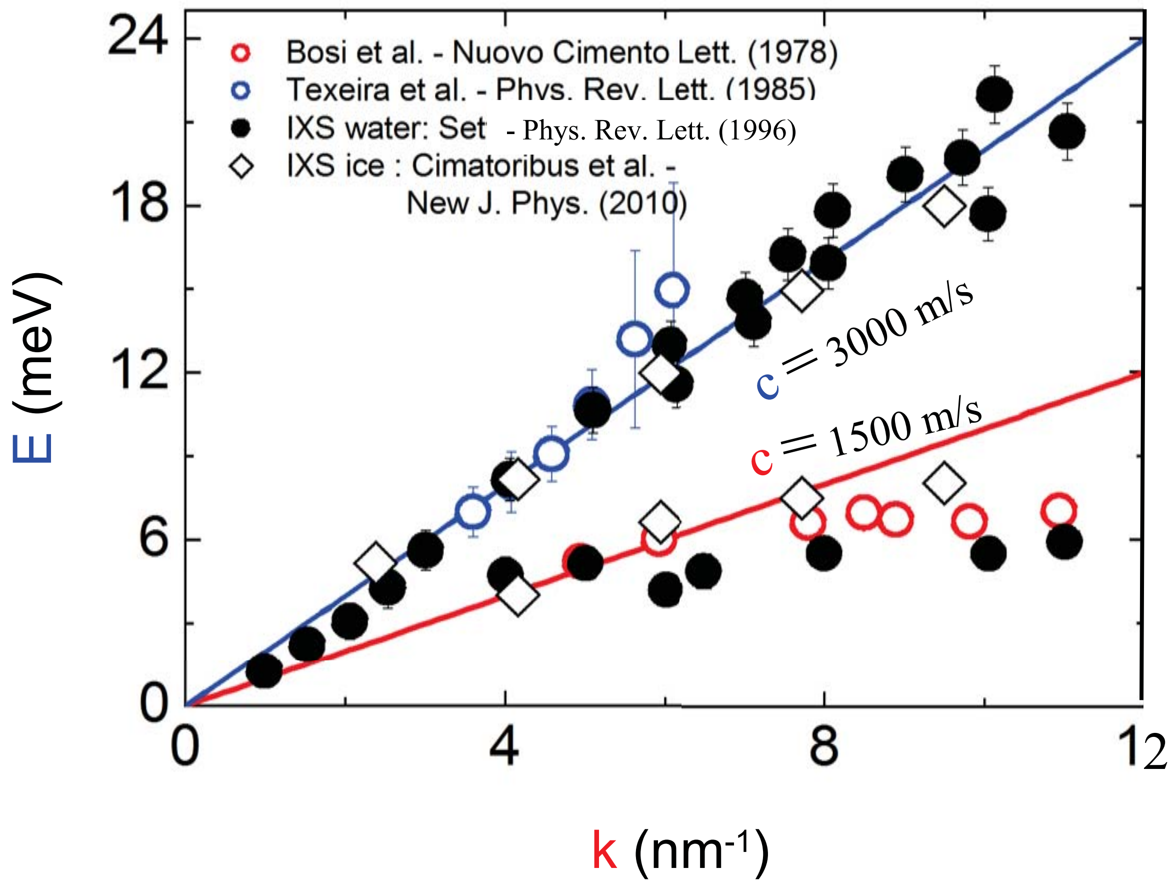

Data analysis

Lorentian peak (quasi elastic scattering) plus two damped harmonic oscillator (DHO) functions (two pairs of inelastic peaks) – **1.5 meV resoultion**

$$S(k,E) = \frac{A_{qe}}{E^2+\Gamma^2} + \frac{A_{HF}}{(E^2-E_{HF}^2)^2+(E*\Gamma_{HF})^2} + \frac{A_{LF}}{(E^2-E_{LF}^2)^2+(E*\Gamma_{LF})^2}$$

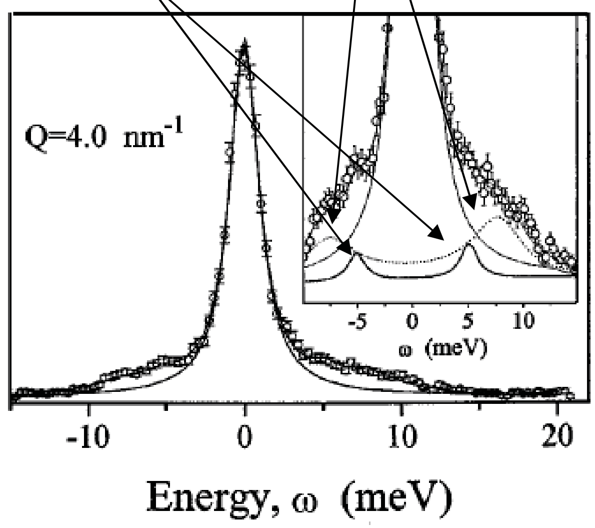

F. Sette et al., PRL 77 (1996)

Experimental highlights (1)

Collective dynamics in water (transverse mode)

Improving experiments and data analysis...

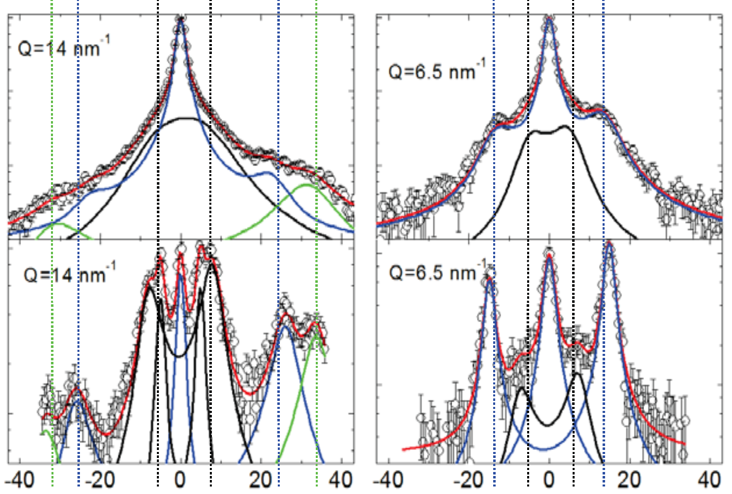

Experiment → High-pressure (3 kbar) and low-T (down to the supercooled liquid phase) for one-to-one comparison with (polycrystalline) ice

Analysis → Viscoelatic model function (quasi elastic and HF peaks) + DHO function (LF peak and the "new" HF peak)

Results → Observed in water a "new" inelastic peak (also present in ice) at frequency higher than those of the "old" HF mode and due to a L-T mixing (in agreement with simulations)

A. Cimatoribus et al., New J. Phys. 12 (2010)

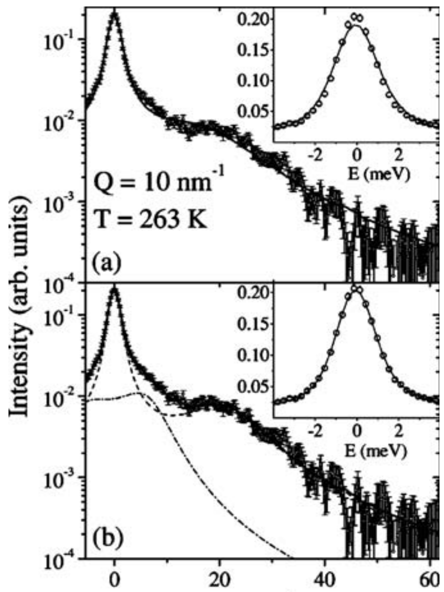

Experiment → High-pressure (3 kbar) vs T

Analysis → Viscoelatic model (HF and quasi elastic peaks) + DHO function (LF peak)

Main result → LF peak shows up in the elastic side of the viscoelastic transition

E. Pontecorvo et al., PRE 71 (2005)

Data analysis

Lorentian peak (quasi elastic scattering) plus two damped harmonic oscillator (DHO) functions (two pairs of inelastic peaks) – **1.5 meV resoultion**

$$S(k,E) = \frac{A_{qe}}{E^2+\Gamma^2} + \frac{A_{HF}}{(E^2-E_{HF}^2)^2+(E*\Gamma_{HF})^2} + \frac{A_{LF}}{(E^2-E_{LF}^2)^2+(E*\Gamma_{LF})^2}$$

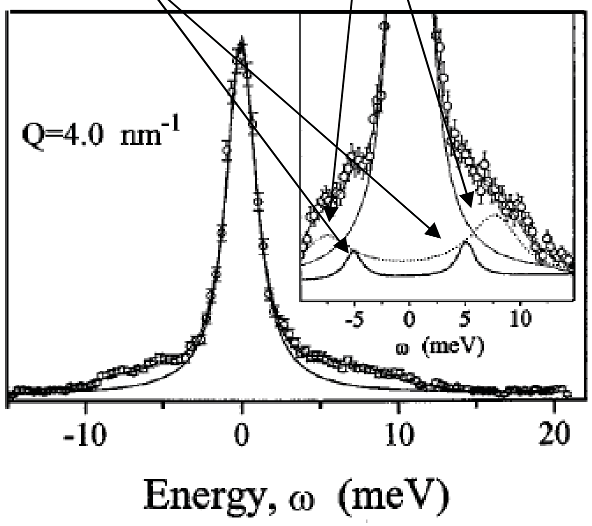

F. Sette et al., PRL 77 (1996)

Experimental highlights (1)

Collective dynamics in water (transverse mode)

Exploiting the complementarity of IXS and INS...

Data analysis

Join (iterative) best fitting of IXS and INS spectra at having the same k; viscoelastic model (quasi elastic and longitudinal) plus a DHO function (transverse).

Water @ room-P and ~ 10 °C

IXS (HERIX @ Argonne National Lab): **1.6 meV** resolution

INS (CNCS @ Oak Ridge National Lab): **0.1 meV** resolution using cold neutrons (E_n=3.7 meV)

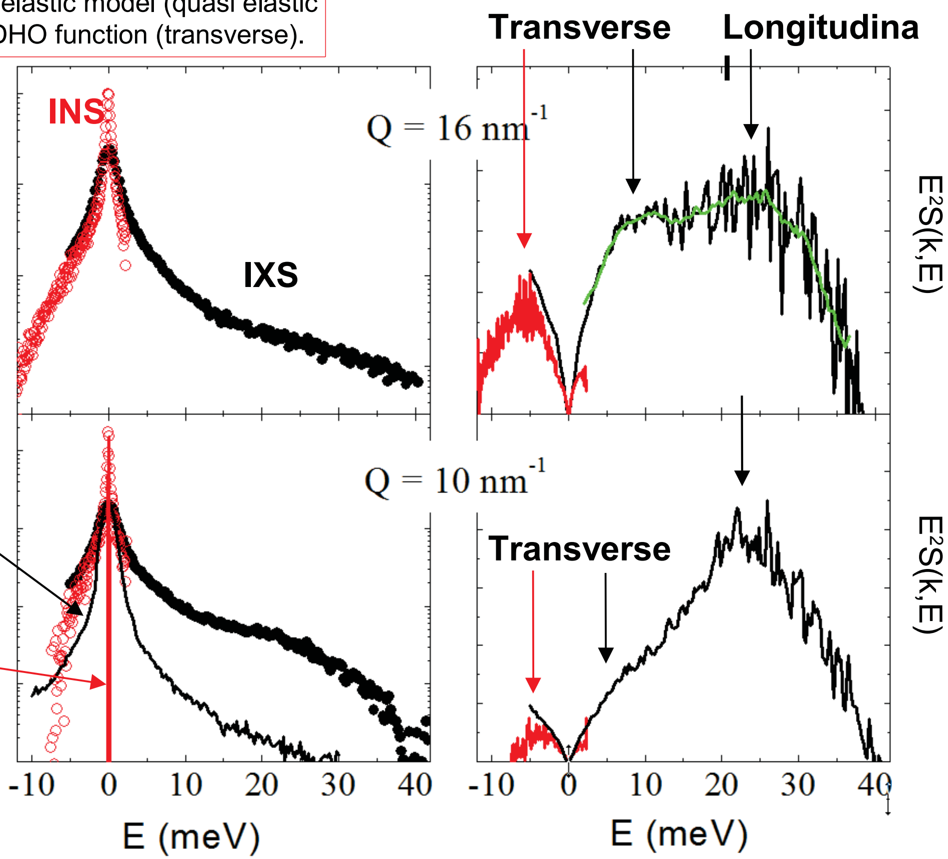

INS spectra

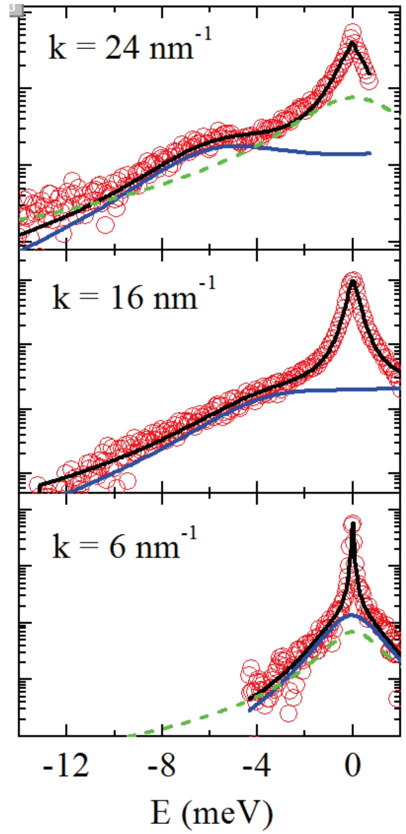

Fit results for the transverse peak

Expected lineshape (Lorentian with FWHM equal to the shear viscosity times k^2), according to classical hydrodynamics

Note

A peak in the $E^2S(k,E)$ lineshape does not necessarily implies a peak (i.e. a propagating inelastic mode) in the corresponding S(k,E)!

A. Cunsolo et al., submitted to PRB

Experimental highlights (1)

Collective dynamics in water (transverse mode)

Exploiting the complementarity of IXS and INS...

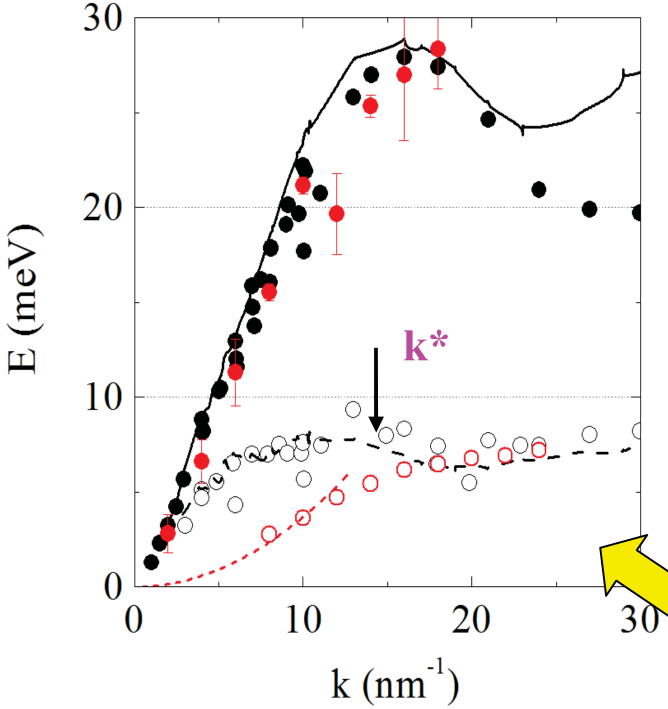

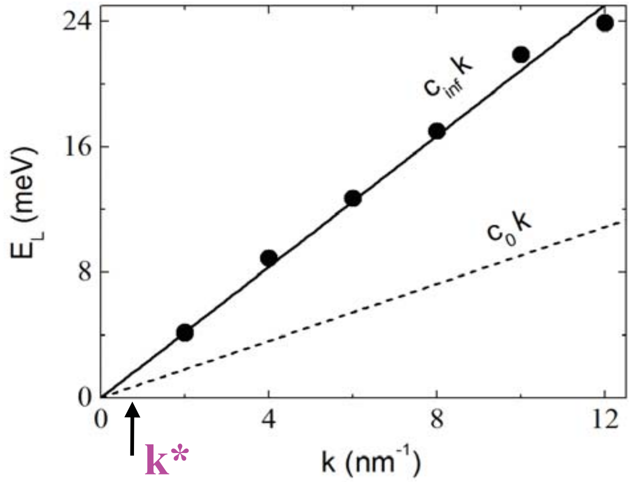

At k > 3 nm^{-1} we are in the “elastic side” of the viscoelastic transition, occurring at some **k***
(belove 3 nm^{-1} in this case)

We observe a diffusive transverse mode (it is **not propagating**). Propagation occurs for k > **k****
(~15 nm^{-1} in this case)

INS spectra

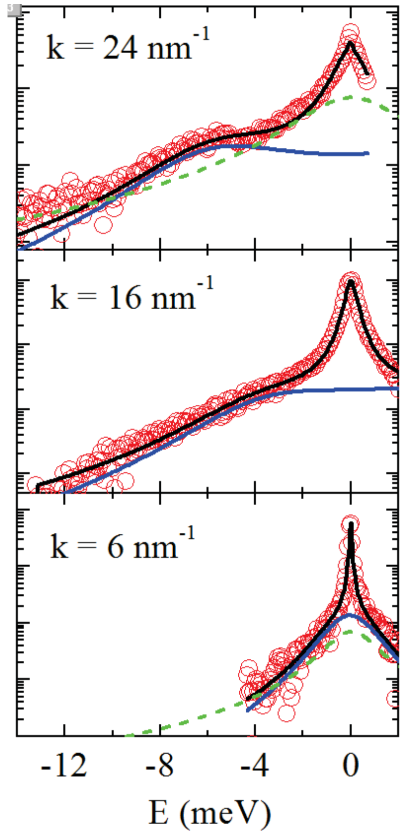

Fit results for the transverse peak

Expected lineshape (Lorentian with FWHM equal to the shear viscosity times k^2), according to classical hydrodynamics

Observability of transverse modes (L-T coupling) and their propagation occurs at different k's, **k*** and **k****. The former is related with the viscoelstic crossover, the latter probably not. A strong P-T dependence of **k**** is expected.

A. Cunsolo et al., submitted to PRB

Experimental highlights (2)

Liquids vs supercritical fluids

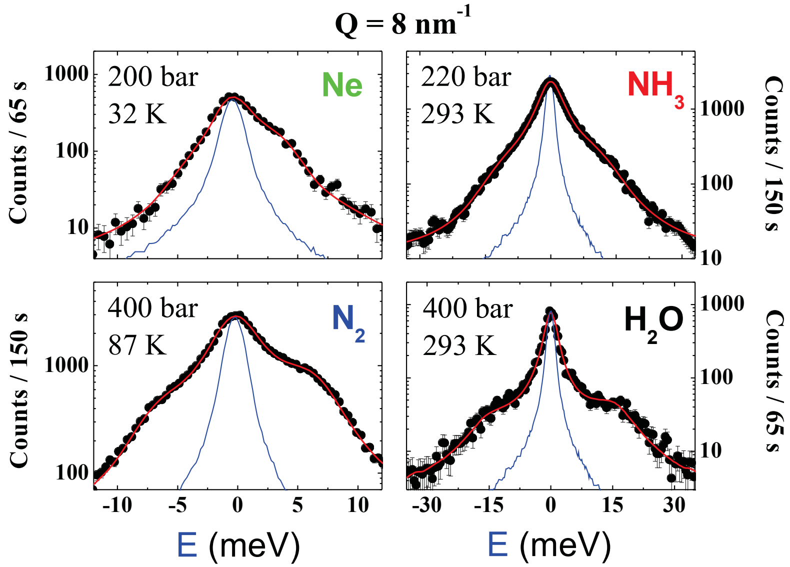

1) Positive sound dispersion in all samples; **<u>"negative" sound dispersion</u>** (c_0 from c_s to c_T – adiabatic to isothermal) in some cases.[a]
2) For **<u>$T > T_c$</u>** relaxation time proportional to mean free time between **<u>collisions</u>**; for **<u>$T < T_c$</u>** relaxation time proportional to exp{E_a/kBT}, where E_a is the energy of intermolecular bonds.[b]

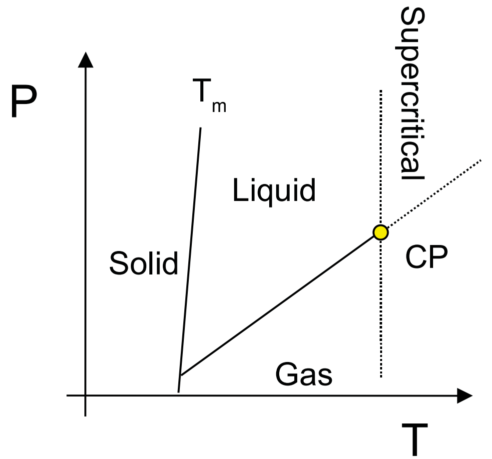

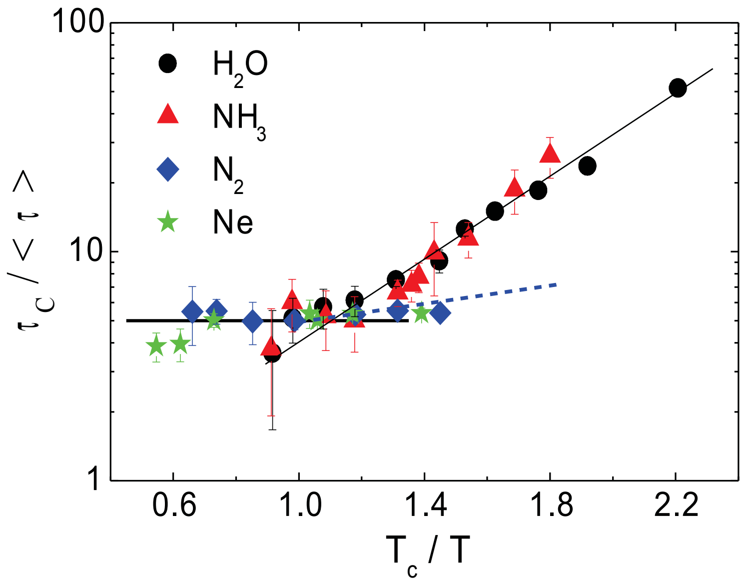

F. Bencivenga et al., JCP 130 (2009)

a) F. Bencivenga et al., Europhys Lett. 75 (2006)
b) F. bencivenga et al., PRL 98 (2007)

Experimental highlights (2)

Liquids vs supercritical fluids

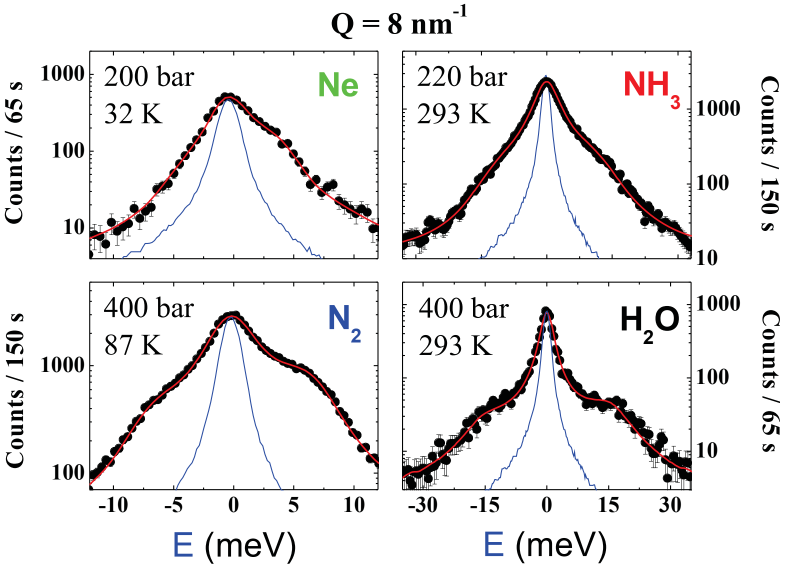

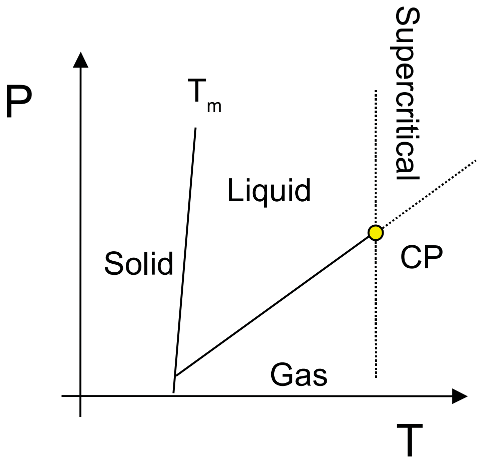

Test of Generalized Collective Modes (GCM) theory:[a]

→ $E_{inel}=c_{hyd}*k + \beta*k^3$; for $k < k_{hyd}$.

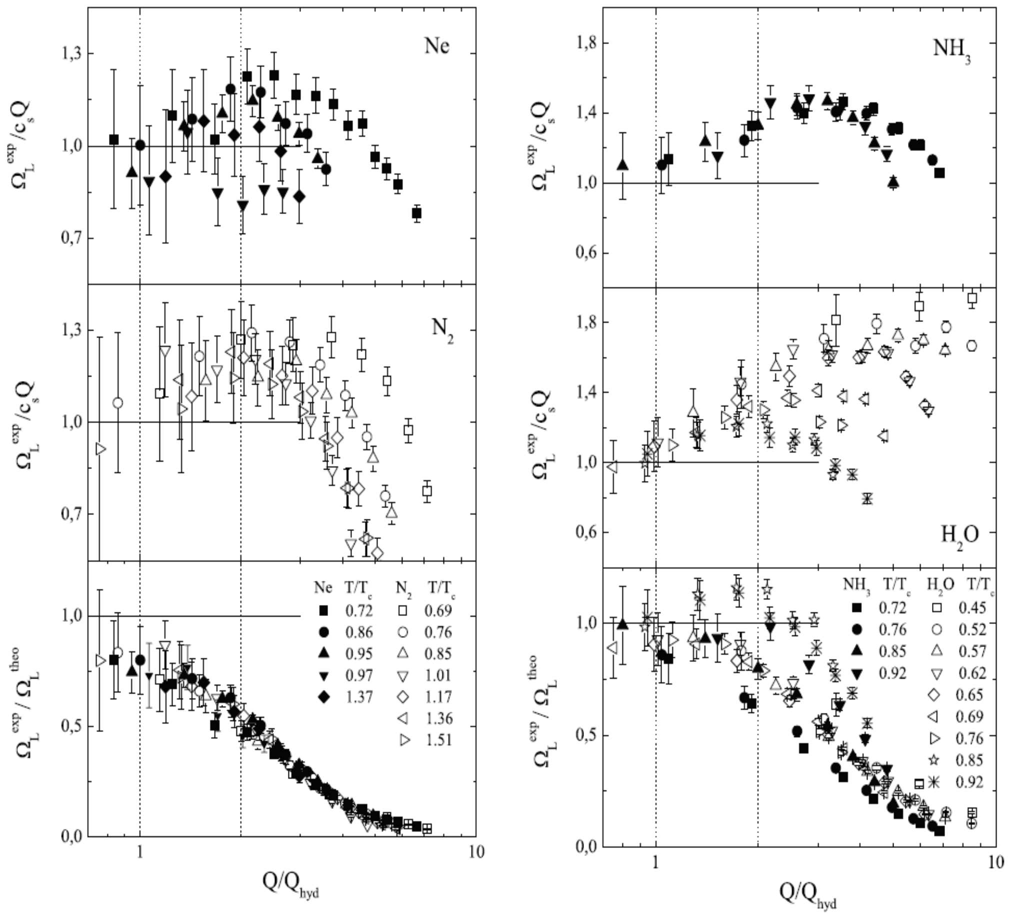

a) T. Bryk et al., JCP 133 (2010)

F. Bencivenga et al., JCP 136 (2012)

Experimental highlights (3)

Experimental test of Sachs-Teller theory[a]

Liquid I_2 (T=388 K);

k = 25 – 150 nm^{-1} ($\gg$ $k^* \sim 7.5\ nm^{-1}$);

ΔE = 3 meV

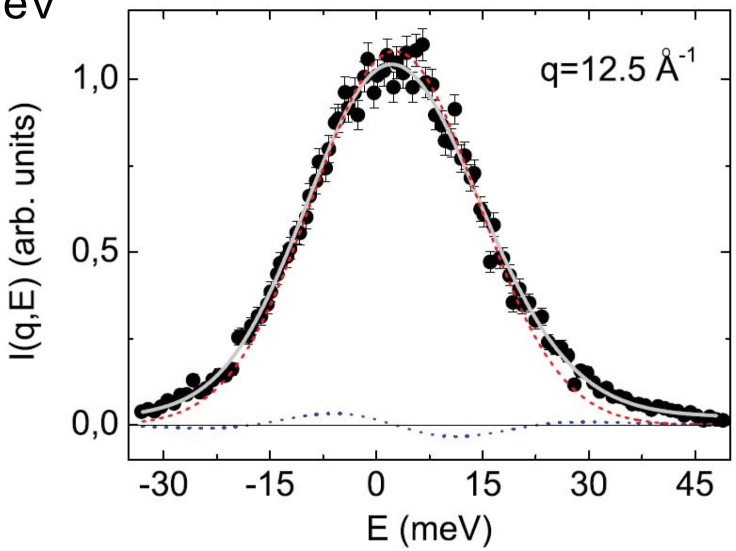

$$S_{IA}(k,E) = (const/\mu_2)*\exp\{-(E-E_R)^2/2\mu_2\}$$
$$*[1-(\mu_3/2\mu_2^2)*(E-E_R)*(1-(E-E_R)^2/3\mu_2)]$$

$E_R=\hbar^2k^2/2M_{ST}$; $\mu_2=(\hbar^2k^2/M_{ST}^2)*\langle p_k^2\rangle$;

$\mu_3=(\hbar^4k^2/6M_{ST}^2)*\langle\nabla U(r)\rangle$

$M \rightarrow M_{ST}$

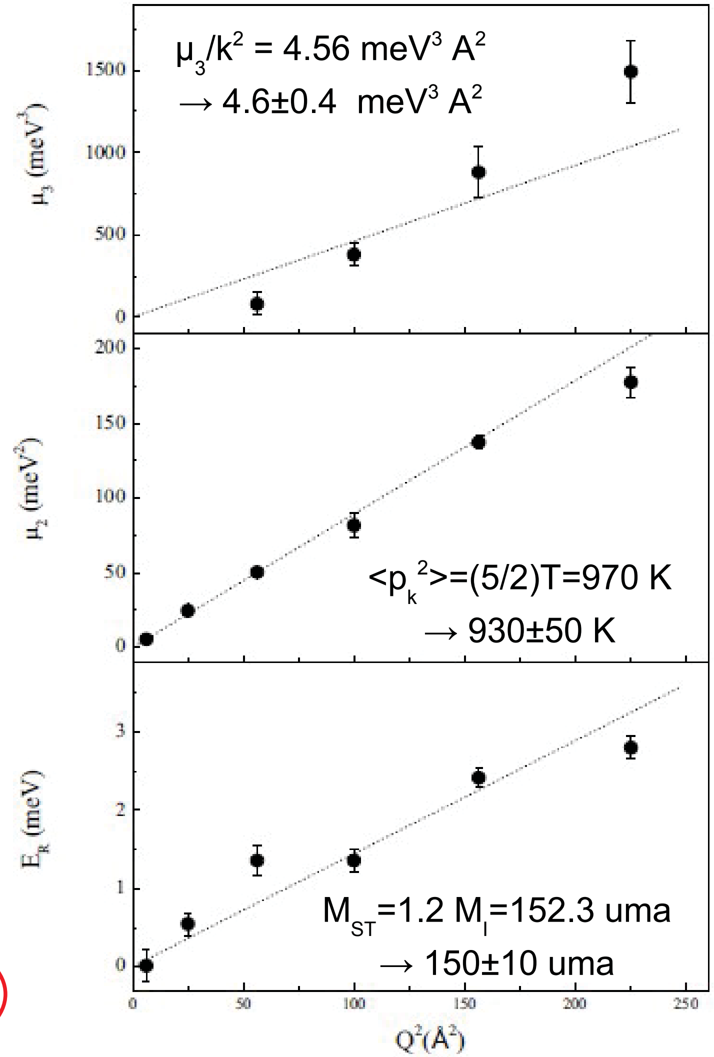

M.G. Izzo et al., JCP 133 (2010)

a) R.G. Sachs et al., Phys. Rev. 60 (1941)

Experimental highlights (4)

(sub)surface sensitivity of IXS

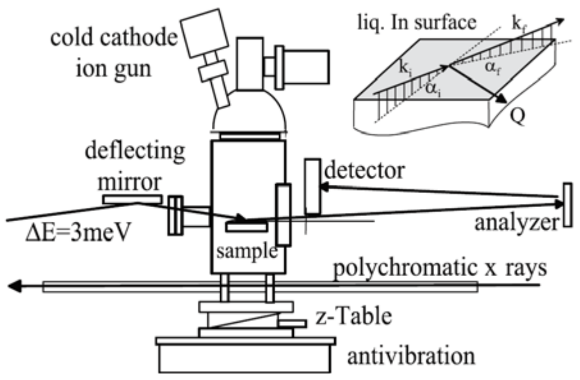

Surface (IXS in "reflection")

X-ray incidence below the critical angle (0.16°, <u>penetration depth</u> ~4.6 nm)

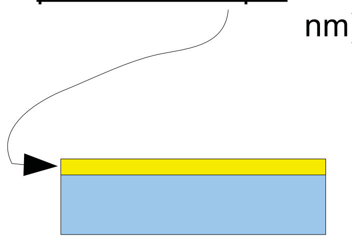

Diamond windows

Bulk

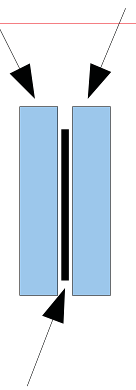

Sample (Indium – optimal thickness ~ 50 μm)

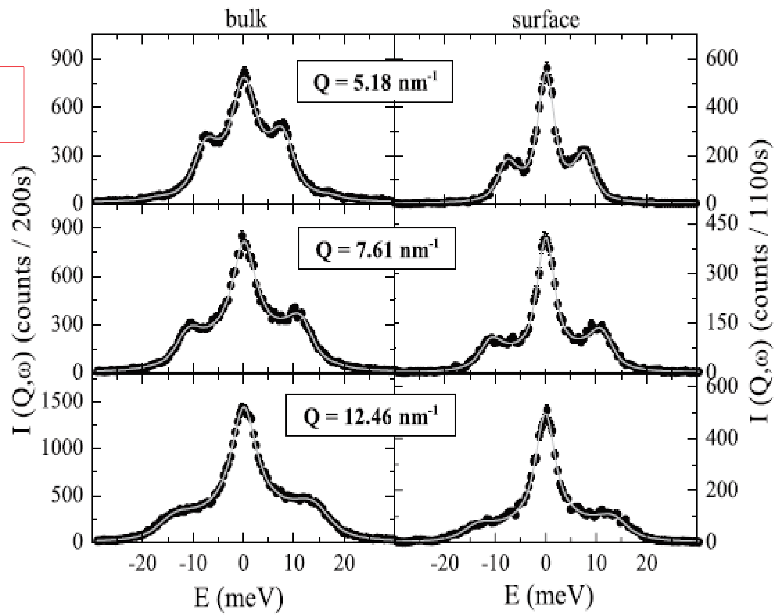

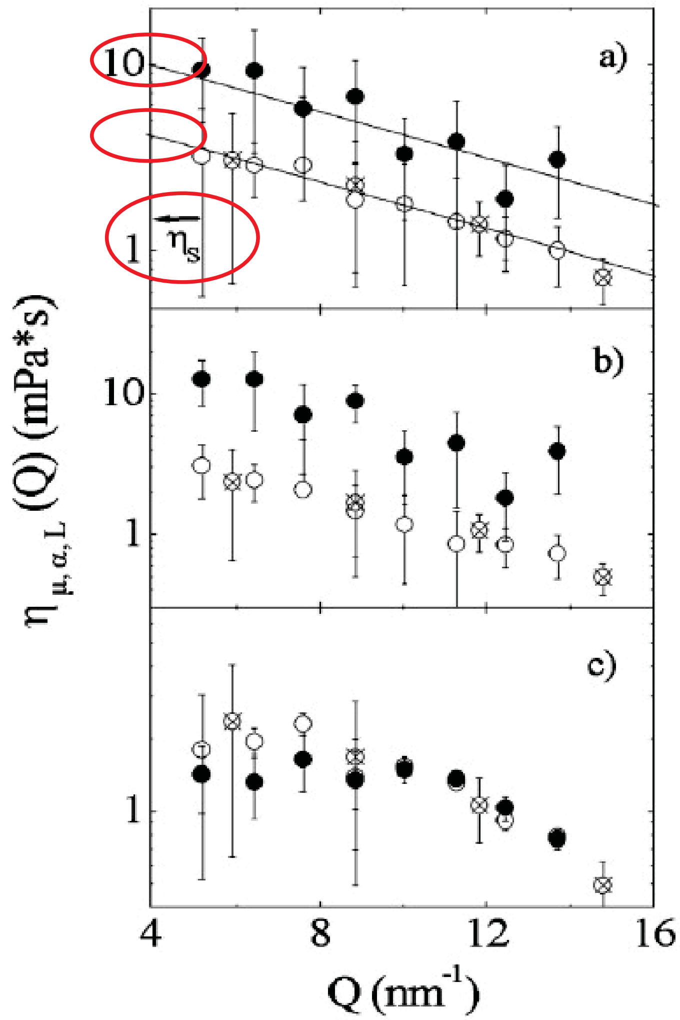

"Sub-surface viscosity increases by a factor 3 with respect to the bulk

H. Reichert et al., PRL 98 (2007)

Experimental highlights (5)

Phonon dispersions in Plutonium: conventional IXS experiment" on a "non-conventional" sample (IXS used for the <u>tight focusing</u>)

<u>Plutonium is one of the most fascinating and exotic element:</u>

- Multitude of unusual properties
  - Central role of 5f electrons

<u>ID28 at ESRF</u>

- Beam size: 20 x 60 μm² (HxV)
- Grain size: ~ 80 μm²
- On-line diffraction analysis

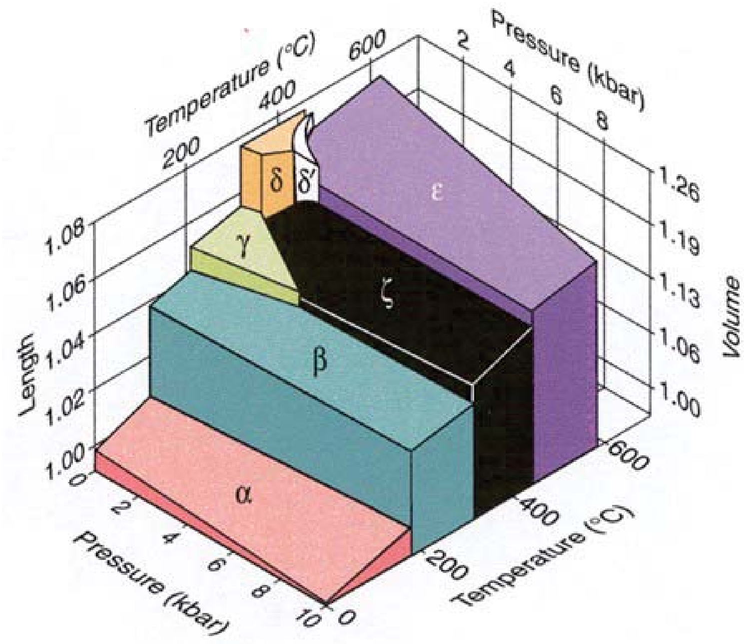

J. Wong et al., Science 301 (2003)

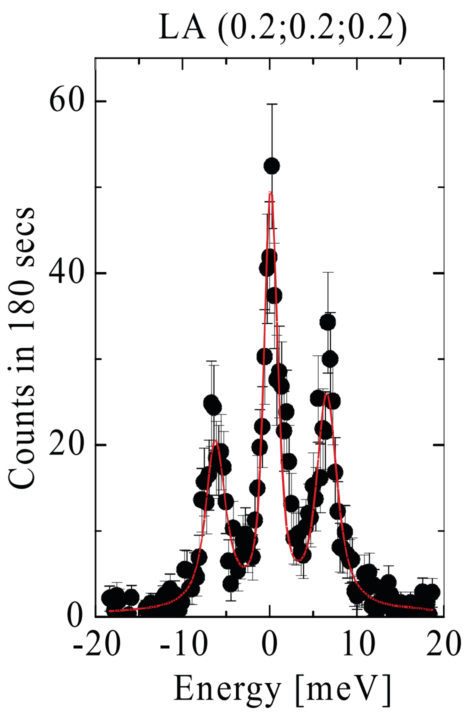

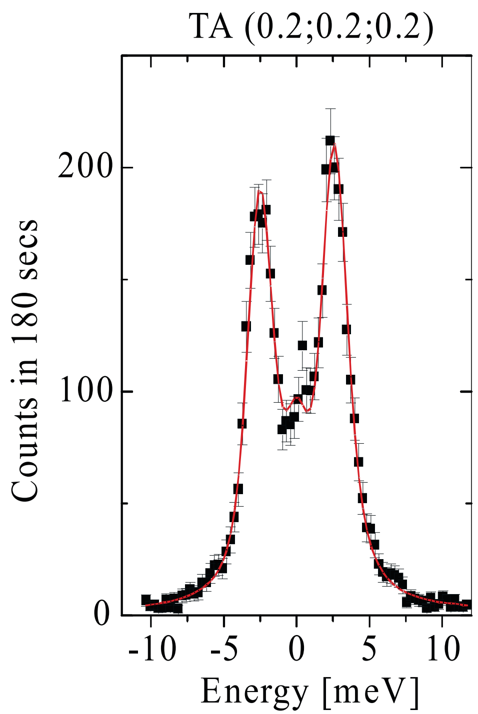

Experimental highlights (5)

Phonon dispersions in plutonium

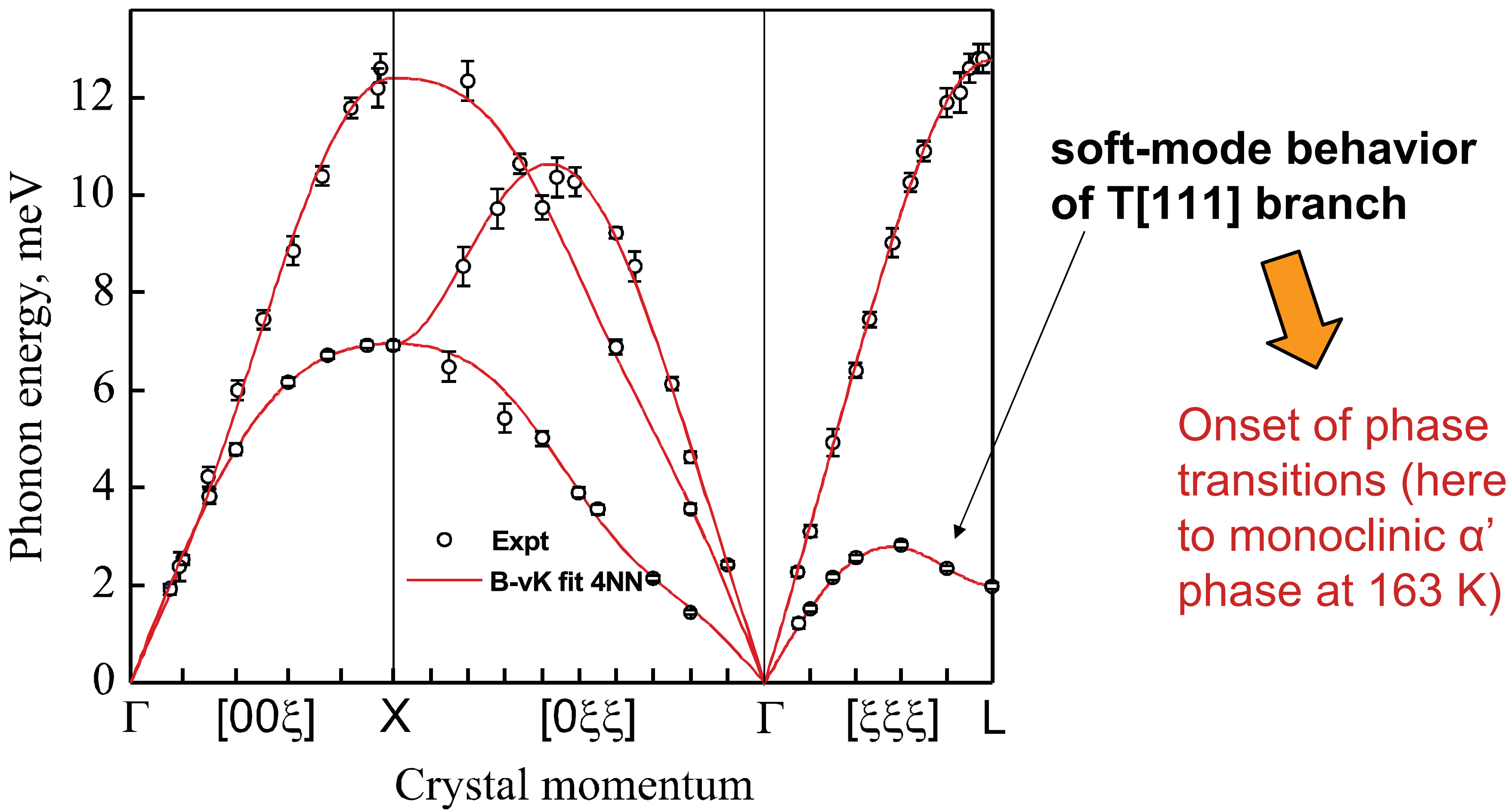

• **Born-von Karman force constant model fit** (fourth nearest neighbors)

J. Wong et al., Science 301 (2003)

Experimental highlights (5)

Phonon dispersions in plutonium

Close to Γ-point: E = **V**q/ħ

$\mathbf{V}_L[100] = (C_{11}/\rho)^{1/2}$

$\mathbf{V}_T[100] = (C_{44}/\rho)^{1/2}$

$\mathbf{V}_L[110] = ([C_{11}+C_{12}+2C_{44}]/\rho)^{1/2}$

$\mathbf{V}_{T1}[110] = ([C_{11} - C_{12}] /2\rho)^{1/2}$

$\mathbf{V}_{T2}[110] = (C_{44}/\rho)^{1/2}$

$\mathbf{V}_L[111] = [C_{11}+2C_{12}+4C_{44}]/3\rho)^{1/2}$

$\mathbf{V}_T[111] = ([C_{11}-C_{12}+C_{44}]/3\rho)^{1/2}$

C_{11} = 35.3±1.4 GPa

C_{12} = 25.5±1.5 GPa

C_{44} = 30.5±1.1 GPa

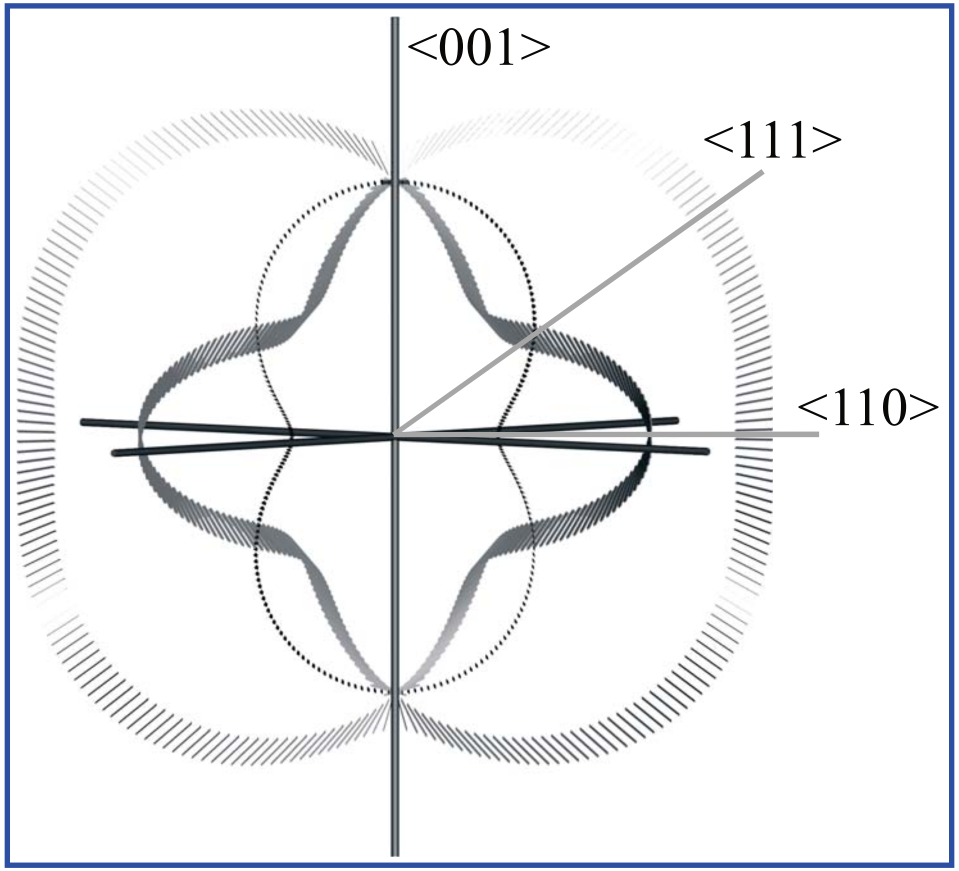

highest elastic anisotropy of all known fcc metals

J. Wong et al., Science 301 (2003)

Experimental highlights (5)

Phonon dispersions in plutonium

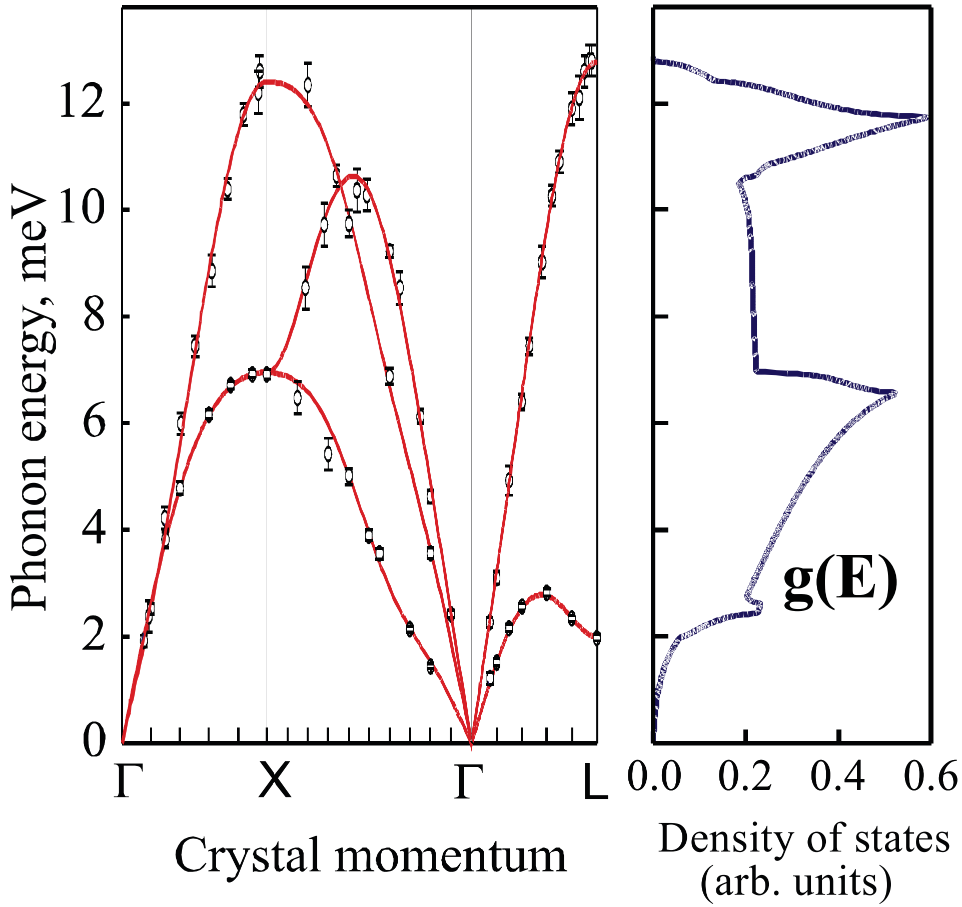

• **Born-von Karman fit**

Specific heat:

$$C_v = 3Nk_B \int_0^{E_{\max}} \left(\frac{E}{k_BT}\right)^2 \frac{\exp(E/k_BT)g(E)dE}{(\exp(E/k_BT)-1)^2}$$

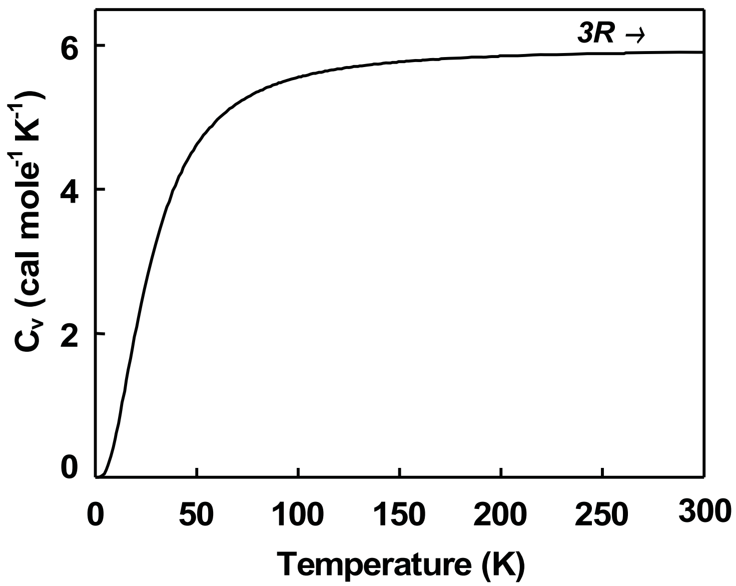

J. Wong et al., Science 301 (2003)

Experimental highlights (6)

Elasticity at high pressure (small focus)

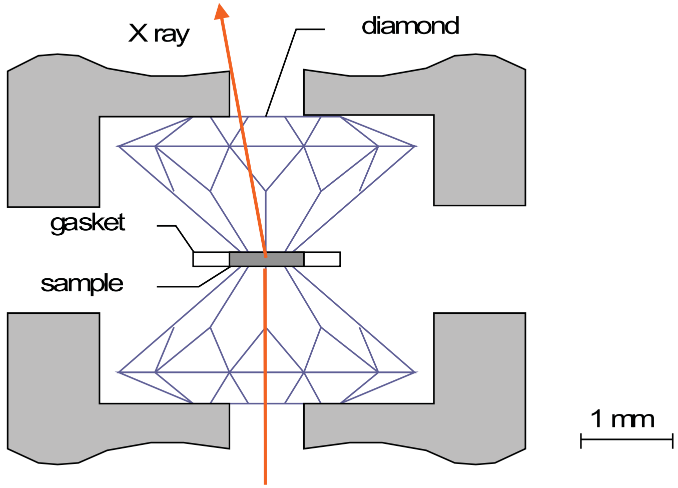

<u>Elasticity of hcp-metals under very high pressure (up to 1 Mbar):</u>

- Geophysical interest (Earth core)
- DAC sample environment + IXS

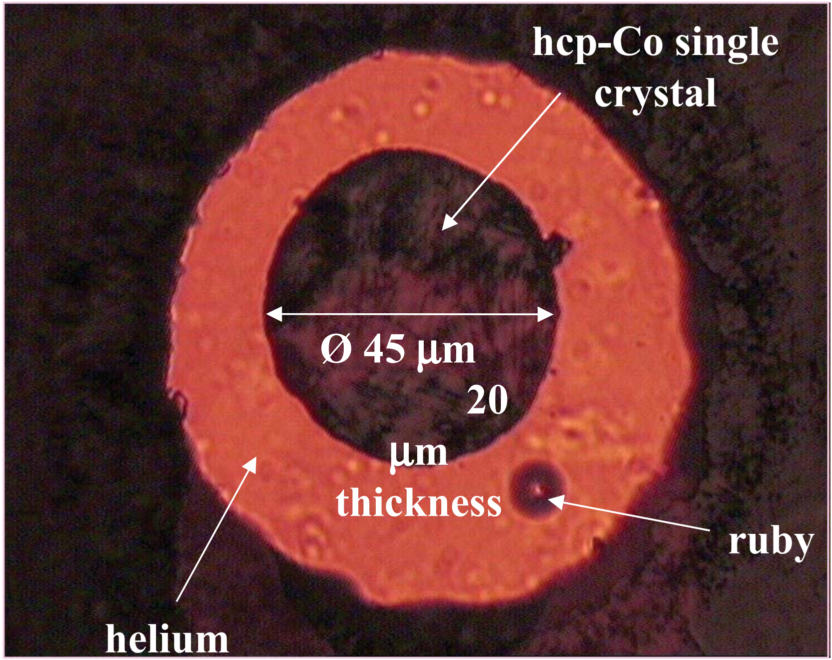

D. Antonangeli et al., PRL 93 (2004)

<u>hcp-structure:</u>

5 independent elastic moduli

$V_L[001] = (C_{33}/\rho)^{1/2}$

$V_L[100] = (C_{11}/\rho)^{1/2}$

$V_{T1}[110] = ([C_{11} - C_{12}] /2\rho)^{1/2}$

$V_{T2}[110] = (C_{44}/\rho)^{1/2}$

$V_{QL}[101] = f(C_{ij},\rho) \rightarrow C_{13}$

Experimental highlights (6)

Elasticity at high pressure

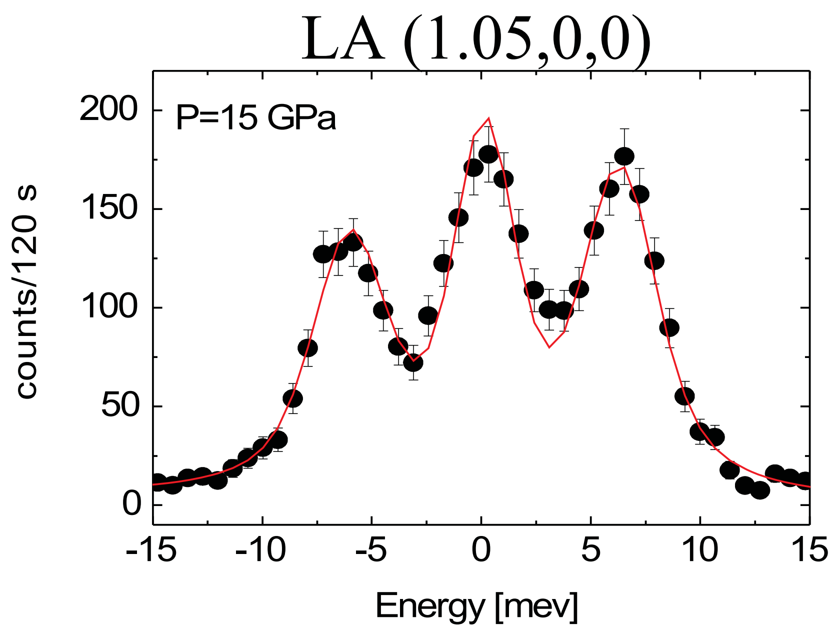

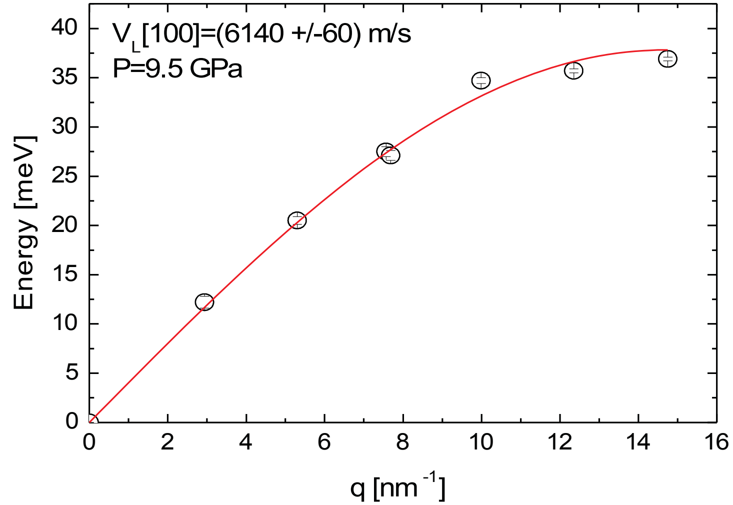

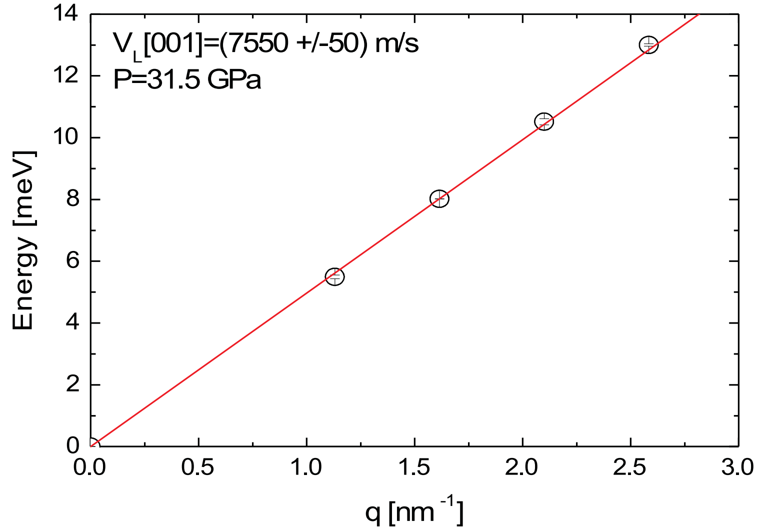

D. Antonangeli et al., PRL 93 (2004)

Experimental highlights (6)

Elasticity at high pressure

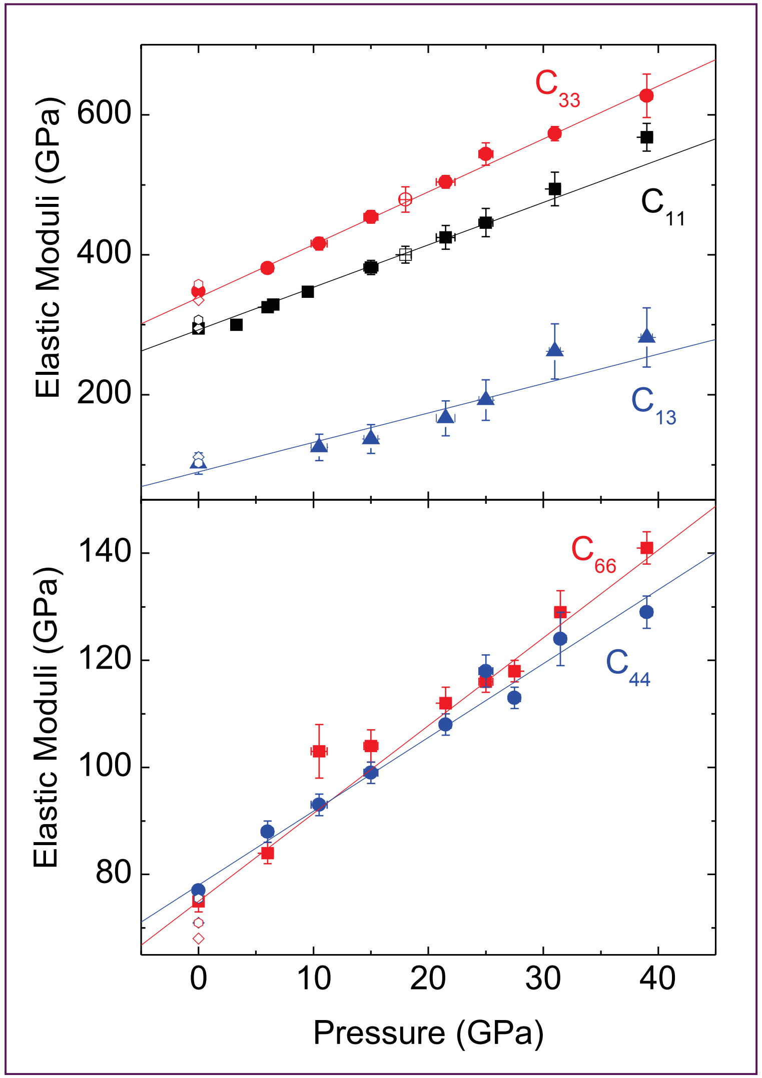

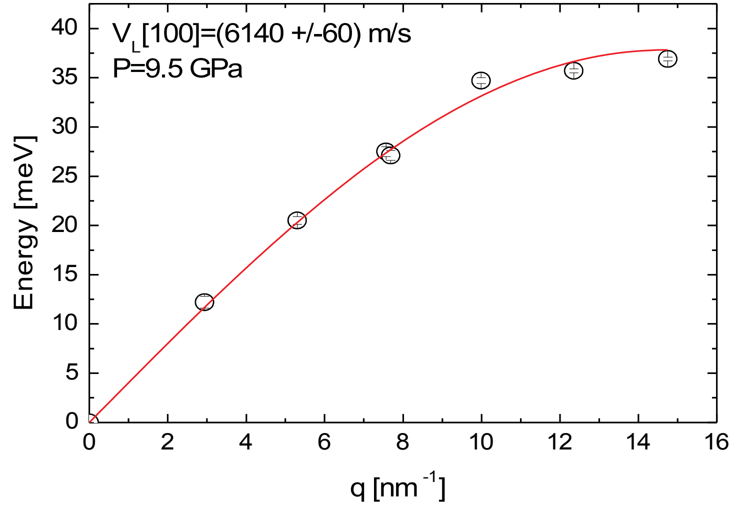

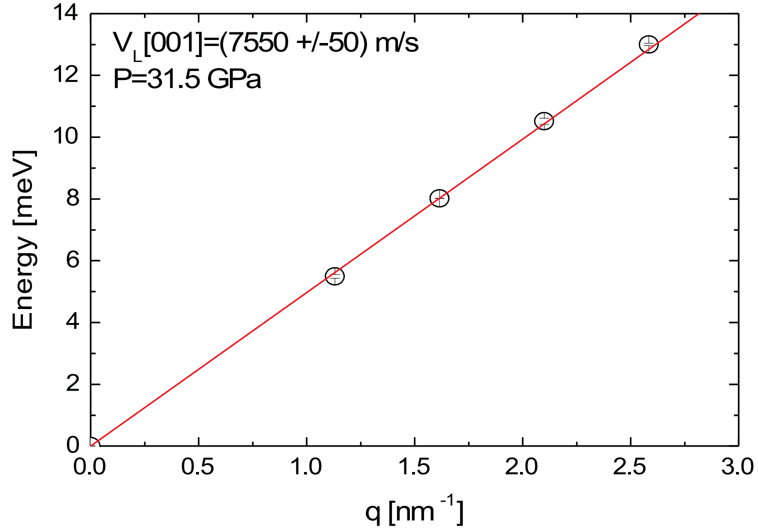

D. Antonangeli et al., PRL 93 (2004)

Experimental highlights (7)

Glassy GeO_2 under pressure (kinematic contraints + tigth focus)

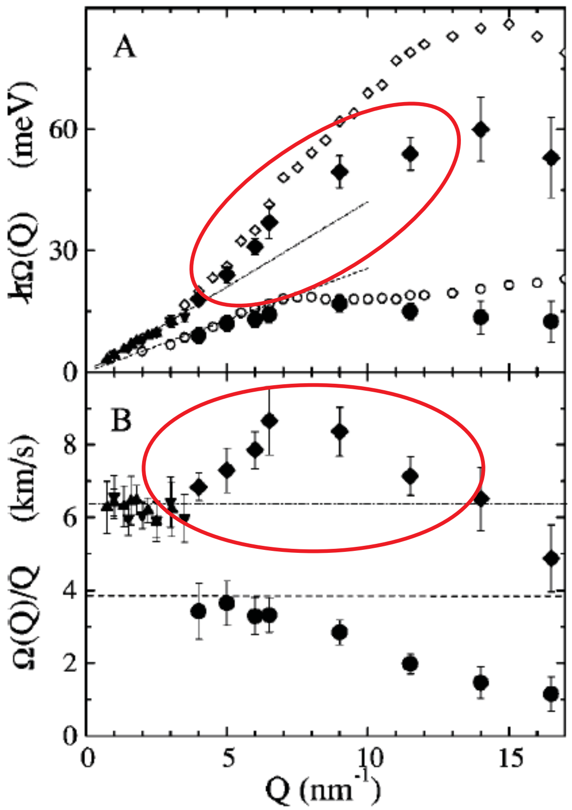

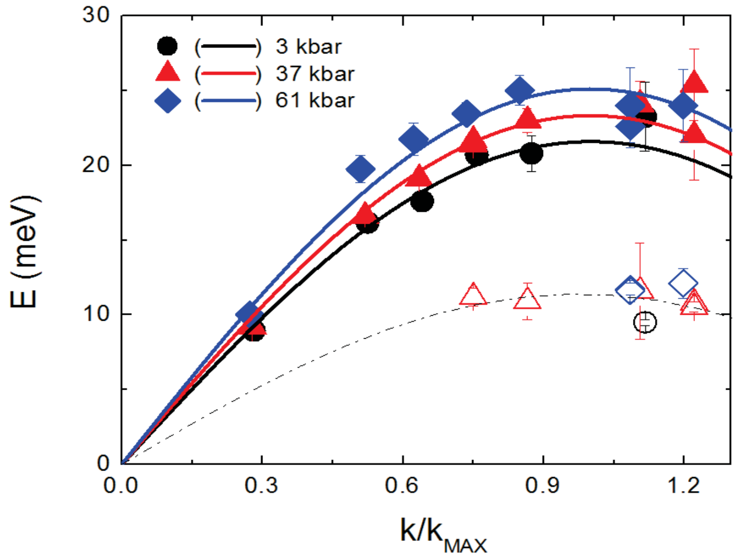

No “anomalies” observed in the crystalline phase; positive dispersion in the glassy phase (weak P-dependence).
Structural transition in glassy GeO_2 at P=0-7 GPa (coordination from 4 to > 10 GPa)

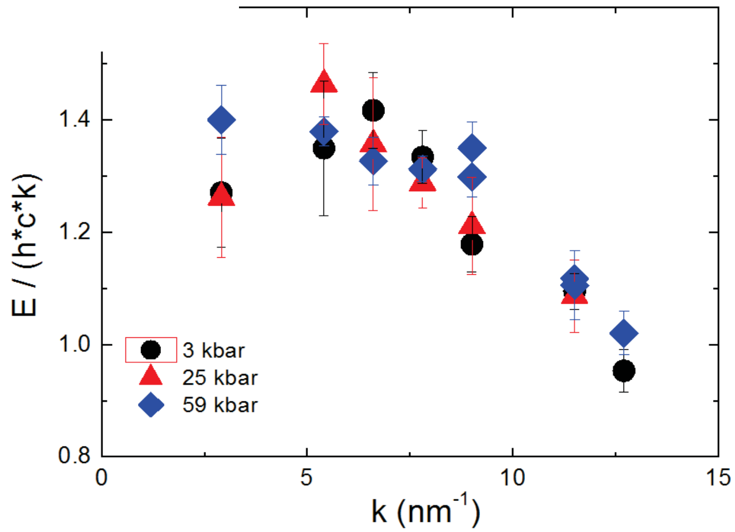

Positive sound dispersion in amorphous **solids** (SiO_2)[a]:
→ Also observed in GeO_2 and $GeSe_2$ (by IXS and INS)
→ Predicted by MD simulations for “harmonic glasses”[b]
→ Related to anharmonicity or structural disorder?

a) B. Ruzicka et al. PRBR 69 (2004); b) G. Ruocco et al., PRL 84 (2000)

F. Bencivenga et al., unpublished

X-ray Raman Scattering (XRS)

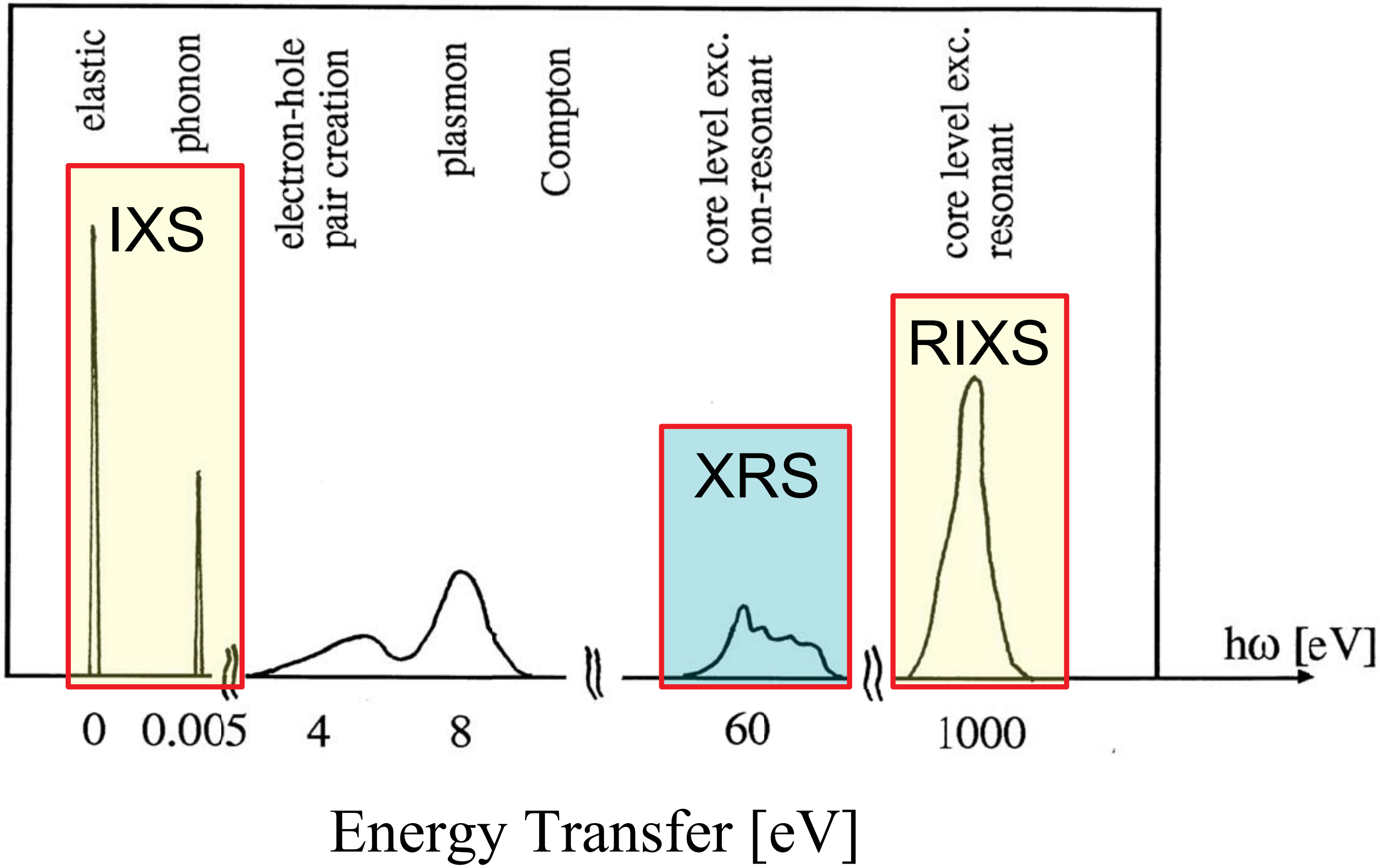

Basic instrumentation (XRS/RIXS)

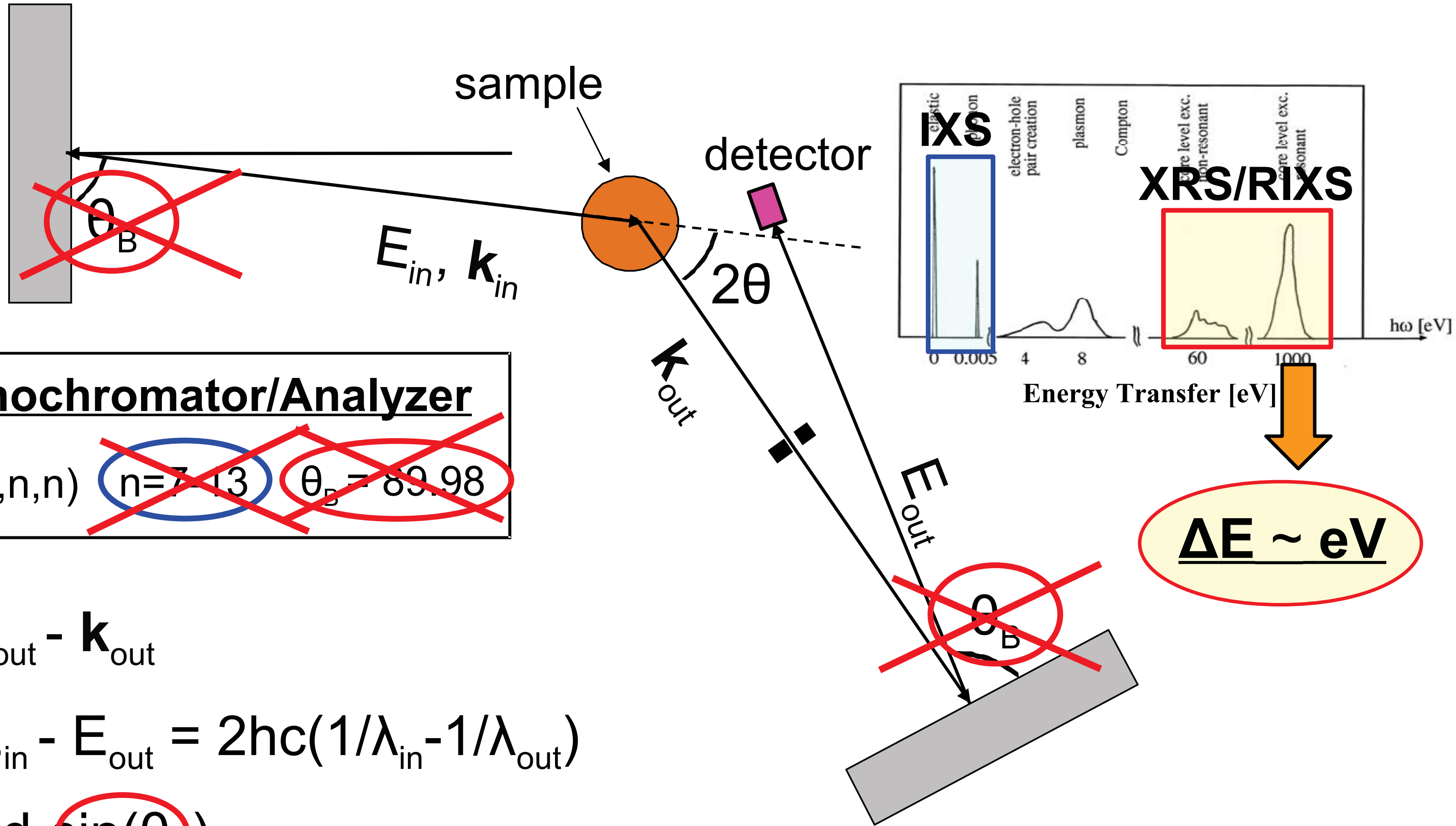

Monochromator/Analyzer

Si(n,n,n) ~~n=7-13~~ ~~θ_B = 89.98~~

$\mathbf{k} = \mathbf{k}_{out} - \mathbf{k}_{out}$

$E = E_{in} - E_{out} = 2hc(1/\lambda_{in} - 1/\lambda_{out})$

$\lambda = 2d_n \sin(\theta_B)$

~~**backscattering**~~ + ~~**high order reflections**~~ = ~~**ΔE ~ meV**~~

Basic instrumentation (XRS/RIXS)

Monochromator

Si(1,1,1); (2,2,0); …

λ_{in} (**tunable**)

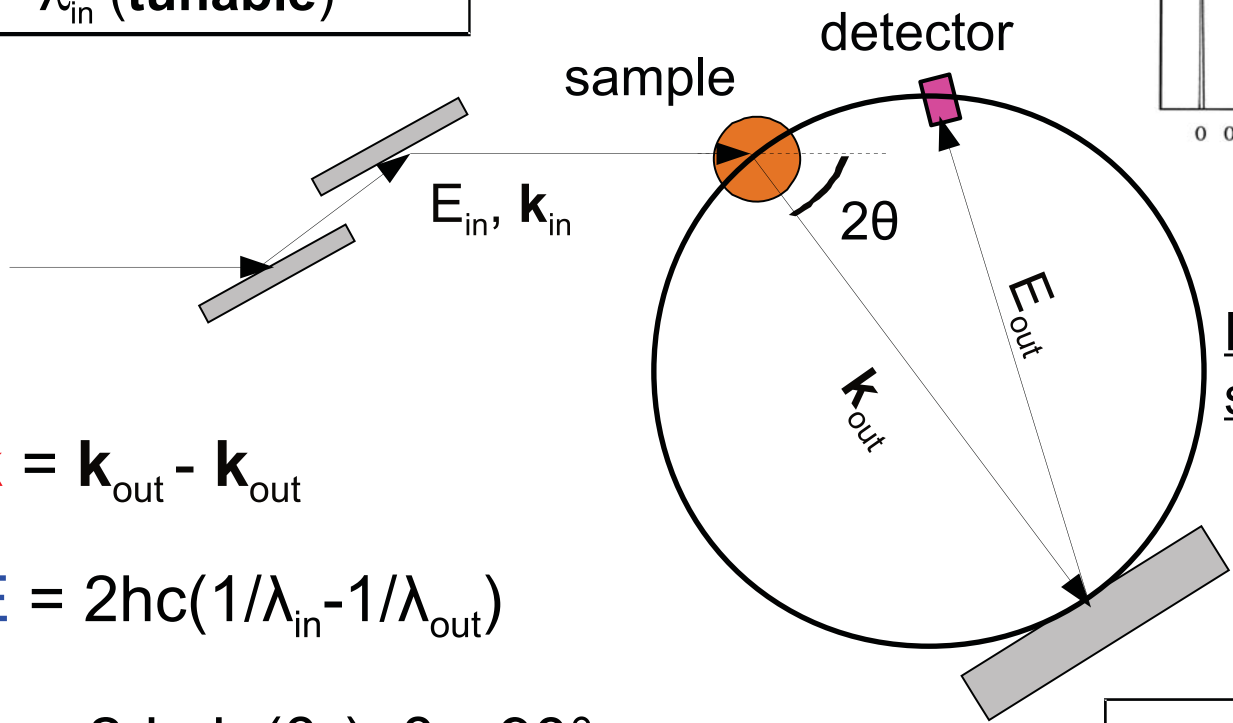

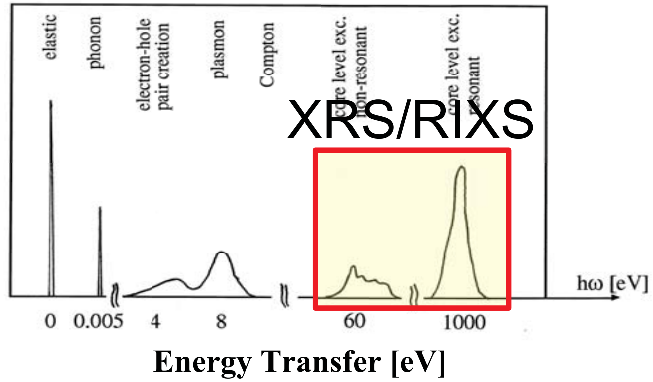

Rowland circle spectrometer (1 m)

$\mathbf{k} = \mathbf{k}_{out} - \mathbf{k}_{out}$

$E = 2hc(1/\lambda_{in} - 1/\lambda_{out})$

$\lambda = 2d_n \sin(\theta_B);\ \theta_B < 90°$

Analyser

Si(h,k,l) λ_{out} (**tunable**)

Basic instrumentation (XRS/RIXS)

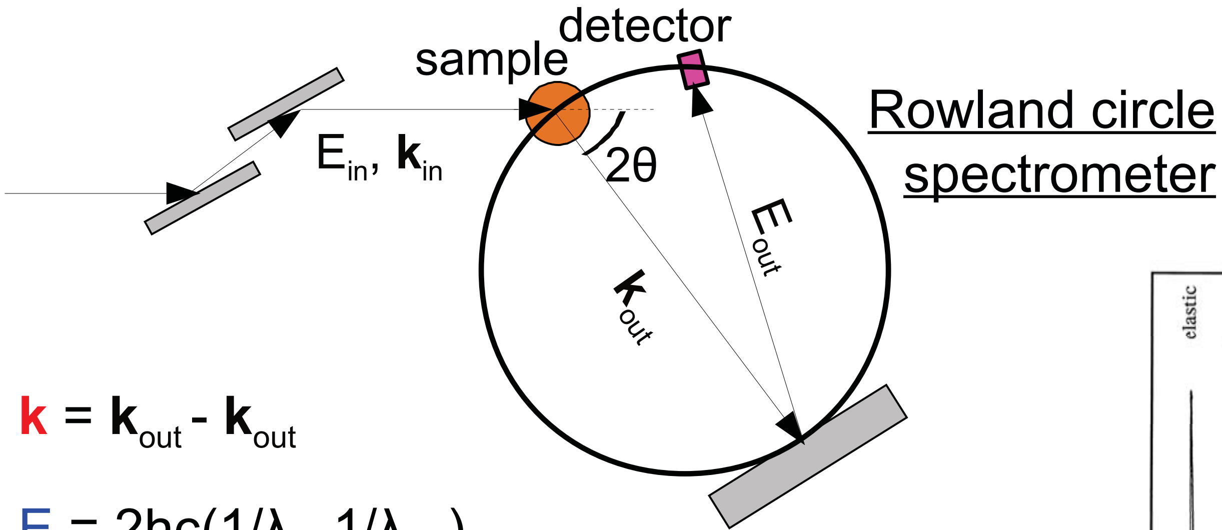

$\mathbf{k} = \mathbf{k}_{out} - \mathbf{k}_{out}$

$E = 2hc(1/\lambda_{in} - 1/\lambda_{out})$

$\lambda = 2d_n \sin(\theta_B)$; $\theta_B < 90°$

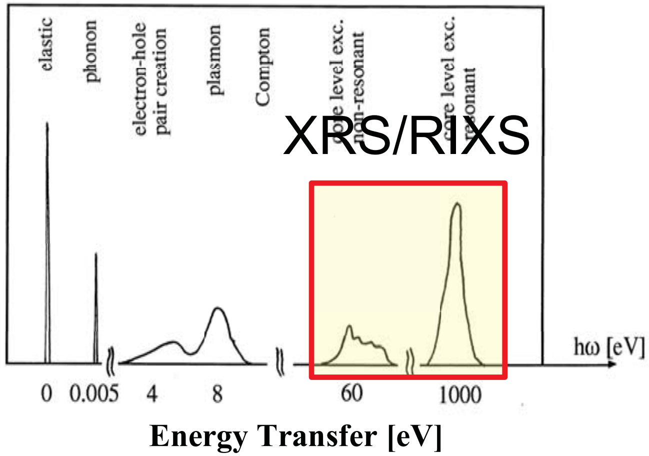

Scanning strategy

1. E_{out} fixed, scanning E_{in} - IXS, XRS, RIXS
2. E_{in} fixed, scanning E_{out} (rotating crystal and follow with the detector) - RIXS
3. Scanning E_{in} and E_{out} keeping E constant - RIXS

Basic theoretical aspects (XRS)

$$H_{int}=(e/m_ec)\sum_j[(e/2c)\mathbf{A}_j\cdot\mathbf{A}_j+\mathbf{A}_j\cdot\mathbf{p}_j]$$

A: vector potential of electromagnetic field

P: momentum operator of the electrons

j: summation over all electrons of the system

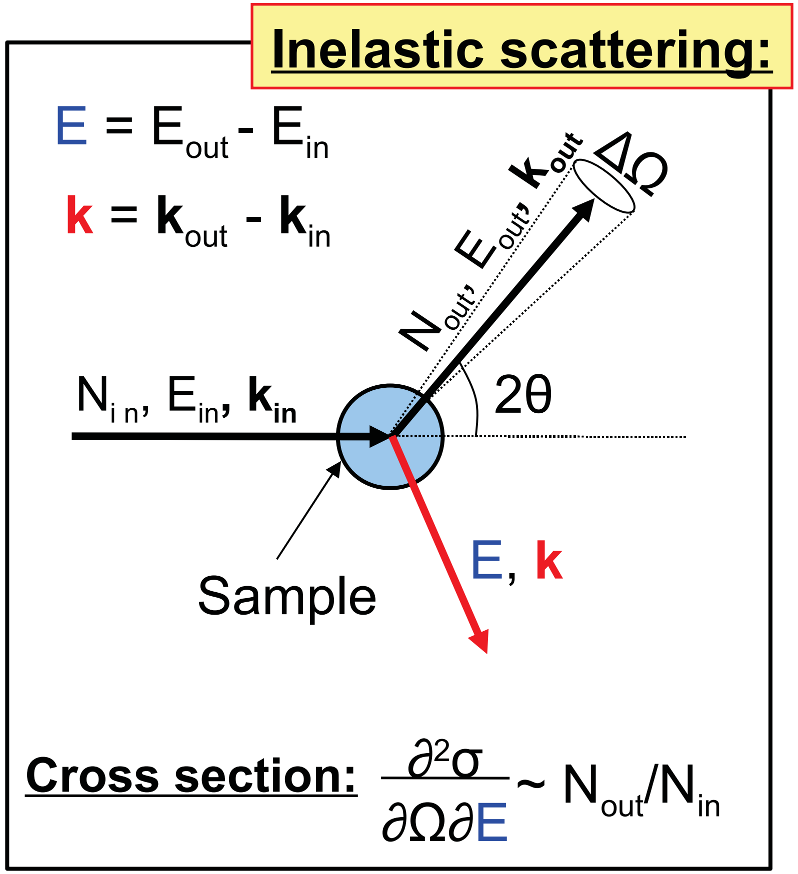

A·A → non-resonant scattering (example: IXS)

A·p → resonant scattering, absorption followed by emission

Basic theoretical aspects (XRS)

Non resonant IXS cross section:

$$\frac{\partial^2\sigma}{\partial\Omega\partial E} = r_0^2(\boldsymbol{\varepsilon}_{in}\cdot\boldsymbol{\varepsilon}_{out})^2(k_{in}/k_{out})\sum_I P_I|\langle I|\exp\{i\mathbf{k}\cdot\mathbf{r}_j\}|F\rangle|^2\delta(E-E_F+E_I)$$

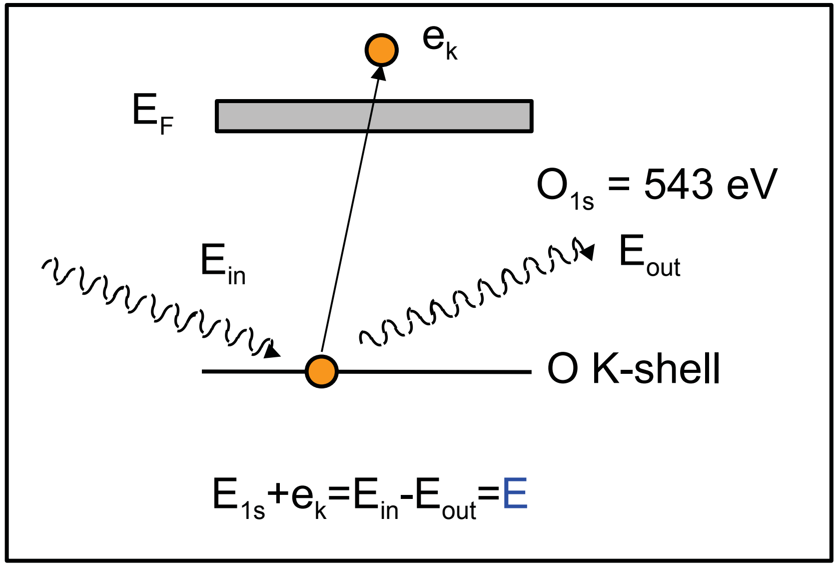

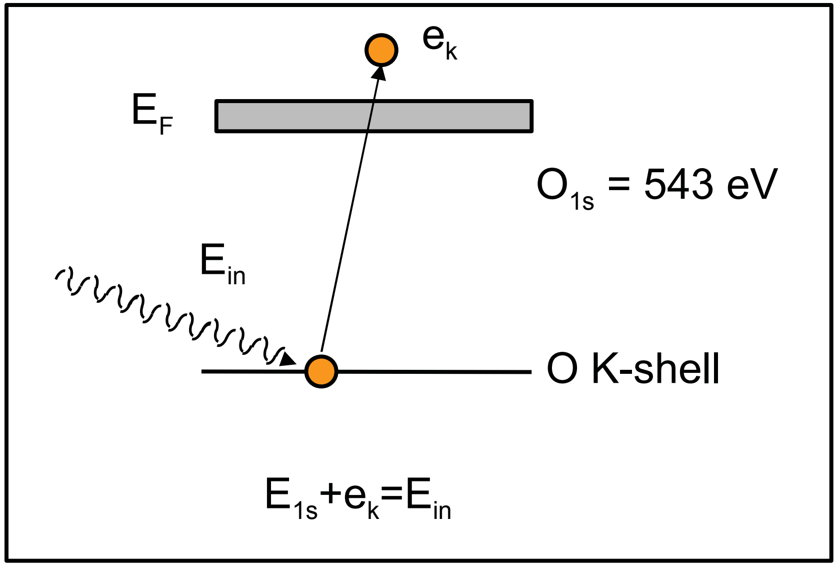

X-ray absorption cross section (dipolar approximation):

$$\frac{\partial\sigma}{\partial E_{in}} = 4\pi^2\alpha E_{in}\sum_I P_I|\langle I|\boldsymbol{\varepsilon}_{in}\cdot\mathbf{r}_j|F\rangle|^2\delta(E_{in}-E_F+E_I)$$

Basic theoretical aspects (XRS)

Non resonant IXS cross section:

$$\frac{\partial^2\sigma}{\partial\Omega\partial E} = r_0^2(\boldsymbol{\varepsilon}_{in}\cdot\boldsymbol{\varepsilon}_{out})^2(k_{in}/k_{out})\sum_I P_I|\langle I|\exp\{i\mathbf{k}\cdot\mathbf{r}_j\}|F\rangle|^2\delta(E-E_F+E_I)$$

$\mathbf{k}\cdot\mathbf{r}_j << 1 \rightarrow e^{i\mathbf{k}\cdot\mathbf{r}} \sim 1 + i\mathbf{k}\cdot\mathbf{r}_j$

$\mathbf{k}\cdot\mathbf{r}_j <<1 \rightarrow$ Dipolar regime: identical to photon absorption, where:

i)The momentum transfer ($\mathbf{k}$) plays the role of the photon polarization vector ($\boldsymbol{\varepsilon}_{in}$)

ii)The energy transfer (E) plays the role of the incident energy (E_{in})

X-ray absorption cross section (dipolar approximation):

$$\frac{\partial\sigma}{\partial E_{in}} = 4\pi^2\alpha E_{in}\sum_I P_I|\langle I|\boldsymbol{\varepsilon}_{in}\cdot\mathbf{r}_j|F\rangle|^2\delta(E_{in}-E_F+E_I)$$

Basic theoretical aspects (XRS)

Non resonant IXS cross section:

$$\frac{\partial^2\sigma}{\partial\Omega\partial E} = r_0^2(\boldsymbol{\varepsilon}_{in}\cdot\boldsymbol{\varepsilon}_{out})^2(k_{in}/k_{out})\sum_I P_I|\langle I|\exp\{i\mathbf{k}\cdot\mathbf{r}_j\}|F\rangle|^2\delta(E-E_F+E_I)$$

X-ray Raman Scattering (XRS)

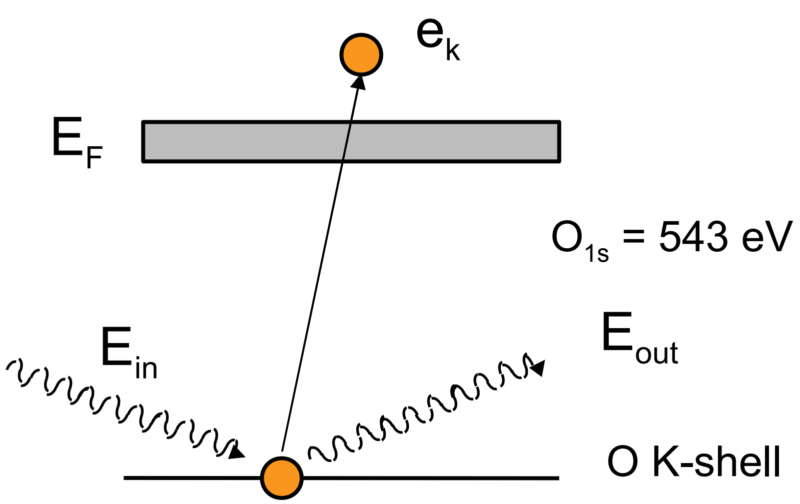

$$E_{1s}+e_k=E_{in}-E_{out}=E$$

Motivation: element-selective probe for local atomic structure

XRS is alternative to:

- Neutron scattering (with isotopic substitution)
- X-ray (anomalous) scattering
- XANES and EXAFS

Experimental highlights (XRS)

XRS from O K-edge in water and ice

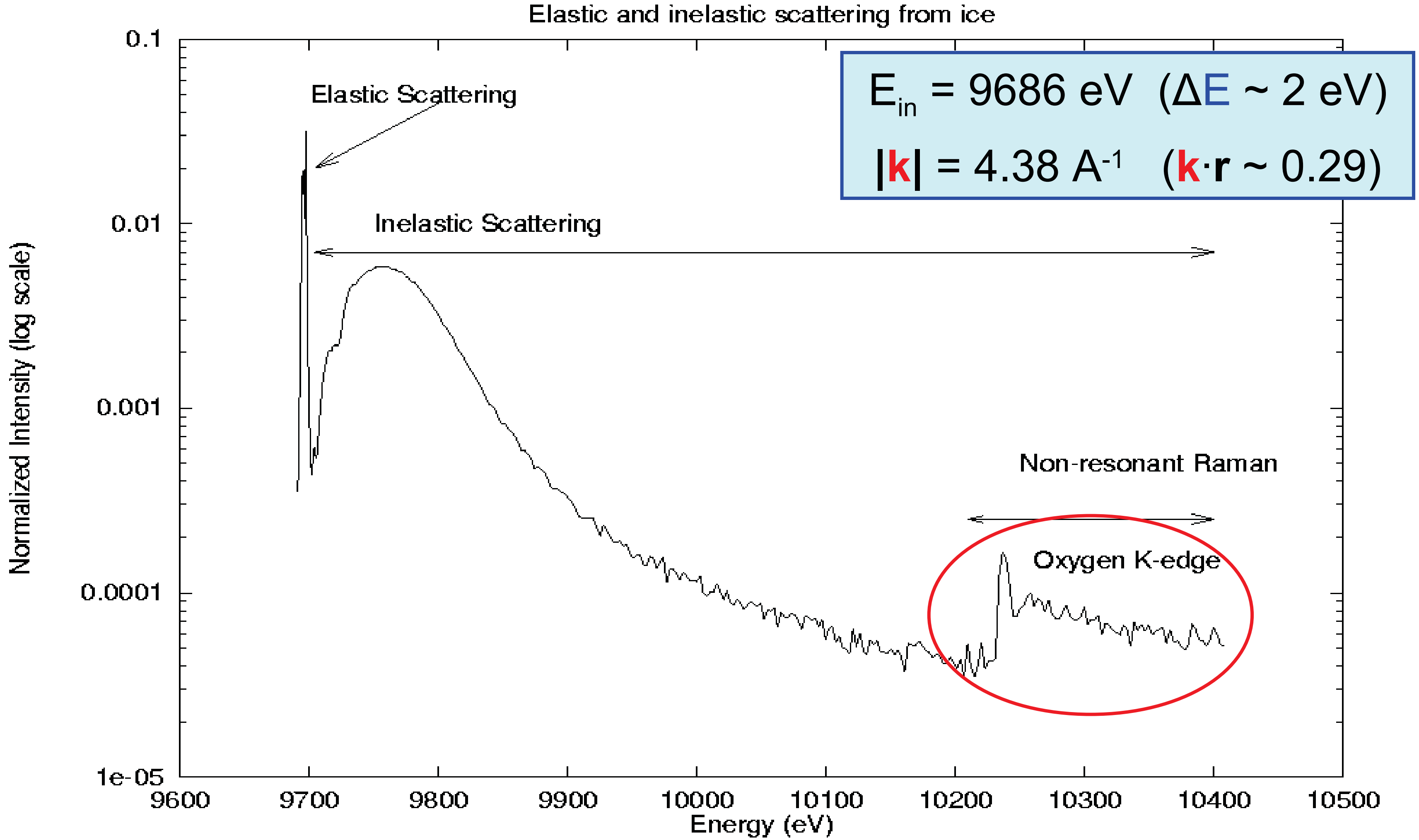

D.T. Bowron et al., PRB 62 (2000)

Experimental highlights (XRS)

XRS from O K-edge in water and ice (EXAFS)

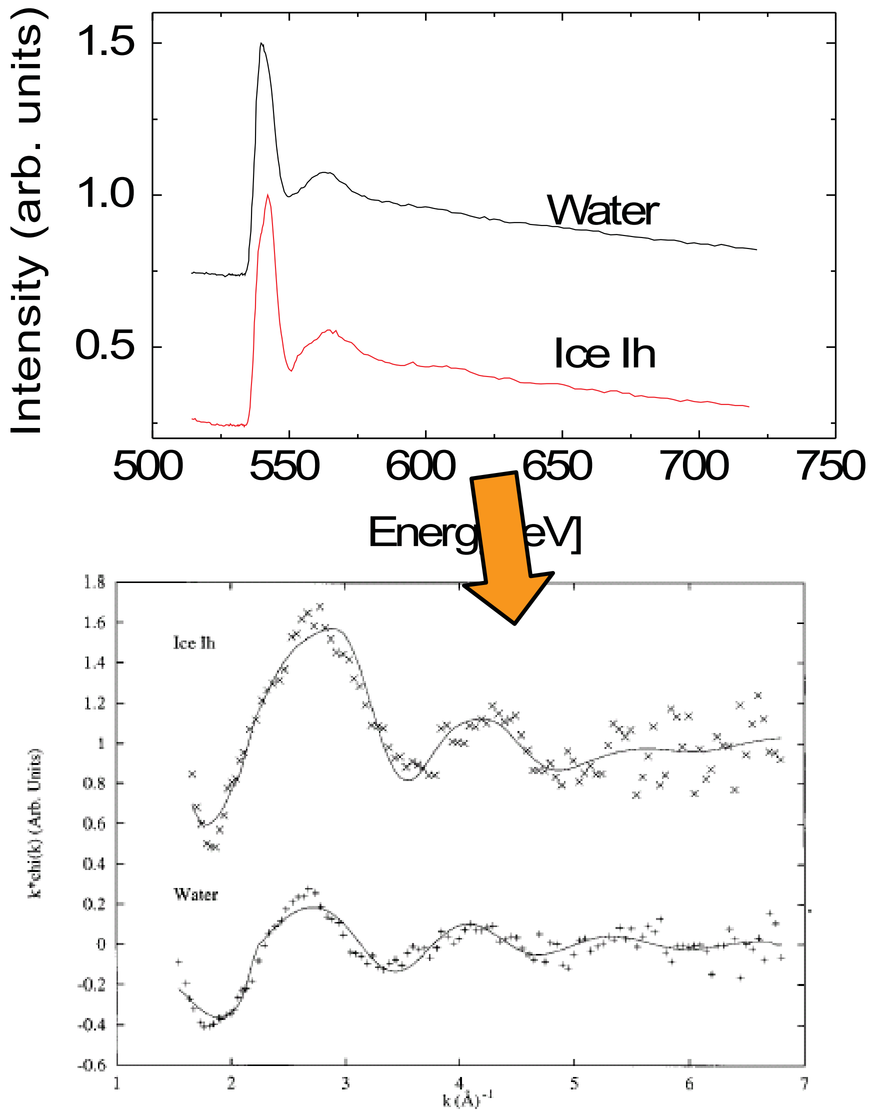

D.T. Bowron et al., PRB 62 (2000)

Experimental highlights (XRS)

XRS from O K-edge in water and ice (EXAFS)

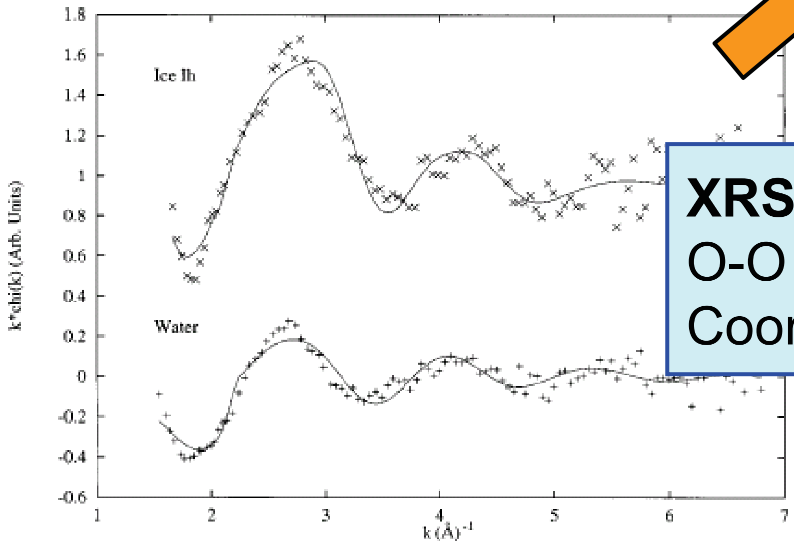

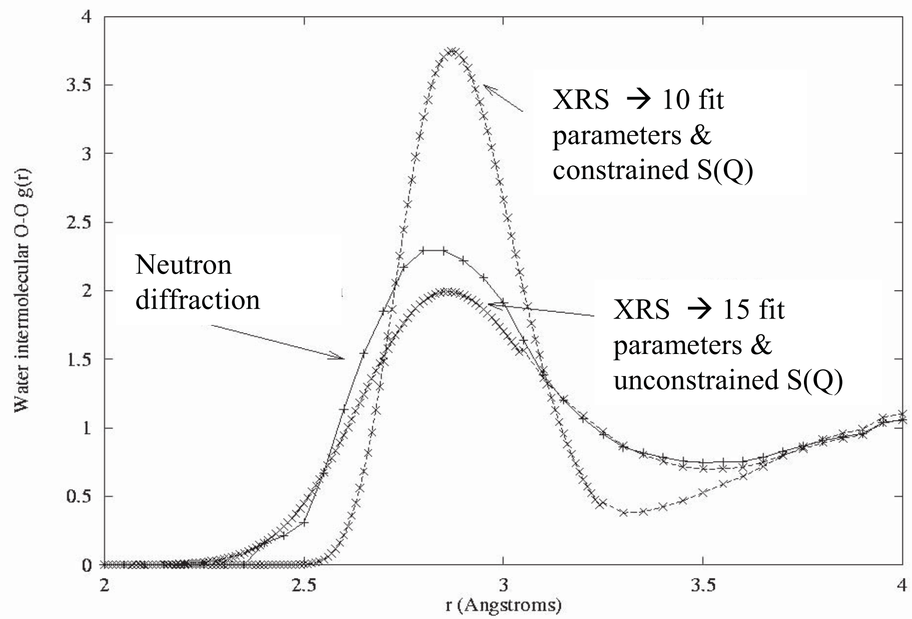

XRS:
O-O distance: 2.87 Å
Coordination: 4 - 7

Neutrons:
O-O distance: 2.85 Å
Coordination: 4.4

D.T. Bowron et al., PRB 62 (2000)

Experimental highlights (XRS)

XRS from O K-edge in water and ice (XANES)

XANES sensitive to the number and "type" of hydrogen bonds (HB)

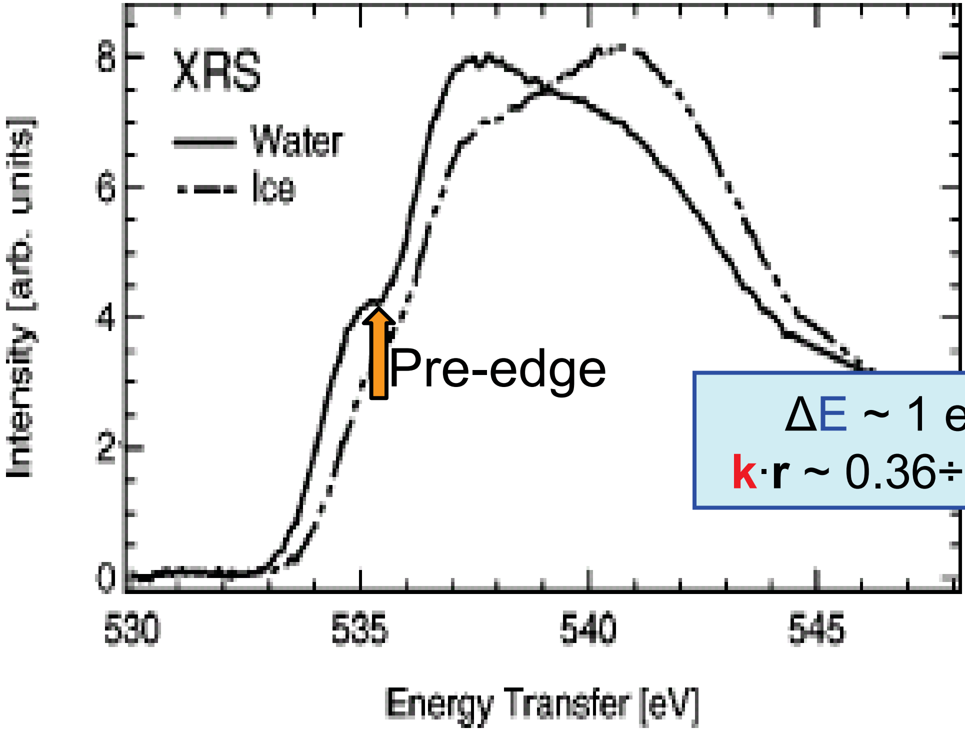

ΔE ~ 1 eV
k·**r** ~ 0.36÷0.57

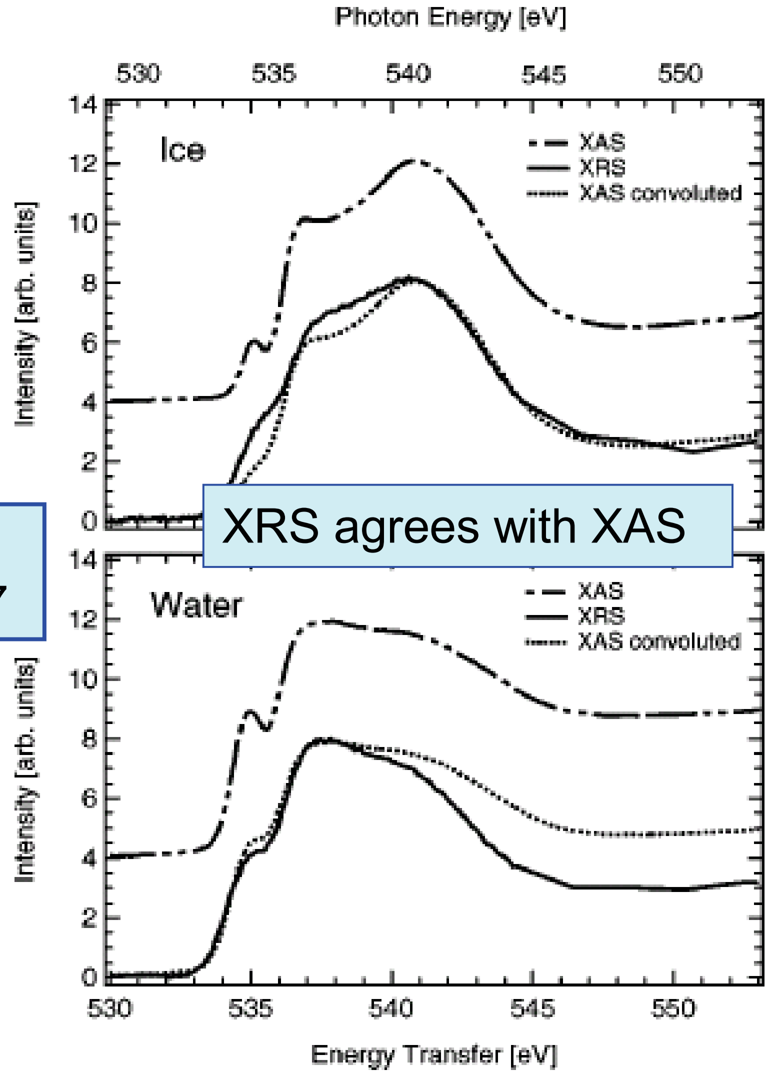

XRS agrees with XAS

- Pre-edge indicates a large number (~ 70%) of distorted or broken HB (supported by calculation)

D.T. Bowron et al., PRB 62 (2000)

Experimental highlights (XRS)

XRS from O K-edge in ice under high pressure

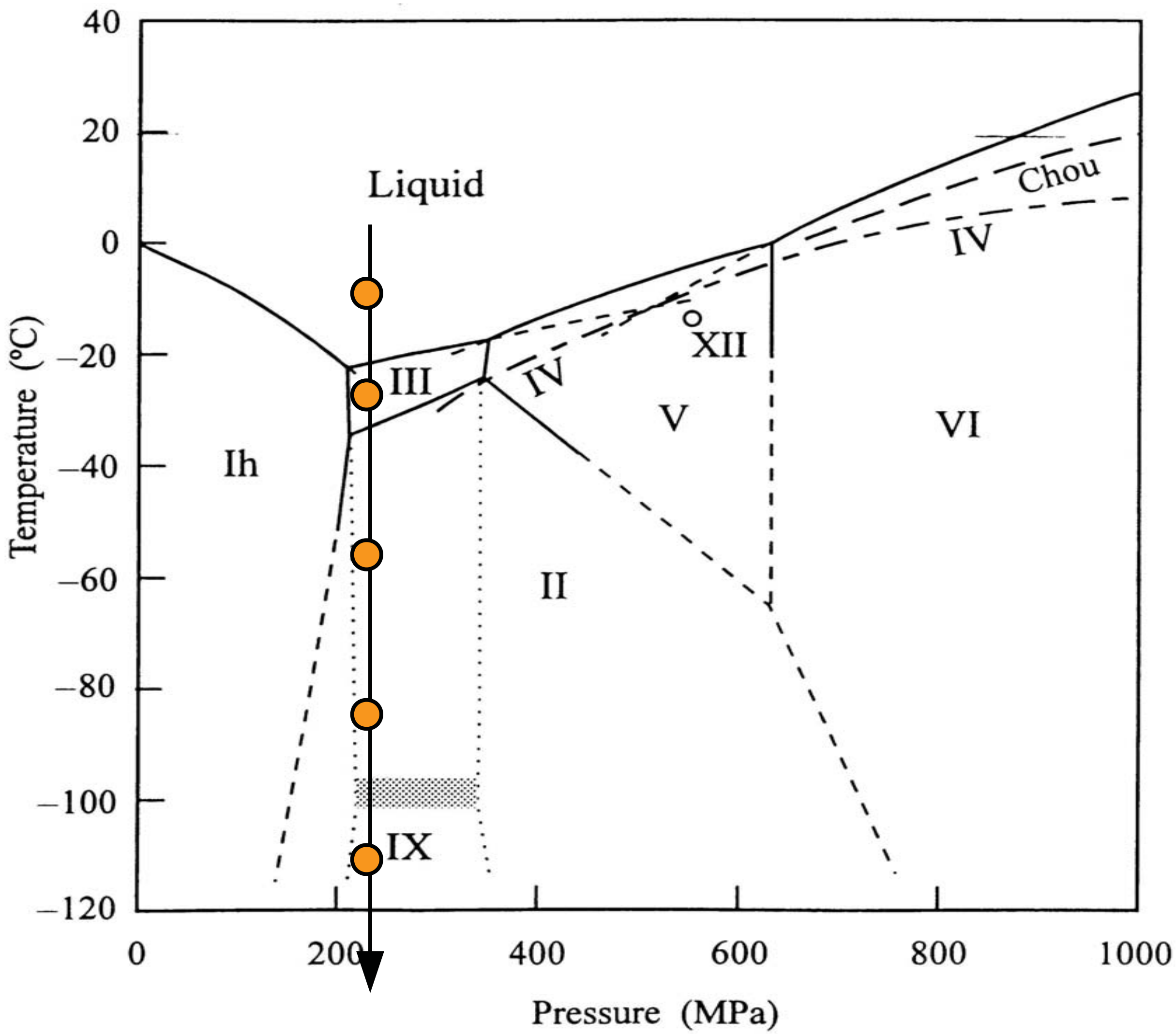

Y.Q. Cai et al., PRL 94 (2005)

E_{out} = 9885 eV
(ΔE ~ 0.2÷0.3 eV)
|**k**| ~ 3 A^{-1} (**k**·**r** ~ 0.2)

DAC sample environment: hard x-ray needed

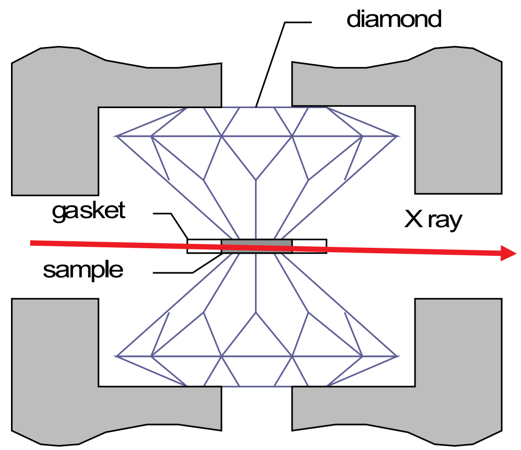

Experimental highlights (XRS)

XRS from O K-edge in ice under high pressure

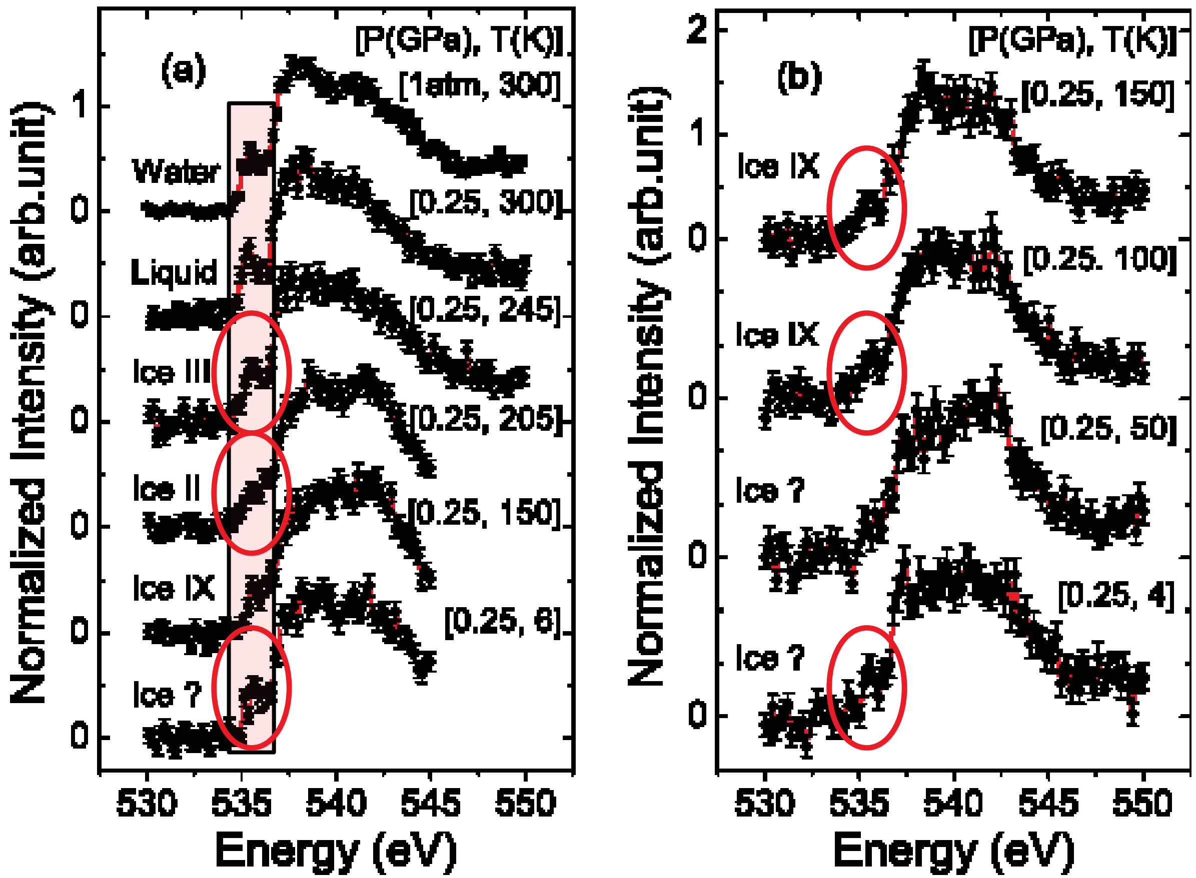

- Slight increase of pre-edge with P (larger HB distortion)
- Increasing order of HB from liquid → Ice III (tetrahedral) → Ice II / IX
- New pre-edge increase @ low-T: new Ice phase?

Observation of spectral changes:
Need of much better statistics and theory to extract quantitative information

Y.Q. Cai et al., PRL 94 (2005)

XRS in summary

Soft x-ray spectroscopy in the hard x-ray regime

Advantages

"simpler" sample environment (high pressure/temperature, etc…) + bulk sensitive
→ indicated for studying (bulk) Oxygen and Carbon

Drawbacks

- "weak probe" (practically limited to $Z < 14$)
→ limited quality for structural analysis (EXAFS), reasonable quality in the XANES region

Exploit information in the near-edge region